

**EXPERIMENTAL INVESTIGATION
OF RECOVERY FACTORS AND
FRICTION FACTORS FOR AIR
FLOWING IN A TUBE AT
SUPERSONIC VELOCITIES**

BY

**RAYMOND VINCENT WELCH
JOSEPH EUGENE VOLONTE**

Library
U. S. Naval Postgraduate School
Annapolis, Md.

MASSACHUSETTS INSTITUTE OF TECHNOLOGY

77 Massachusetts Avenue

Cambridge, Massachusetts

May 19, 1950

Professor J. P. Den Hartog
Chairman of Departmental Committee on Graduate Students
Mechanical Engineering Department
Massachusetts Institute of Technology
Cambridge, Massachusetts

Dear Professor Den Hartog:

We take pleasure in submitting this thesis entitled "Experimental Investigation of Recovery Factors and Friction Factors for Air Flowing in a Tube at Supersonic Velocities" in partial fulfillment of the requirements for the degree of Master of Science in Mechanical Engineering.

Respectfully,

Theses
W3935

EXPERIMENTAL INVESTIGATION OF
RECOVERY FACTORS AND FRICTION FACTORS
FOR AIR FLOWING IN A TUBE AT SUPERSONIC VELOCITIES

by

RAYMOND VINCENT WELCH

B.S., United States Naval Academy (1941)

and

JOSEPH EUGENE VOLONTE

B.S., United States Naval Academy (1942)

SUBMITTED IN PARTIAL FULFILLMENT OF THE
REQUIREMENTS FOR THE DEGREE OF
MASTER OF SCIENCE

in

MECHANICAL ENGINEERING

at the

MASSACHUSETTS INSTITUTE OF TECHNOLOGY

May 19, 1950

Thesis
W392

ACKNOWLEDGMENTS

It is with pleasure that we acknowledge our indebtedness to our instructors and colleagues for the aid they have so generously given during the course of this investigation.

Professor Joseph Kaye, under whose personal supervision this research was carried out, gave constant help and guidance. Professor Joseph H. Keenan, who is associated with the project under which this investigation was carried out, furnished invaluable advice.

Professor Ascher H. Shapiro made suggestions which facilitated the design and selection of a supersonic nozzle. Professor Samuel C. Collins, was most cooperative in providing dry air from his Low Temperature Laboratory for some of the experimental work.

Mr. Robert H. Shoulberg, who was in charge of the experimental work of the project when the authors commenced their work, provided the necessary guidance during the initial stages of the investigation.

Mr. Gordon J. Van W ylen rendered much assistance during the first part of the program.

The Messrs. Tau-Yi Toong and William O. Young, who are currently working on this project and who will continue the research commenced during this investigation, made it possible for the authors to complete the experimental work necessary to the preparation of this thesis.

Miss Barbara Healy assisted in the computations necessary for the determination of the final results.

We wish to thank Chief Engineer Chester B. Dolber and his assistant,
Mr. Chester H. Babcock, for their cooperation and aid in the Steam
Laboratory.

TABLE OF CONTENTS

<u>Chapter</u>		<u>Page</u>
I	Summary	I-1
II	Nomenclature	II-1
III	Introduction	III-1
	Recovery Factors	III-1
	Friction Factors	III-5
IV	Investigation Procedure	IV-1
V	Description of Apparatus	V-1
	Air Supply	V-3
	Air Dehumidification	V-3
	Air Flow and Temperature Control	V-4
	Recovery Factor Apparatus	V-5
	Downstream Air Path	V-7
	Vacuum System	V-8
	Pressure Measuring System	V-8
	Temperature Measuring System	V-9
VI	Discussion of Results	VI-1
	General	VI-1
	Recovery Factors	VI-2
	Friction Factors	VI-4
	Effect of Vacuum System	VI-5
	Preliminary Results with Modified Apparatus	VI-6
VII	Conclusions	VII-1
VIII	Recommendations	VIII-1
 <u>Appendix</u>		
A	Brief History of Project DIC 6418	A-1
B	Calculation of Recovery and Friction Factors	B-1
C	Calculation Data, Constants and Coefficients	C-1
D	Sample Calculation	D-1
E	Design of Nozzle	E-1
F	Description of Sauer Method of Nozzle Design	F-1
G	Nozzle Calibration	G-1
H	Thermocouple Calibration	H-1
I	Vacuum System Precautions	I-1
J	Orifice	J-1
K	Modification to Recovery Factor Apparatus	K-1
L	Effect of Measurement Errors	L-1
M	Bibliography	M-1

LIST OF FIGURES AND ILLUSTRATIONS

<u>Figure</u>		<u>Following Page</u>
V-1	Schematic Drawing of Air System	V-3
V-2	Assembly (drawing)	V-7
	Assembly (photograph)	V-7
	Reducer, nozzle, test section and end plates (photograph)	V-7
V-3	Reducer and Collar (drawing)	V-7
V-4	Nozzle (drawing)	V-7
	Reducer, upstream end plate and nozzle (photograph)	V-7
V-5	Test Section (drawing)	V-7
	Test Section (photograph)	V-7
V-6	End Plates (drawing)	V-7
V-7	Outer Tube (drawing)	V-7
V-8	Adapter (drawing)	V-7
V-9	Gaskets (drawing)	V-7
V-10	Schematic Drawing of Pressure Measuring System	V-8
VI-1	Pressure ratio vs L/D	VI-7
VI-2	Temperature ratio vs L/D	VI-7
VI-3	Recovery Factor vs Mach number	VI-7
VI-4	Recovery Factor vs Reynolds number (diameter)	VI-7
VI-5	Recovery Factor vs Reynolds number (length)	VI-7
VI-6	Mean Apparent Friction Factor vs Reynolds No. (length)	VI-7
VI-7	Mean Apparent Friction Factor vs L/D	VI-7
VI-8	Mean Apparent Friction Factor vs Reynolds No. (diameter)	VI-7
VI-9	Mach Number vs Reynolds Number (length)	VI-7
VI-10	Recovery Factor vs Mach Number Comparison Curve	VI-7
B-1	Comparison of Calculation Methods	B-4
C-1	Mach Number vs $(1/C_w) (P_w/P_{us})$	C-5
C-2	Nozzle coefficient vs Reynolds Number (throat diameter)	C-5
C-3	Viscosity vs Temperature for Air	C-5
C-4	Pressure Conversion Factors	C-5
E-1	Nozzle Contour Regions	E-2
E-2	Comparison of Nozzle Throat to Exit Contours	E-2
F-1	Mach Net - Physical Plane	F-3
F-2	Velocity Net	F-3
F-3	Physical Plane M_I	F-3
F-4	Velocity Plane G_0	F-6
F-5	Physical Plane Corrected to give Parallel Outflow	F-6
G-1	Schematic Diagram of Nozzle Calibration Apparatus	G-2
G-2	Schematic Diagram of Nozzle Calibration Apparatus	G-2
G-3	Nozzle Calibration C_w vs Reynolds No. (throat diameter)	G-3
J -1	Orifice Calibration Curve	J -3



<u>Figure</u>		<u>Following Page</u>
L-1	Effect of Measurement Errors on Calculated Mach No.	L-3
L-2	Effect of Errors in Mach No. on Calculated R'	L-3
L-3	Effect of Errors in T_{aw} on Calculated R'	L-3

<u>Table</u>		<u>Page</u>
	Tables of Results	VI-8
C-1	Temperature Conversions	C-5
D-1	Sample Calculation	D-7
G-1	Summary of Results of Nozzle Calibration	G-5

CHAPTER I

Summary

Recovery factor and friction factor data are presented here for air at a stagnation temperature of 110°F flowing through a cylindrical tube at Mach numbers ranging from 1.3 to 2.6 and at inlet diameter Reynolds numbers from 0.47×10^5 to 4.8×10^5 .

Varying from a value of about 0.81 at a Mach number of 1.3 to about 0.905 at a Mach number of 2.6, the recovery factor has been shown to be an almost linear function of only Mach number over the entire range of inlet diameter Reynolds numbers. Although the results obtained indicate three flow regimes, there appears to be no dependency of the recovery factor on the diameter Reynolds number at inlet. In addition, there apparently is no simple relationship between recovery factors and Prandtl number involving fractional exponents.

The mean apparent friction factors are in good agreement with the results of Keenan and Neumann¹⁷ and Ketchum¹⁰. From a plot of mean apparent friction factor as a function of length Reynolds number three flow regimes which are essentially laminar, transitional, and turbulent can be identified with the transitional regime apparently lying between length Reynolds numbers of 15×10^5 and 30×10^5 . The friction factor attains a minimum value of about 0.0013 at the transition region and after transition decreases steadily with increasing length Reynolds number from a maximum value of about 0.0035.

Preliminary results were obtained with the recovery factor apparatus modified to reduce heat transfer to the test section; although neither extensive nor conclusive, these data indicate that the recovery factors obtained will be from one-half to one percent lower than those determined with the unmodified apparatus and that recovery factor is independent of stagnation temperature.

CHAPTER II

Nomenclature

Symbol	Meaning
A	cross-sectional area of test section (in^2)
A^*	cross-sectional area of nozzle throat (in^2)
c_p	specific heat at constant pressure (Btu/lb-F)
C_w	nozzle flow coefficient (dimensionless)
D	diameter of test section (in)
D^*	diameter of nozzle throat (in)
f	local apparent friction factor; friction factor which is the mean of the values for two adjacent stations in the test section (dimensionless)
\bar{f}	mean apparent friction factor; friction factor which is the mean of the values for the first station and another station in the test section (dimensionless)
g	gravitational acceleration (ft/sec^2)
G	mass velocity in test section (lb/sec-ft^2)
G^*	mass velocity in nozzle throat (lb/sec-ft^2)
h_1	height of mercury in leg of McLeod gage (cm)
h_2	height of mercury in capillary tube of McLeod gage (cm)
J	proportionality constant (ft-lb/Btu)
k	specific heat ratio (dimensionless)
k	thermal conductivity (Btu/hr-ft-F)

Symbol	Meaning
L	longitudinal distance from exit plane of nozzle to a point in the test section (in or ft)
L_{\max}	longitudinal distance from entrance to cylindrical tube (exit plane of nozzle) to a point where the Mach number is 1.0 (in or ft)
M	Mach number (dimensionless)
p, P	static pressure; P_{bar} - barometer; P_{ds} - downstream stagnation tank; P_{gas} - gasometer tank; P_{ol} - upstream of orifice; ΔP_{o} - pressure differential across orifice; P_{us} - upstream stagnation tank; P_{w} - wall of test section; P_{vac} - evacuated chamber surrounding test section (psi or psia)
Pr	Prandtl number (dimensionless)
R	gas constant (ft-lb/lb-F)
R'	recovery factor (dimensionless)
Re	Reynolds number; Re_D - based on test section diameter; Re_L - based on distance from exit plane of nozzle; Re_x - based on distance from nozzle throat (dimensionless); Re_D^* - based on nozzle throat diameter
\bar{Re}	mean Reynolds number; value which is a mean for two adjacent stations of test section (dimensionless)
r_s	radius of station temperature thermocouple (in)
Δr_s	radial distance between differential temperature thermocouples (in)

Symbol	Meaning
r_w	radius of test section wall (in)
t	temperature ($^{\circ}\text{F}$); t_{aw} - adiabatic wall temperature; t_{ds} - downstream stagnation temperature; t_{gas} - temperature in gasometer; t_m - mean stream temperature; t_{room} - room temperature; t_s - temperature at station thermocouple; Δt_s - temperature differential between differential temperature thermocouples; t_{us} - upstream stagnation temperature;
T	temperature ($^{\circ}\text{Fabs}$); same subscripts as for t
w	mass rate of flow (lb/sec); w_o - mass rate of flow through orifice; w_s - isentropic mass rate of flow; w^* - mass rate of flow through nozzle; w_{gas} - mass rate of flow into gasometer
x	longitudinal distance from nozzle throat to a point in the test section (in)
μ	viscosity (lb/sec-ft); μ_m - viscosity evaluated at mean stream temperature; μ^* - viscosity at nozzle throat
ϕ	dimensionless group, $\frac{4fL_{max}}{D}$

CHAPTER III

Introduction

The experimental work reported in this thesis is part of Project DIC 6418 sponsored by the Office of Naval Research to determine recovery factors, friction factors and heat transfer coefficients for air flowing at supersonic velocities. More extensive knowledge of the heat transfer coefficient is becoming increasingly important in the design of aircraft, aircraft coolers, missiles, compressor and turbine blading. However, the heat transfer coefficients as defined for air flowing at supersonic speeds cannot be determined without a prior knowledge of recovery factors, data for which is currently insufficient and inadequate. It is the purpose of this thesis to determine the magnitude of recovery factors and the parameters upon which the recovery factor depend in the flow of air at supersonic speeds through a cylindrical tube. In addition, data on closely related friction factors are to be obtained incidental to the determination of recovery factors.

Recovery Factor

The coefficient of heat transfer for compressible flow is defined as the rate of heat flow per unit area per degree temperature difference between wall temperature and the adiabatic wall temperature:

$$h = \frac{q/A}{T_w - T_{aw}} \quad (1)$$

The temperature difference, $T_w - T_{aw}$, is now almost universally accepted where any compressibility effects are encountered since its use yields

values of h which are independent of the temperature difference at high subsonic and supersonic speeds. In earlier investigations, however, the heat transfer coefficients were often based on the temperature difference between T_w and T_m or T_o .

Since T_{aw} is defined as the temperature the wall would have if it were in equilibrium with the stream and thermally isolated from its surroundings, i.e., an adiabatic wall, it cannot be measured when heat is being transferred by the wall. However, by determining the value of the recovery factor defined in terms of T_{aw} and the stream properties found in an adiabatic test, T_{aw} can be predicted under the conditions when heat is being transferred by the wall.

The definition of the recovery factor used is the dimensionless quantity:

$$R' = \frac{T_{aw} - T_m}{T_o - T_m} \quad (2)$$

in which the stagnation temperature T_o can be measured at a point in the stream where the velocity is zero; T_{aw} can be measured in an adiabatic test; and the mean stream temperature T_m can be evaluated from a one-dimensional analysis of wall and stagnation pressure measurements.

Since in steady, one dimensional flow of a perfect gas in a duct of constant cross-sectional area in the absence of heat exchange

$$T_o - T_m = \frac{V^2}{2gJ C_p} \quad (3)$$

where V is the velocity of the mean stream at the point where T_m is evaluated,

$$R' = \frac{T_{aw} - T_m}{V^2 / 2gJ C_p} \quad (4)$$

$$\text{and} \quad T_{aw} = T_m + R' \frac{V^2}{2gJ C_p} \quad (5)$$

Equation (5) thus furnishes a method of predicting the value of T_{aw} when heat is being transferred by the wall, provided R' has been previously determined from adiabatic tests.

From Equation (5), it can be seen that physically the recovery factor may be thought of as the proportion of the mean stream kinetic energy that is recovered at the wall as the air is retarded to zero velocity at the wall surface. It is also seen that T_{aw} may be less or greater than T_o depending upon whether R' is greater or less than 1.0.

In general, T_{aw} will not equal T_o since there is a velocity gradient in the fluid layers near the walls as the fluid is brought to rest which indicates also the presence of a temperature gradient. The temperature gradient in the fluid causes heat to flow from the layers near the wall to those further removed which are at a lower temperature. The velocity gradient, however, causes a transfer of work energy towards the wall in overcoming the viscous forces present in the boundary layer. The ratio of heat flow away from the wall to the work energy directed toward the wall determines whether T_{aw} will be greater or less than T_o .

Since the flow of heat away from the wall is controlled by the thermal diffusivity $\alpha = k/\rho C_p$ and the flow of work energy toward the wall is

controlled by the momentum diffusivity, or kinematic viscosity, $\nu = \frac{\mu}{\rho}$, it might be expected that the net effect is controlled by the ratio of α to ν which is $k/\mu C_p$, the Prandtl number.

Pohlhausen²⁴ in a study of adiabatic wall temperature of an incompressible fluid flowing over a non-conducting flat plate with a laminar boundary layer predicted that the recovery factor was a complex function of only the Prandtl number.

Emmons and Brainerd¹⁸ using a differential analyzer to solve the differential equations of compressible and incompressible flow over a flat plate with a laminar boundary layer found that the recovery factor was a function of the Prandtl number with some dependence upon the Mach number. For Prandtl numbers greater than 0.5 and Mach numbers less than 2.7, they predicted that the relationship, $R' = (Pr)^{\frac{1}{2}}$ would be valid to within two percent.

Eckert and Weise¹⁹ and Ackerman²⁰ predict that the recovery factor is of the order of $(Pr)^{\frac{1}{3}}$ for a turbulent boundary layer.

Recovery factors for subsonic flow of air in brass tubes were measured by Nicolai²¹ who reported values of 0.80 to 0.905 for Mach numbers ranging from 0.1 to 1.0. Czapek and Marcuse in similar measurements reported values of 0.85 to 0.96.

Eber²² measured surface temperatures on various types of probes placed in a supersonic stream and found that for Mach numbers between 1.5 and 3.0, the recovery factors varied from 0.85 to 0.96 with increasing Mach numbers.

Ketchum,¹⁰ who compiled the recovery factor data obtained by Junge and Margolskee² and Connors and Helfrich¹ in previous theses on this Project using apparatus similar to that used in this thesis, found that the recovery factor for air flowing in a lucite tube at Mach numbers from 1.0 to 2.6 is a function of the Mach number only, provided the flow is turbulent and indicated that the flow became turbulent at inlet diameter Reynolds numbers of 1.1×10^5 . Ketchum's values of recovery factor, 0.88 at $M = 2.53$, 0.84 at $M = 1.78$ and 0.80 at $M = 1.41$ were about 3% lower than the recovery factors obtained by Eber. At inlet diameter Reynolds numbers less than 1.1×10^5 , Ketchum found recovery factors that were somewhat erratic but which gave a mean line that for the higher Mach numbers agreed with the recovery factors obtained at the higher Reynolds numbers, but which at the intermediate Mach numbers gave recovery factors two to four percent higher than those obtained at the higher Reynolds numbers. At the low Mach numbers the two curves remained parallel.

Friction Factors

The determination of friction factors in this thesis was undertaken to furnish data for the design of any future recovery factor or heat transfer apparatus and to supplement existing data on friction factors for air at supersonic velocities in a tube.

The apparent friction factor or coefficient is an approximation of the true friction coefficient. The latter is defined in terms of the shear

stress at the duct wall and is extremely difficult to measure. Previous studies indicate the desirability of using the apparent friction factor as a convenient form of evaluating results. It is defined in terms of the stream pressures, stagnation state and flow per unit area and may be evaluated from one-dimensional compressible flow functions for adiabatic flow at constant area from the Gas Tables.⁷ See Appendix B.

Experimental results and literature on the subject of apparent friction factors in tubes is very limited. Frossel's²³ data for supersonic flow indicated agreement at fully developed flow with the von Karman-Nikuradse relation between friction factor and Reynolds number for incompressible flow. Keenan and Neumann¹⁷ also obtain results that show that the friction factor approaches that of incompressible flow at distances in excess of 50 diameters from pipe inlet. In addition, they show that during the development of the boundary layer for a fixed value of L/D greater than 30, the mean apparent friction factor decreases as the Reynolds number increases.

Ketchum, in his analysis of the friction factor data obtained by Helfrich and Connors, found that the apparent friction factors obtained in supersonic flow in textolite and lucite tubes were in good agreement with the results obtained by Keenan and Neumann.

CHAPTER IV

Investigation Procedure

The investigation of recovery factors for air flowing adiabatically at supersonic velocities resolves itself into a determination of the values necessary to the calculation of recovery factors by the following formula:

$$R' = \frac{T_{aw} - T_m}{T_{us} - T_m} = \frac{(T_{aw}/T_{us}) - (T_m/T_{us})}{1 - (T_m/T_{us})}$$

In order to determine these values the work reported in this thesis was started under a plan, the basic features of which were:

1. The use of dry air at various stagnation temperatures and over a wide range of stagnation pressures;
2. The use of a converging-diverging nozzle to obtain supersonic velocities with a maximum Mach number of about 2.6;
3. The passage of the air at supersonic speeds through a cylindrical tube with L_{max}/D of about 41 and with facilities for measurement of wall temperatures and static pressures at regular intervals along its length; and
4. The reduction to a minimum of heat transfer to the supersonic stream by providing thermal insulation in the forms of low conductivity plastic materials and of an evacuated chamber surrounding the lucite cylindrical tube.

In view of the results obtained by previous investigators whose work apparently led to the conclusion that the recovery factor is a function of the

stagnation temperature, it was considered desirable to conduct experimental runs at the following temperature levels: 32°, 65°, 110°, and 130°F. In addition, in order to cover a reasonably wide range of Reynolds numbers, it was decided to vary the upstream stagnation pressure from about 8 psia to 80 psia, the upper limit having been imposed by the inability of a downstream ejector to handle greater flow rates. In all runs critical flow through the nozzle was maintained by the use of a steam-driven air ejector which maintained very low pressures in the section of the apparatus downstream of the nozzle.

In order to reduce the effect of condensation shock on the static pressure the specific humidity of the air entering the test apparatus was maintained at about 1.5×10^{-5} . It has been estimated that the presence of this amount of water vapor would cause a condensation shock which would affect the static pressures in the negligible amount of about 1 part in 100,000.¹⁶

A pressure tap was located in each of the eleven bosses spaced at two-inch intervals along the test section, and since the pressure gradient across the boundary layer can be considered negligible, the pressure recorded was essentially the mean stream static value. As described in Appendix B these pressure readings (P_w) were used to evaluate the Mach Number of the flow at each station, from which the T_m/T_{us} values could be determined.

Of the three thermocouples located in each boss one was used to measure the temperature at a point 0.089 inches radially outward from the tube wall and the other two were used to measure the temperature differential between two points displaced 0.45 inches radially. From the differential value the radial temperature gradient (degrees per inch) was determined and the wall temperature was computed by extrapolation. In the absence of any heat transfer to the test section, the wall temperature thus measured would very closely approximate the adiabatic wall temperature at that point.

Since it was suspected that the previously obtained conclusion regarding the variation of recovery factor with the upstream stagnation temperature was caused by the fact that the tests were not actually adiabatic, it was deemed imperative that the heat transfer be rendered negligible. As a result the design and recommendations set forth in reference 4 were used in an effort to obtain the predicted temperature differential across the bosses of 0.001°F .

Recovery factor runs were made at the following stagnation temperatures: 32° , 65° , and 110°F ; but preliminary calculations indicated that the results would be similar to those obtained by Helfrich and Connors, namely, that the recovery factor varied with stagnation temperature. It was, therefore, found necessary to disregard the twenty-one runs made at 32° and 65° and to devote further effort to the reduction of heat transfer. The fourteen runs made at 110° were retained and their results submitted for

the reasons indicated in Chapter VI.

Subsequent investigation indicated that the heat transfer to the test section could be substantially reduced by effecting the modifications to the apparatus as described in Appendix K. Preliminary calculations of recovery factors obtained with the modified apparatus indicate that the values for a stagnation temperature of 110°F will not be appreciably affected but that those at other temperatures will be modified in such a direction as to show that the recovery factor is independent of the stagnation temperature. A more complete discussion of these preliminary results can be found in Chapter VI; however, the final results will not be available until reported by the investigators who are continuing the work of this project.

CHAPTER V

Description of Apparatus

The apparatus used in this thesis is largely that originally designed by Klingensmith³ and Wyant¹⁵ and assembled by Junge and Margolskee² except for the recovery factor test section which was designed mainly by Shoulberg⁴ and assembled by the authors with some changes. The major improvements of the present apparatus over that used by Junge and Margolskee and Connors and Helfrich¹ for determining recovery factors are:

- (1) Use of lucite test section similar to that used by Connors and Helfrich but surrounded by a vacuum chamber to thermally insulate the test section and to reduce the time required to reach thermal equilibrium.
- (2) Use of differential thermocouples to measure temperature gradients in the station bosses of the test section in order to more accurately determine adiabatic wall temperatures.
- (3) Improved method of construction and installation of the test section thermocouples.
- (4) Use of a shorter nozzle to reduce the boundary layer effect upon determination of recovery factors.
- (5) An improved method of joining the nozzle to the test section to reduce misalignments to a minimum.
- (6) Alterations to the pressure measuring system to provide a method of measuring absolute pressures at wall of test section by means of DC703 Silicone oil manometers.

- (7) Installation of a standard orifice and alterations to the downstream piping to provide sufficient straight lengths of uninterrupted piping for the orifice.
- (8) Installation of a source of dry air from the Low Temperature Laboratory.
- (9) Installation of a copper coil with a larger I.D. and a larger coil radius in the constant temperature bath to reduce the pressure drop in the coil.
- (10) Installation of several pressure gages and valves throughout the system to reduce the pressure losses and to aid in the control of the air and the testing of the system for leakage.
- (11) Installation of piping to permit calibration of nozzle and orifice by means of gasometer flow. (Piping is uncoupled at the apparatus when not in use and does not appear in any of the illustrations of this chapter.)

A brief description of the components of the system appears in the following paragraphs with the exception of the orifice installation which is described in Appendix J. A recent modification to the test section, made after the data for this thesis was obtained, is described in Appendix K. Drawings and pictures of the apparatus, as it appeared prior to Run F-36 and prior to the modification just mentioned, follow the description.

Air Supply:

Air is available from four sources;

<u>Source</u>	<u>Maximum Pressure</u> (psi)	<u>Approximate Capacity</u> (CFM)
Ingersoll-Rand, steam driven, 2 stage	180	124.0
Chicago , " " 1 "	100	69.6
Joy , motor " 2 "	200	250.0
Low Temperature Laboratory	150	---

The last source is obtained from the excess dry air of the air liquefying process in the Low Temperature Laboratory which uses the Joy air compressor for its air supply. Only air from the Ingersoll-Rand compressor or dry air from the Low Temperature Laboratory was used in the runs of this thesis.

Air dehumidification:

Refer to Figure 1. Air from the Ingersoll-Rand compressor is passed through a coil immersed in an ice-water bath and a filter composed of glass wool and copper sponges to remove dirt and to condense oil and water vapor. The filter is equipped with a drain to vent the condensate to the atmosphere. The air then passes through a trap cooled by the ice-water bath and passes upward through a three-tube counter flow, regenerative cooler whose temperature approaches -60°F and in which the remaining water vapor is condensed out of the air in a solid phase. Leaving the top of the regenerator, the air enters a coil immersed in a dry ice-alcohol bath which cools the air several degrees, then passes through a filter of glass wool and copper sponges where any solid phase is removed and returns downward through the regenerator. A thermocouple (T_c) measures the temperature entering

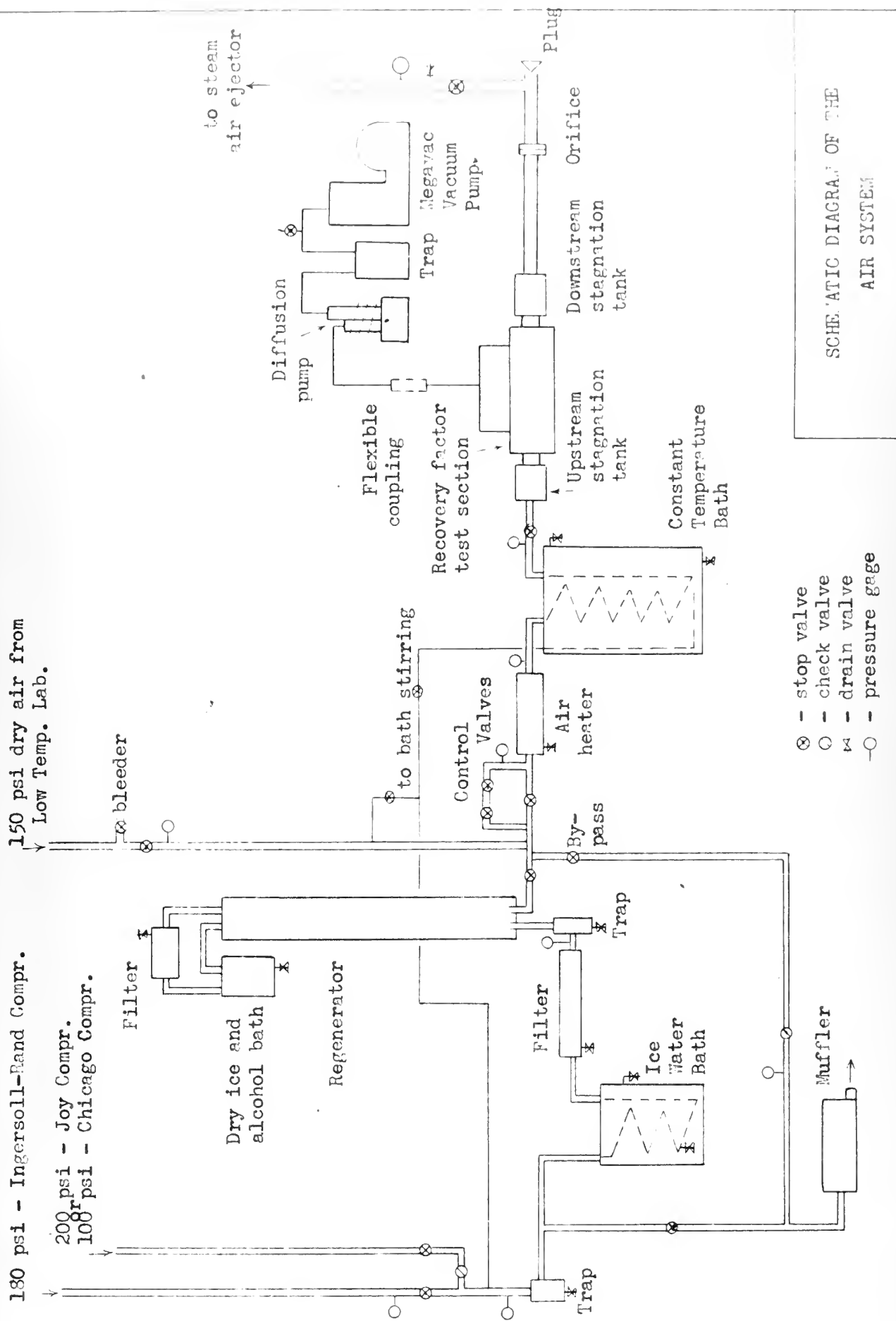


Figure V -1

the filter; and to prevent moisture condensation shocks, air from the dehumidifier is not admitted to the test section when T_c is higher than -40°F . During its downward path, the air removes heat from the upward flowing air and emerges from the regenerator as warm dry air. The dehumidification process is by-passed when air from the Low Temperature Laboratory is used since it has already been dehumidified in the air-liquefying process.

Air Flow and Temperature Control:

Air from the regenerator or from the Low Temperature Lab now passes through the control valves which consist of a needle and a stop valve in parallel with a larger globe stop valve. Fine control of the air flow is obtained by opening the large valve to the approximate upstream pressure desired and then using the needle valve to maintain the exact pressure. A by-pass valve is also provided just before the control valves to vent excess air to the atmosphere through a muffler. A shell-and-tube type Ross air heater, through which a mixture of steam and water is circulated, is used to heat the air to within approximately 5°F of the temperature of the constant temperature bath through which the air proceeds next. This is a large water bath in which the air is heated to approximately the desired upstream stagnation temperature as it passes through a copper coil (40' uncoiled length) immersed in the water. The water is heated by means of steam to the approximate temperature desired and the temperature is then regulated by means of an electric heating coil in the bath with an automatic temperature regulator thermostatic control which operates to

maintain the desired temperature within 0.2°F . Air is bubbled through the bath to stir the water and make the temperature uniform. After leaving the bath the air enters the upstream stagnation tank (3" diameter) in which the air is slowed to a uniform low velocity by means of baffles and wire screening. In the tank are nine thermocouples distributed in a plane perpendicular to the flow and equipped with radiation shields to prevent radiation to the tank walls. The thermocouples are used to measure the stagnation temperature (T_{us}) and the temperature distribution of the air in the stagnation tank. A pressure tap provides a means of measuring P_{us} .

Recovery Factor Apparatus:

The air from the upstream stagnation tank enters the recovery factor apparatus through a convergent textolite reducer (Figure 3) which has an exit diameter of 1.25". The reducer, upstream end plate and the nozzle are bolted together firmly with Allen head steel bolts. A stainless steel cylindrical ring (Figure 6) with a force fit in the upstream end plate connects the reducer to the nozzle. The ring is machined so that there is a near perfect transition with no discontinuities to interrupt the flow from the reducer to the nozzle.

The convergent-divergent nozzle (Figure 4) is made of stainless steel, with an entrance diameter of 1.25", a throat diameter of 0.2685", and an exit diameter of 0.5015" and was designed for a Mach number of 2.6 and uniform parallel flow at the exit. A flange is provided at each end of the nozzle for securing it to the upstream end plate and reducer and for fastening the nozzle to the test section. The walls of the nozzle are as

thin as possible but still provide the necessary strength. Two thermocouple holes are provided to measure temperature distribution along the wall but the thermocouples were not installed.

The nozzle, collar and lucite test section are bolted together firmly. The collar is provided to insure nearly perfect alignment of the nozzle exit and the test section entrance areas. Special machining and hand fitting was required in manufacturing the lucite collar to make the junction between the nozzle and test section as smooth as possible. The recovery factor apparatus was designed to be dismantled without the necessity of unfastening the nozzle and collar from the test section. Means of re-aligning the three parts is provided, however, should such an eventuality arise.

The lucite test section (Figure 5) is similar to that used by Connors and Helfrich in regard to diameter (0.5015"), length (21.020"), and location of eleven test stations at 2" intervals along the tube. Lucite was used since it is a resin with a low thermal conductivity and reduces the effects of longitudinal heat transfer in the test section to a minimum. At each station, 1.88"-diameter bosses are provided to afford a means of anchoring the pressure tubing compression fittings to the lucite. In between the bosses the tube thickness is reduced to 1/8" to further restrict longitudinal heat transfer along the tube. In order to minimize the effects of turbulence on pressure measurement at further downstream taps the pressure taps are arranged around the tube so that only the first and eleventh pressure tap holes are in alignment. Three thermocouple holes

are provided at each station. One thermocouple is used to determine the wall temperature while the other two, located at different radial distances from the tube wall, indicate the temperature gradient in the boss. The interior of the lucite tube was made as straight and smooth as possible and was given a high polish during manufacture. At the downstream end the test section was bolted to the downstream end plate which is also made of lucite.

Surrounding the test section and bolted to the upstream and downstream end plates is a thick-walled outer tube (Figure 7) made of textolite for strength and low thermal conductivity. In the outer tube are two pipe connections to the vacuum system, used to evacuate the space between the outer tube and the test section, and a smaller pipe connection for the McLeod gage vacuum-measuring system.

The upstream end plate made of lucite contains compression fittings for securing the pressure tubing and a means of leading thermocouple wires out of the apparatus. (See Figure 6).

The recovery factor apparatus is sealed throughout with rubber gaskets and high vacuum grease at every joint to obtain as high a vacuum as possible. Glyptal and air-drying varnish are used externally to seal all joints and fittings.

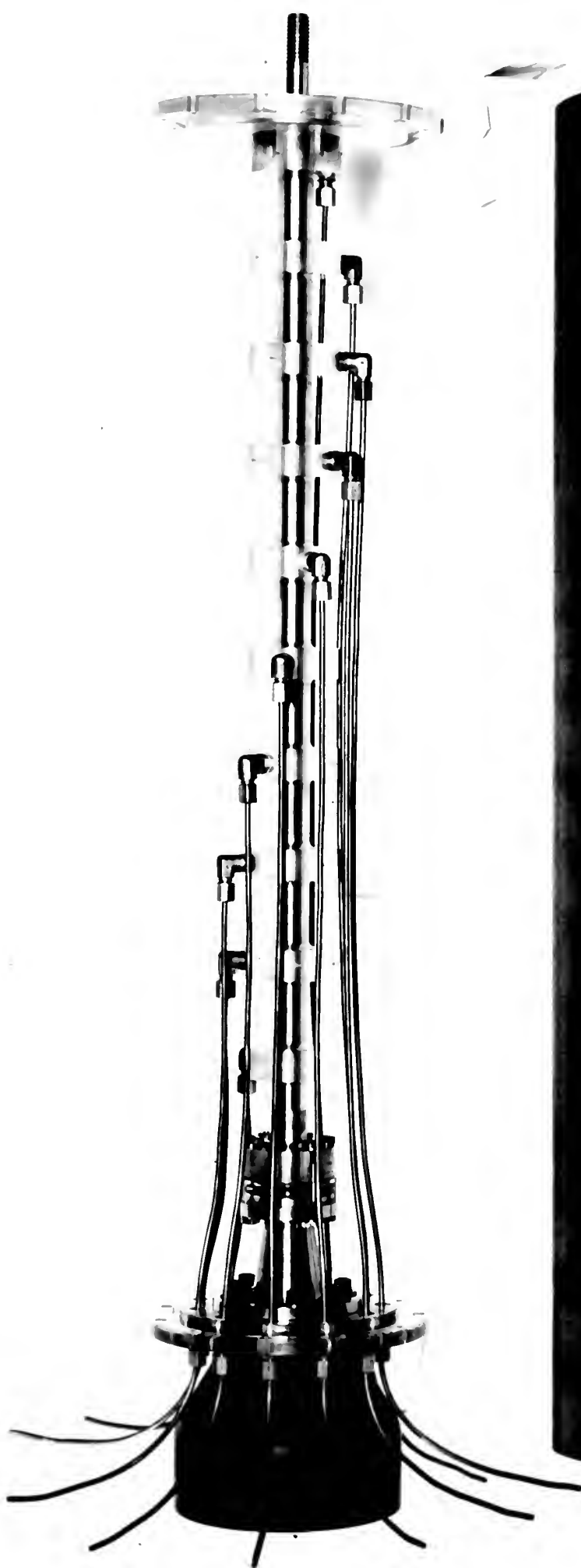
Downstream air path:

The air leaves the recovery factor apparatus through a 4" I.D. sheet steel adapter fastened between the apparatus and the downstream stagnation tank. This tank like the upstream tank contains baffles and wire screens to

ASSEMBLY

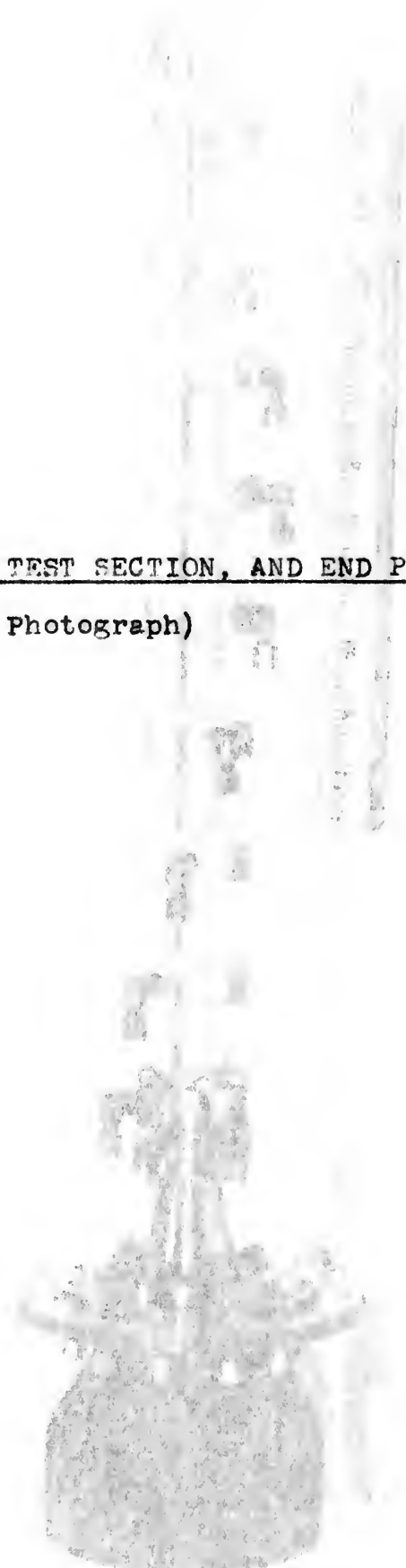
(Photograph)

ASSEMBLY
(Photograph)



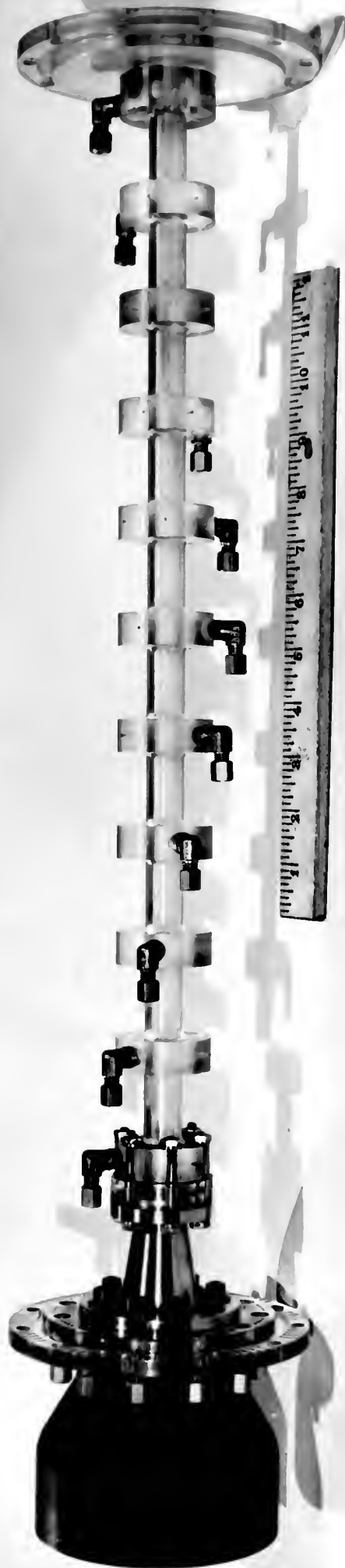
REDUCER, NOZZLE, TEST SECTION, AND END PLATES

(Photograph)



REDUCER, NOZZLE, TEST SECTION, AND END PLATES

(Photograph)



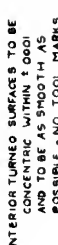
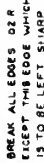


Figure V-4

REDUCER, UPSTREAM END PLATE, AND NOZZLE

(Photograph)

ELSON DVA TAIT

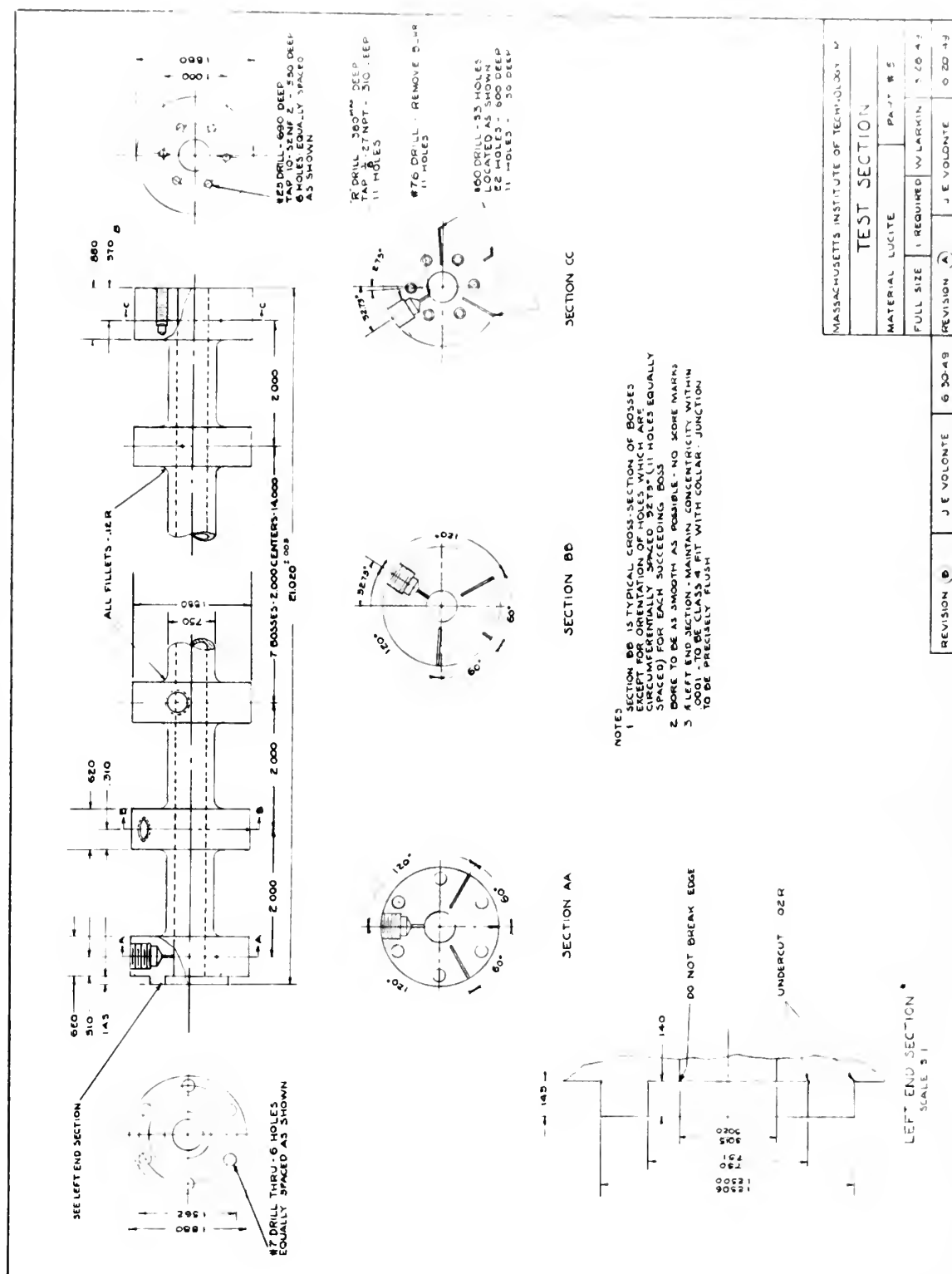
REDUCED, UPSTREAM END PLATE, AND NOZZLE

(Photograph)

ELSON DVA TAIT

(Photograph)





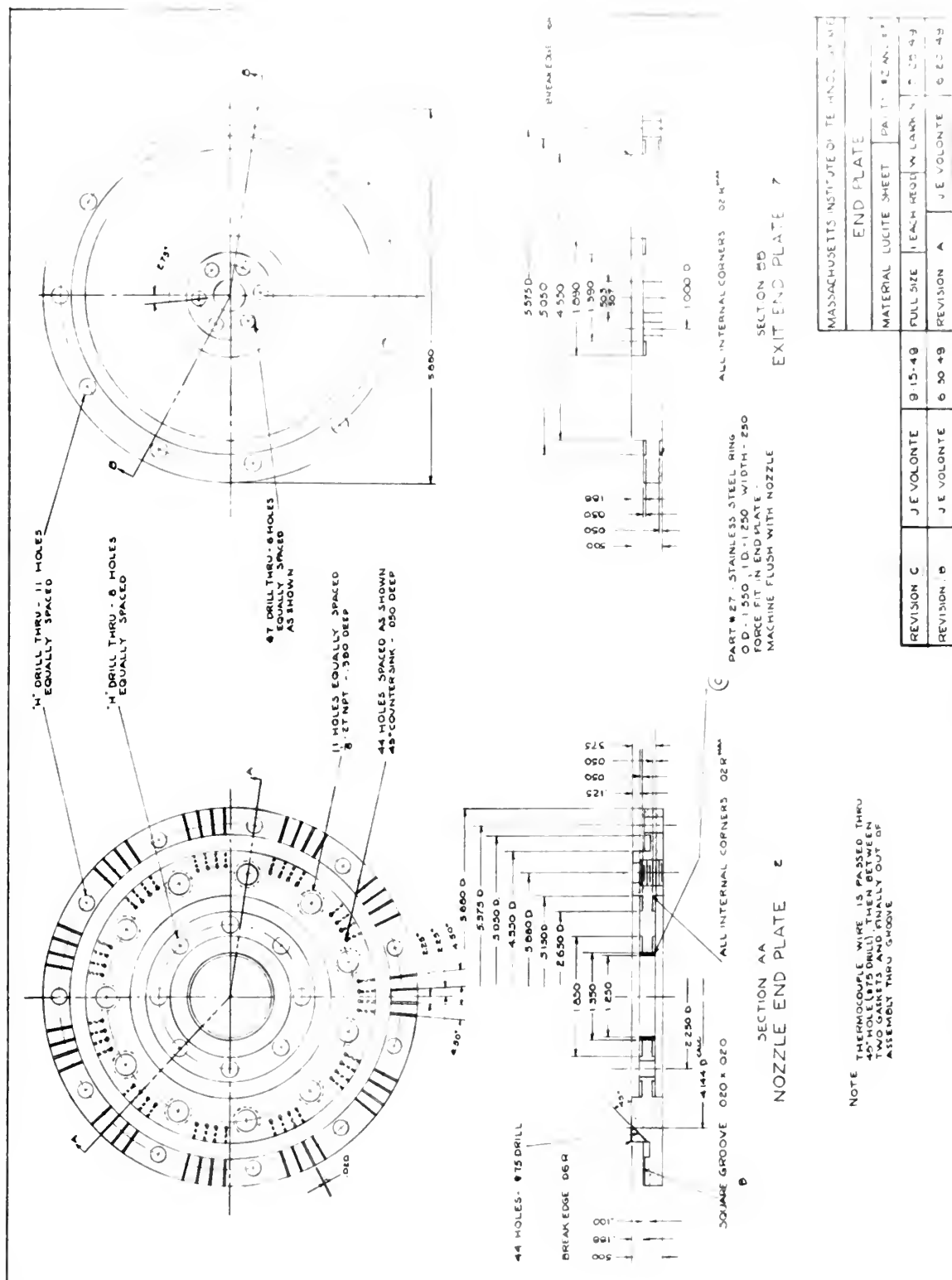
TEST SECTION

(Photograph)

TEST SECTION

(Photograph)





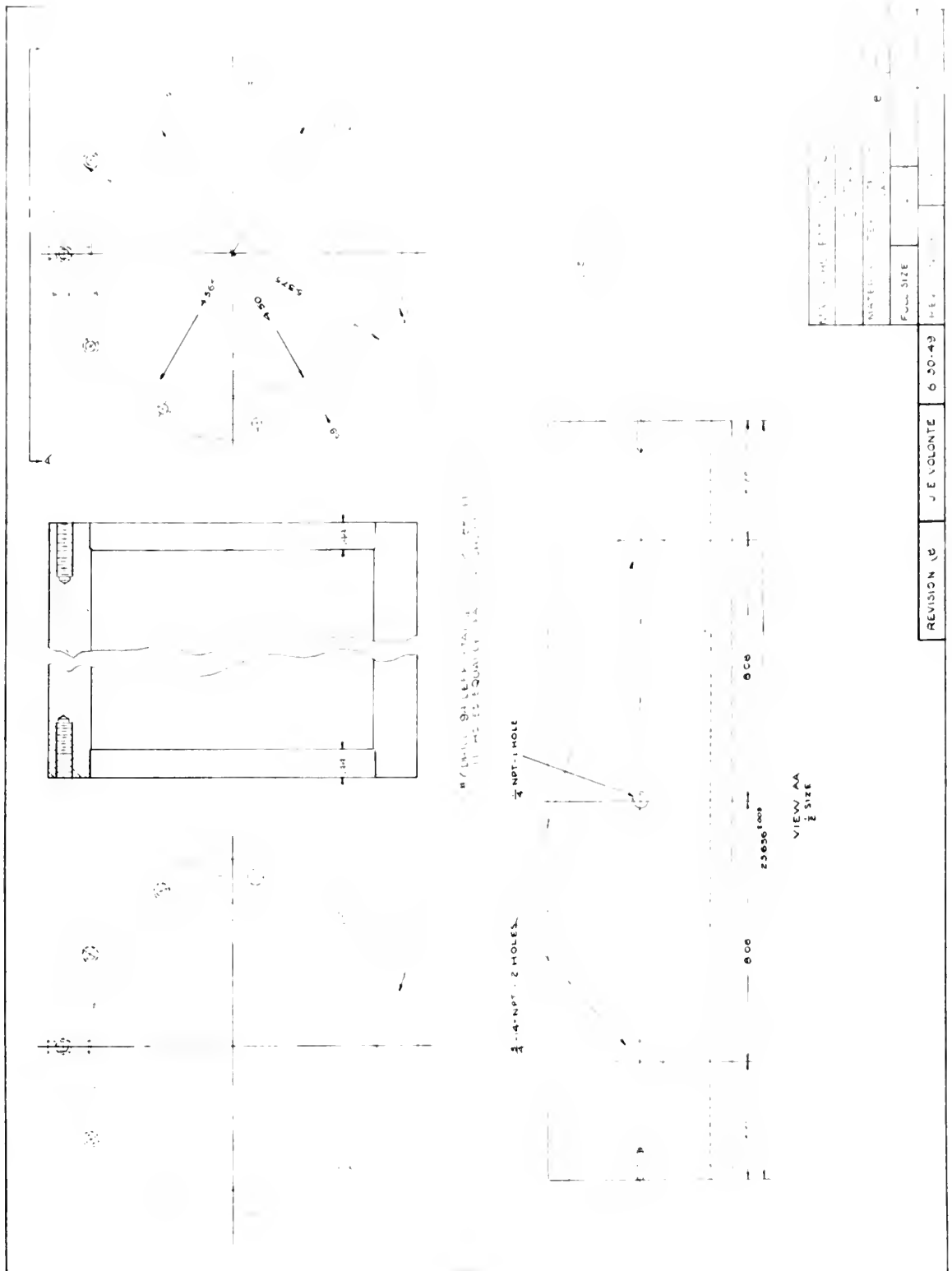


Figure V-7

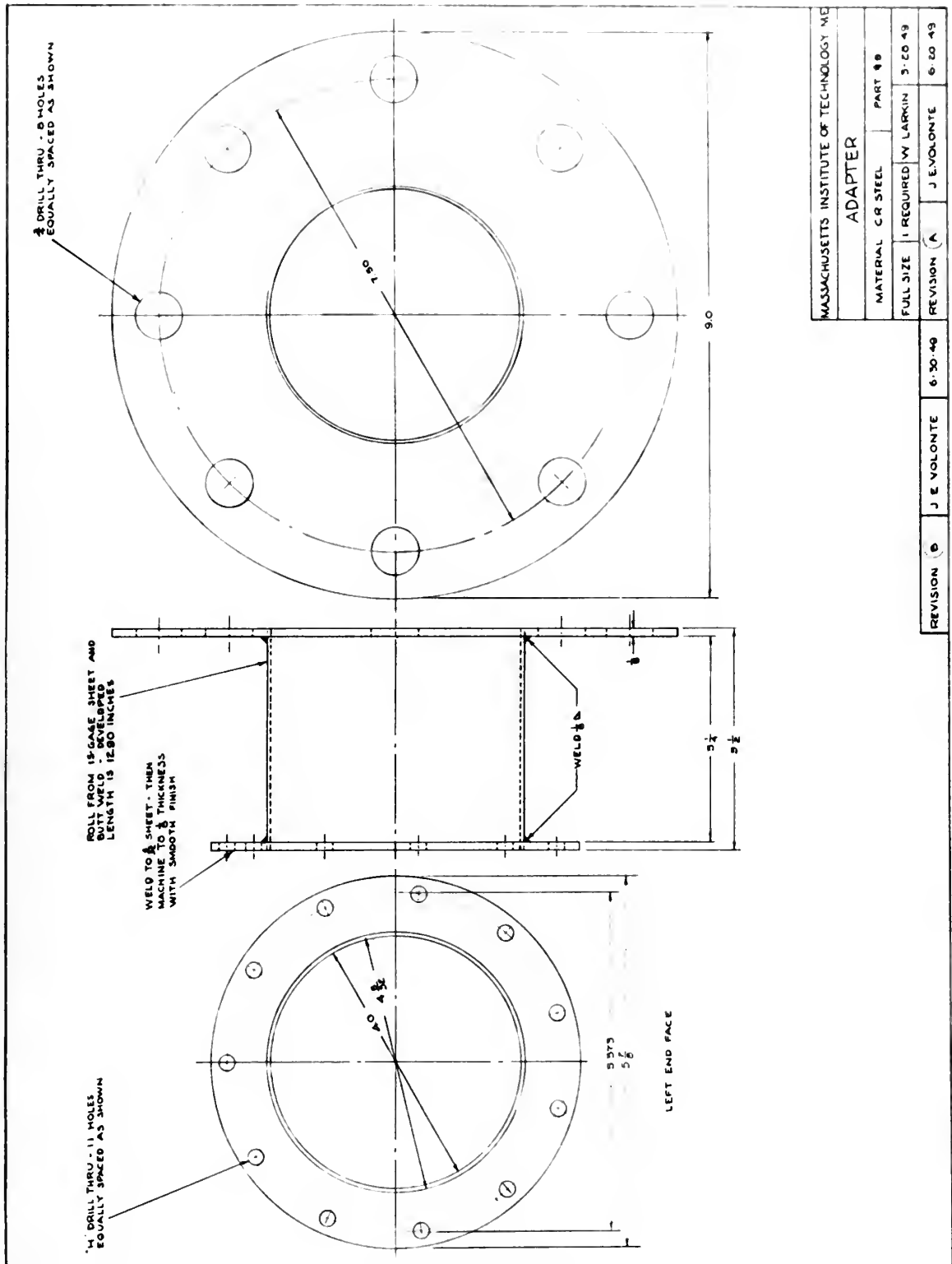


Figure V-8

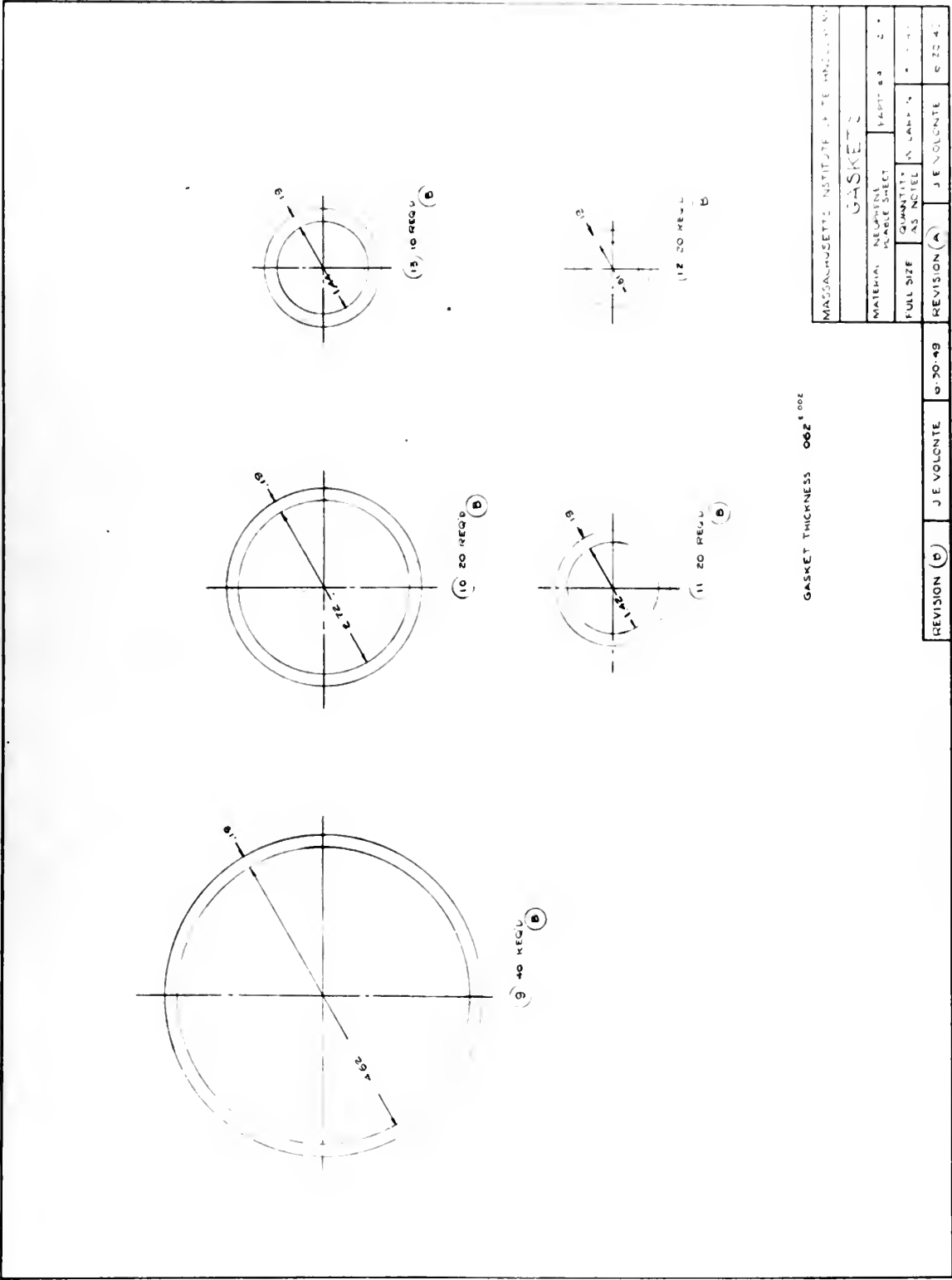


Figure V-9

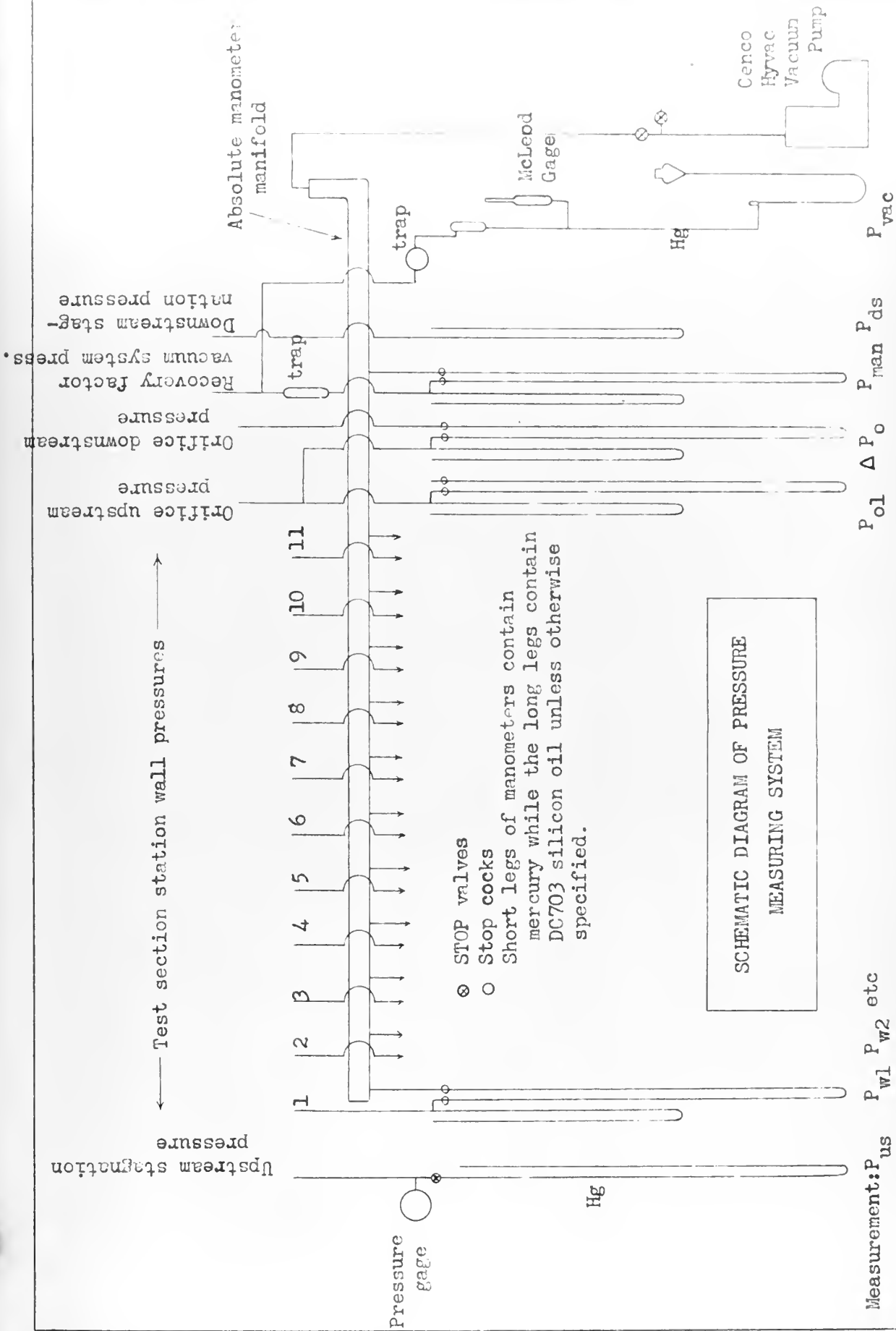
slow the air to a uniform low velocity. Nine thermocouples and a pressure tap are used to determine stagnation temperature (T_{ds}), temperature distribution, and P_{ds} . Leaving the stagnation tank, the air enters a 2 1/2" I.D. pipe leading to the orifice and from thence to the steam driven air ejector located in the Steam Laboratory. The air ejector reduces the pressure in the test section below atmospheric thus insuring supersonic flow through the greater part of the test section even at high rates of flow.

Vacuum system:

The vacuum system (Figure 1) used for evacuating the recovery factor apparatus consists of an all metal diffusion pump, a trap and a Cenco Megavac vacuum pump. The diffusion pump is a fractionating, water cooled, electrically heated vacuum pump using octoil and is capable of maintaining an ultimate vacuum of 10^{-6} mm Hg. The Megavac pump requires a 1/2 hp motor and is capable of maintaining a vacuum of 0.1×10^{-3} mm Hg. A trap is provided between the two pumps to prevent accidental flow of octoil into the Megavac pump. A flexible coupling is provided between the diffusion pump and the apparatus, which effectively reduces the vibrations transmitted from the Megavac pump to the apparatus. All piping joints are soft soldered and sealed with glyptal and air-drying varnish with the exception of two unions which are sealed with high vacuum grease and glyptal. The best vacuum obtained was 1.81×10^{-3} mm Hg.

Pressure-measuring system:

This system provides mercury and silicone oil (Dow-Corning 703) manometers as shown in Figure 10. Provided the pressure in the absolute



manometer manifold is less than 0.1 mm Hg, absolute pressures may be read directly from the silicone manometers which have one leg connected to the absolute manometer manifold which is evacuated by means of a Cenco Hyvac Pump capable of maintaining 3×10^{-4} mm Hg pressure. All silicone manometers are equipped with stop cocks to prevent oil from entering the pressure lines or the absolute manometer manifold. One manometer containing silicone oil is provided to compare the pressure in the absolute manometer manifold with that in the recovery factor apparatus. A McLeod gage calibrated by Junge and Margolskee is used to determine the pressure in the recovery factor apparatus. A Bourdon pressure gage is provided for measuring P_{us} greater than 43 psia. Silicone oil is used because of its low vapor pressure, low air solubility, and a specific gravity (1.09) near that of water. It also does not dissolve the grease used to keep the stop cocks air tight.

Temperature-measuring system:

The upstream and downstream stagnation tank thermocouples are those installed and calibrated by Junge and Margolskee. The thermocouples installed in the test section consist of eleven used to measure station wall temperatures and calibrated as in Appendix H and twenty-two used to measure the temperature gradient across each station boss. The thermocouples were made of #30 constantan and copper wire twisted together for a length of $1/8$ " and soft soldered. The junction was carefully placed in the drilled hole of the station boss and the hole filled with high vacuum grease using a hypodermic needle. The 44 wires were led

out of the apparatus through 45° holes in the upstream end plate and thence between the end plate and the textolite outer tube. An effective seal was obtained by means of high vacuum grease, rubber gaskets, and externally applied glyptal and air-drying varnish. The cold junctions of the station wall thermocouples were placed in an ice water mixture contained in thermos bottles along with the cold junctions of the stagnation tank thermocouples. The temperature reading was obtained by means of a sensitive galvanometer and potentiometer in conjunction with a calibrated standard cell and a 6 volt storage battery. A switchboard was provided for selection of the desired thermocouple reading.

CHAPTER VI

Discussion of Results

General

The results presented here were obtained from fourteen experimental runs, F-1 to F-9 and F-17 to F-21, using the apparatus described in Chapter V. Each run was made with the upstream stagnation temperature and pressure held constant while measurements were made at eleven stations along the test section to obtain data necessary to the determination of recovery factors, friction factors, Mach numbers, and Reynolds numbers. All runs were conducted at an upstream stagnation temperature of about 110°F and at upstream pressures varying from 8 to 80 psia, the range of inlet diameter Reynolds numbers being 0.47×10^5 to 4.8×10^5 .

Runs F-17 to F-21 were carried out as duplicating runs to insure that the results obtained in Runs F-1 to F-9 could be repeated. In general, there was excellent agreement between the data obtained from runs which duplicated each other.

The results of the experimental work are presented in tabular form at the end of this chapter and are shown graphically in Figures VI-1 to VI-10. Except for Figure VI-2 only data for points upstream of a suspected shock were plotted.

Figures VI-1 and VI-2 show the distribution of wall pressures and calculated adiabatic wall temperatures along the test section for the first nine runs. From these plots can be seen the influence of shocks near the downstream end of the cylindrical tube as well as the effects of

heat transfer to the test section at its inlet and outlet ends.

In the pressure-ratio plot, Run F-9, which was made with the lowest inlet diameter Reynolds number, shows a pressure ratio which increases along the length of the tube, a situation which is impossible in the one-dimensional theory used as a basis for the work of this thesis. Since similar results were reported by Kaye, Keenan, and McAdams¹⁶ and Ketchum,¹⁰ it may be concluded that the discrepancy was caused by the limitations of the theory rather than by errors in measurement.

In the temperature-ratio plot Run F-5 shows a distribution which is inconsistent with that of other similar runs. In checking through the original data used to calculate the results of this run, it was found that this was the first of five runs carried out in one day. As a result it is believed that temperature equilibrium had not actually been attained when readings were commenced and that, consequently, all results of Run F-5 should be disregarded.

Recovery Factors

The results which are of primary importance in the determination of recovery factors are those relating the recovery factor to the Mach number; they are shown in Figure VI-3, which includes the results of runs made over the entire range of inlet diameter Reynolds numbers from 0.47×10^5 to 4.8×10^5 . Discounting the values for Run F-5, the deviation of any of the points from a mean line passed through them is less than one percent of the recovery factor.

In attempting to correlate the results presented here with those of previous investigators, a comparison with the data obtained by Ketchum was made. His data led to the apparent conclusion that the recovery factor depended on the inlet diameter Reynolds number as well as the Mach number; as a result he divided his results into two regimes, the line of demarcation being an inlet diameter Reynolds number of 1.05×10^5 . Ketchum concluded that only in the region of higher inlet Reynolds could the recovery factor be regarded as a function of Mach number only. The results presented here do not indicate the necessity for such a division since the recovery factors determined seem to be independent of the Reynolds number. In addition, there is considerably less scatter in the region of low flow rates.

At low values of Mach number the results indicated in Figure VI-3 are in excellent agreement with those obtained by Ketchum in the regime of high rates of flow, but at the higher Mach numbers there is a significant deviation with Ketchum's recovery factors being somewhat lower. The net result of this difference is that the mean of the values presented here is more nearly linear.

In Figure VI-4 recovery factors are plotted against diameter Reynolds number for each run. The plot is interesting in that the lines connecting successive stations for each run are roughly parallel at a slope of 0.47. This suggests a strong dependence of recovery factor on viscosity and, consequently, on the Prandtl number; however, it has been impossible to correlate the results indicated in Figure VI-3 with

simple formulas involving fractional exponents of the Prandtl number.

The plot of recovery factor vs. length Reynolds number (Figure VI-5) shows two flow regimes which can best be characterized by the inlet diameter Reynolds number. If the results of Run F-9 are disregarded on the basis that the one-dimensional theory is inadequate for the conditions of the run, then one regime could be identified with flow for which the inlet Reynolds number is between 0.83×10^5 and 1.8×10^5 and for which the recovery factor could be expressed as a function of length Reynolds number. In the other regime for inlet Reynolds number greater than 1.8×10^5 the recovery factor seems to be independent of the length Reynolds number and to be more dependent on the L/D ratio.

Friction Factors

Although local apparent friction factors were calculated along with the mean apparent values, the preliminary plots of the former showed no consistency and as a result, only the latter values have been plotted and will be considered in this discussion. The local apparent values, however, are included in the tables of results.

The most significant results obtained are those indicated in Figure VI-6, which is a plot of friction factor as a function of length Reynolds number. The plot is quite analogous to the corresponding relationship between friction factor and diameter Reynolds number for incompressible flow. It clearly defines three flow regimes which appear to be essentially laminar, transitional, and turbulent. In this figure the region of transition lies roughly in the range of Reynolds numbers from

15×10^5 to 30×10^5 ; this compares reasonably well with Ketchum's data which indicated that the limits of this regime were 7×10^5 to 25×10^5 .

The friction factor reaches a minimum of about 0.0013 as it reaches the transition region and after transition decreases steadily with increasing Reynolds number from a maximum value of about 0.0035.

In the plot of friction factor vs. L/D ratio (Figure VI-7) the results shown are in good agreement with the results of Keenan and Neumann¹⁷ and Ketchum except for the values at the second station (L/D of about 5). In this report the friction factors for runs conducted at the higher inlet Reynolds numbers increase in going from station 2 to station 3 whereas in the other reports the friction factor decreases. Since the friction factor is dependent only on the Mach number, or the pressure ratio, it is not immediately evident why the difference exists.

Figure VI-8, which is plotted to a linear scale, again shows the presence of three flow regimes with a transition occurring at a diameter Reynolds number of about 10^5 . After transition the friction factor appears to level off at a value of about 0.003 or decrease slightly from that value as the diameter Reynolds number increases. In addition, in the region beyond transition, the friction factor seems to be reasonably independent of the L/D ratio.

Effect of Vacuum System

Although no data was observed for the exclusive purpose of determining the effect of the evacuated chamber on heat transfer, it is interesting to consider the apparent results obtained. Runs F-2 and F-18

were conducted at upstream stagnation pressures which differed by less than two percent and at upstream stagnation temperatures which differed by less than 0.1 percent, but F-2 had a P_{vac} of 0.0035 mm Hg and F-18 of 0.0091 mm Hg. In this case the recovery factors of F-18 were roughly one-half percent higher than those of F-2. Unfortunately no other set of duplicating runs was made under such conditions as to afford a comparison as good as the above since in most cases the temperatures and pressures differed by greater amounts while the values of P_{vac} showed a smaller variation.

Preliminary Results with Modified Apparatus

After the recovery factor apparatus was modified to reduce heat transfer to the test section (See Appendix K), runs were continued in an effort to investigate the effect of stagnation temperature on recovery factor. The initial runs were made at stagnation temperatures of about 110°F to check the validity of the results reported here. In Figure VI-10 the results of two of these runs are compared with data obtained from the original apparatus for approximately the same diameter Reynolds number at inlet. It can be seen that the recovery factor for the more recent runs is lower by about one percent at the higher Mach numbers and that at lower Mach numbers the difference is roughly one-half percent.

The data obtained with the modified apparatus, consequently, more closely approximates that obtained by Ketchum despite the fact that his apparatus was more susceptible to heat transfer than that used for this report. However, since the differences are of such a low order and since

the adiabatic wall temperature for stagnation temperatures of 110°F should be sufficiently close to room temperature to render heat transfer effect negligible, it is felt that the results presented here are sufficiently valid for the purposes for which they will be used.

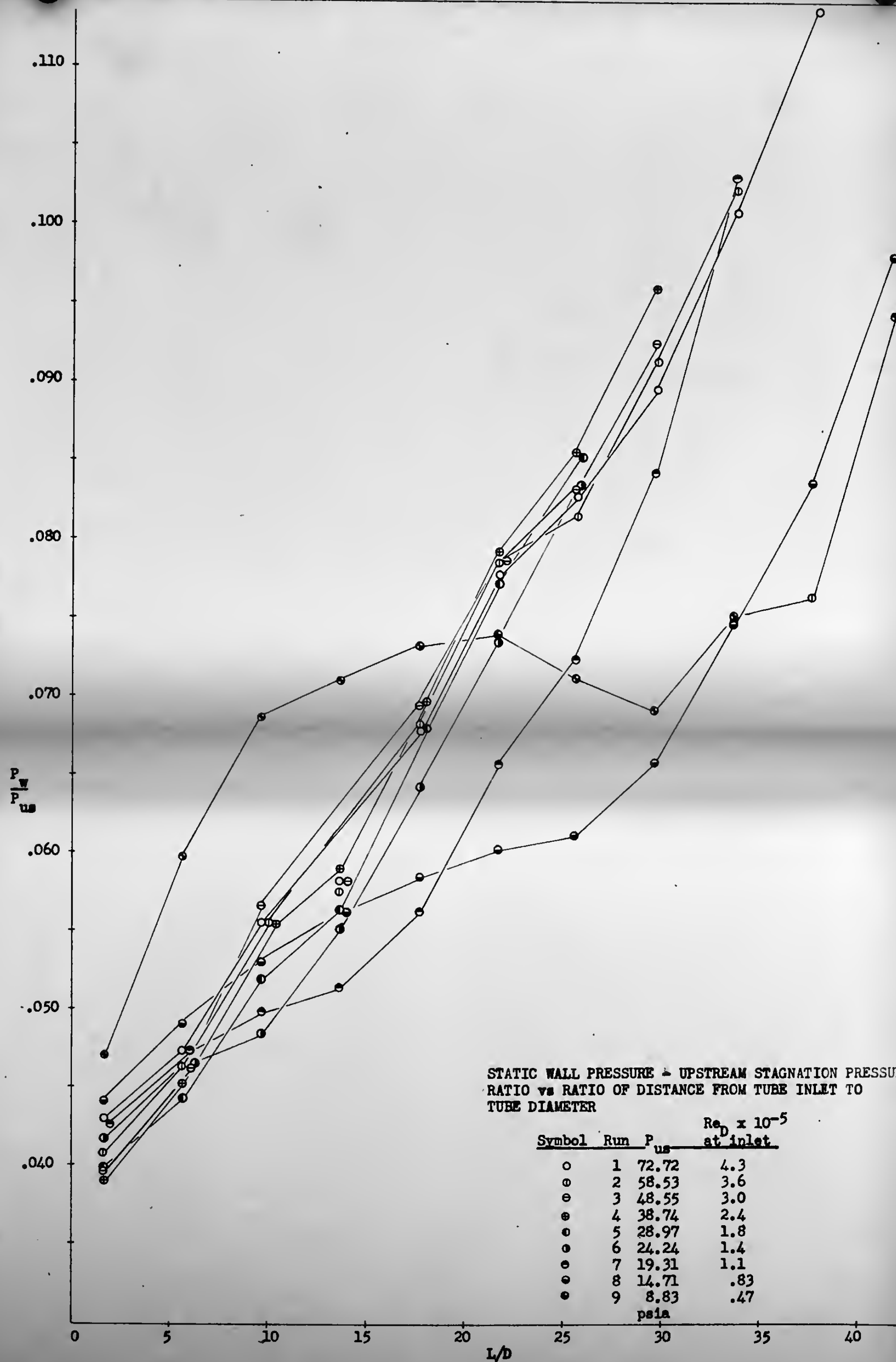


Figure VI-1

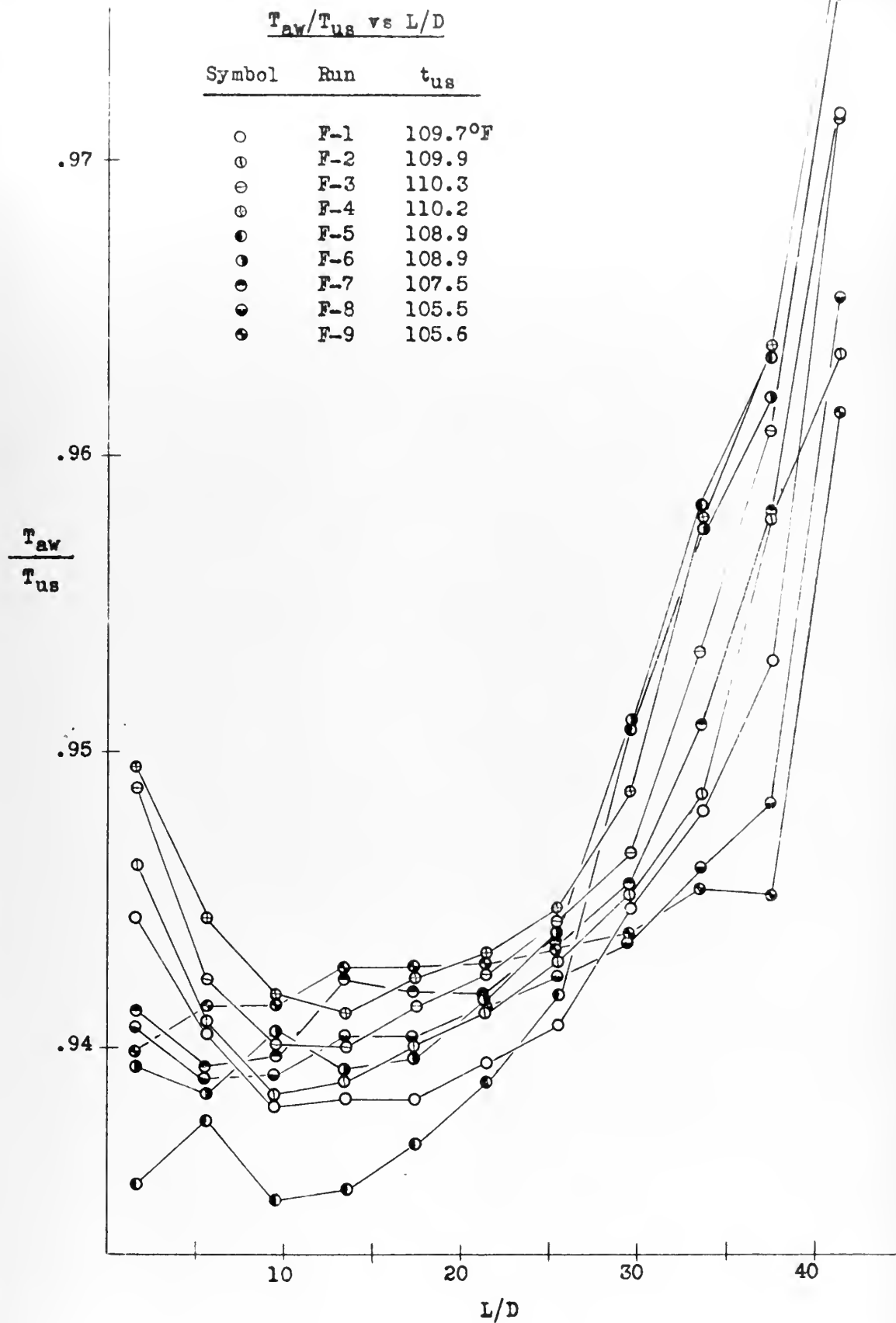


Figure VI-2

Symbol	Run	T_{us}	P_{us}	$Re \times 10^{-5}$ at inlet
F-17		106.74	79.72	4.8
F-1		109.68	72.72	4.3
F-2		109.92	58.53	3.6
F-18		110.23	59.69	3.4
F-3		110.34	48.55	3.0
F-4		110.19	38.74	2.4
F-19		111.61	38.69	2.4
F-5		108.89	28.97	1.8
F-6		108.86	24.24	1.4
F-20		111.31	24.23	1.4
F-7		107.47	19.31	1.1
F-8		105.46	14.71	.83
F-21		110.64	14.66	.81
F-9		105.58	8.83	.47
		of	psia	

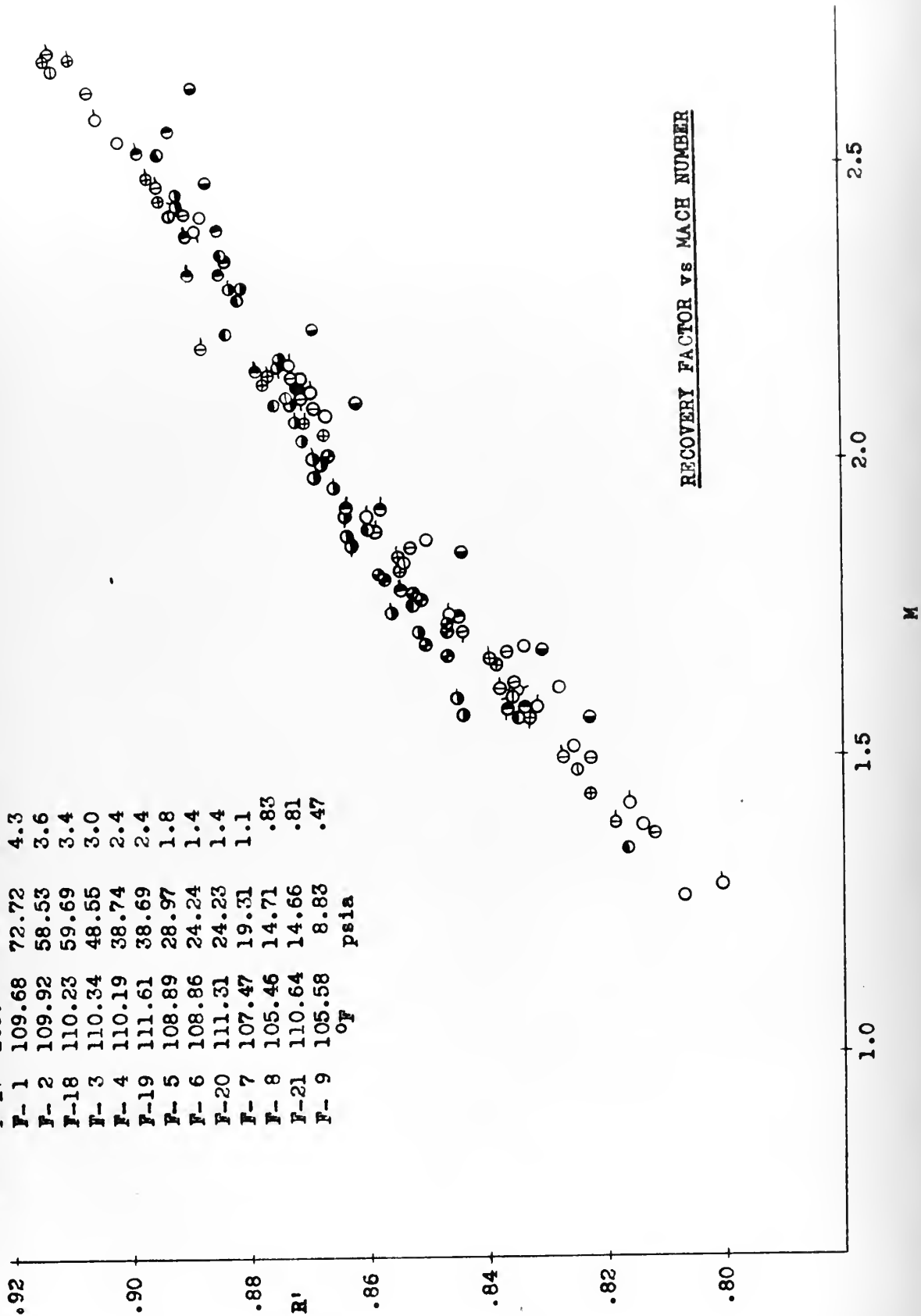
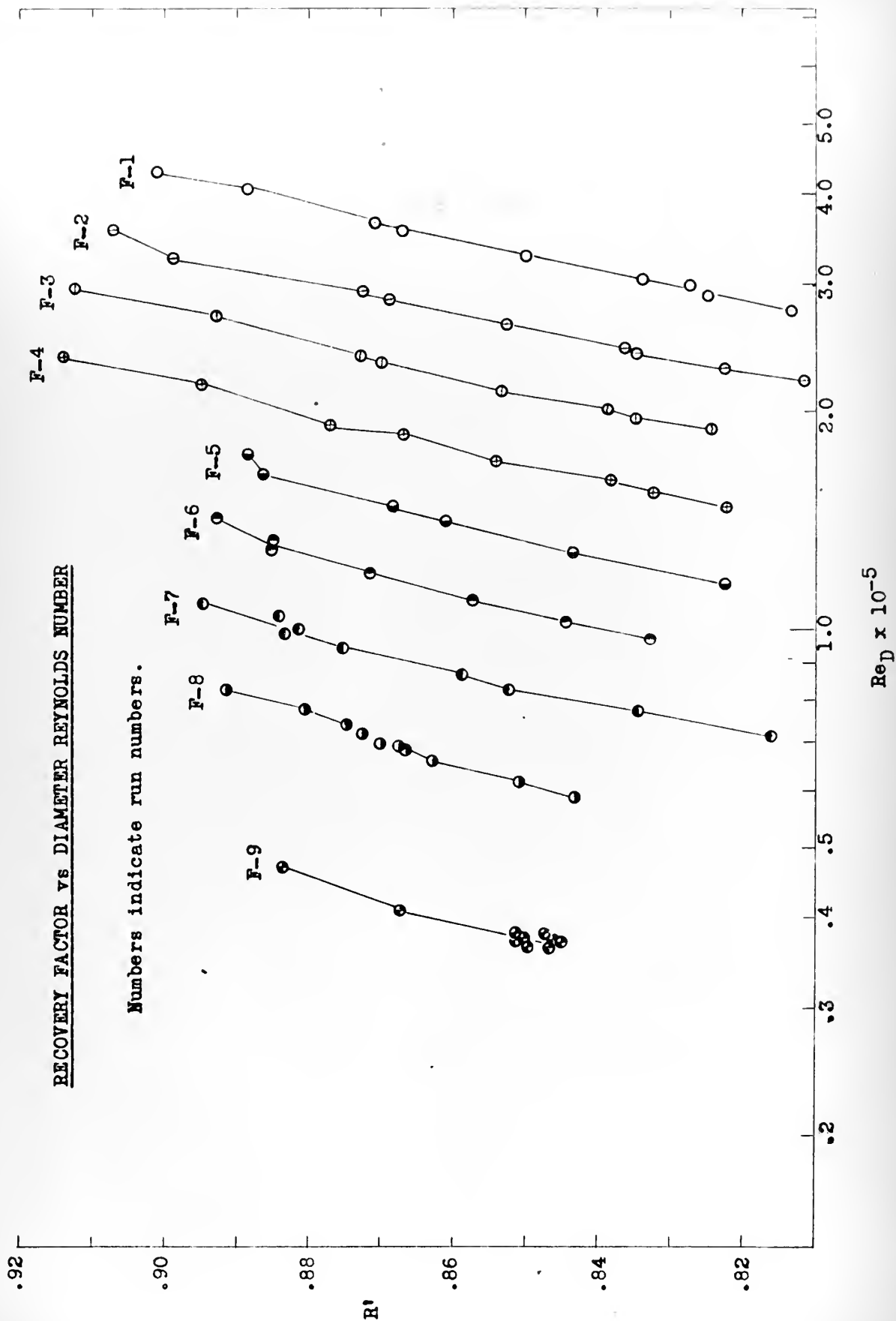


Figure VI-3

RECOVERY FACTOR vs DIAMETER REYNOLDS NUMBER

Numbers indicate run numbers.



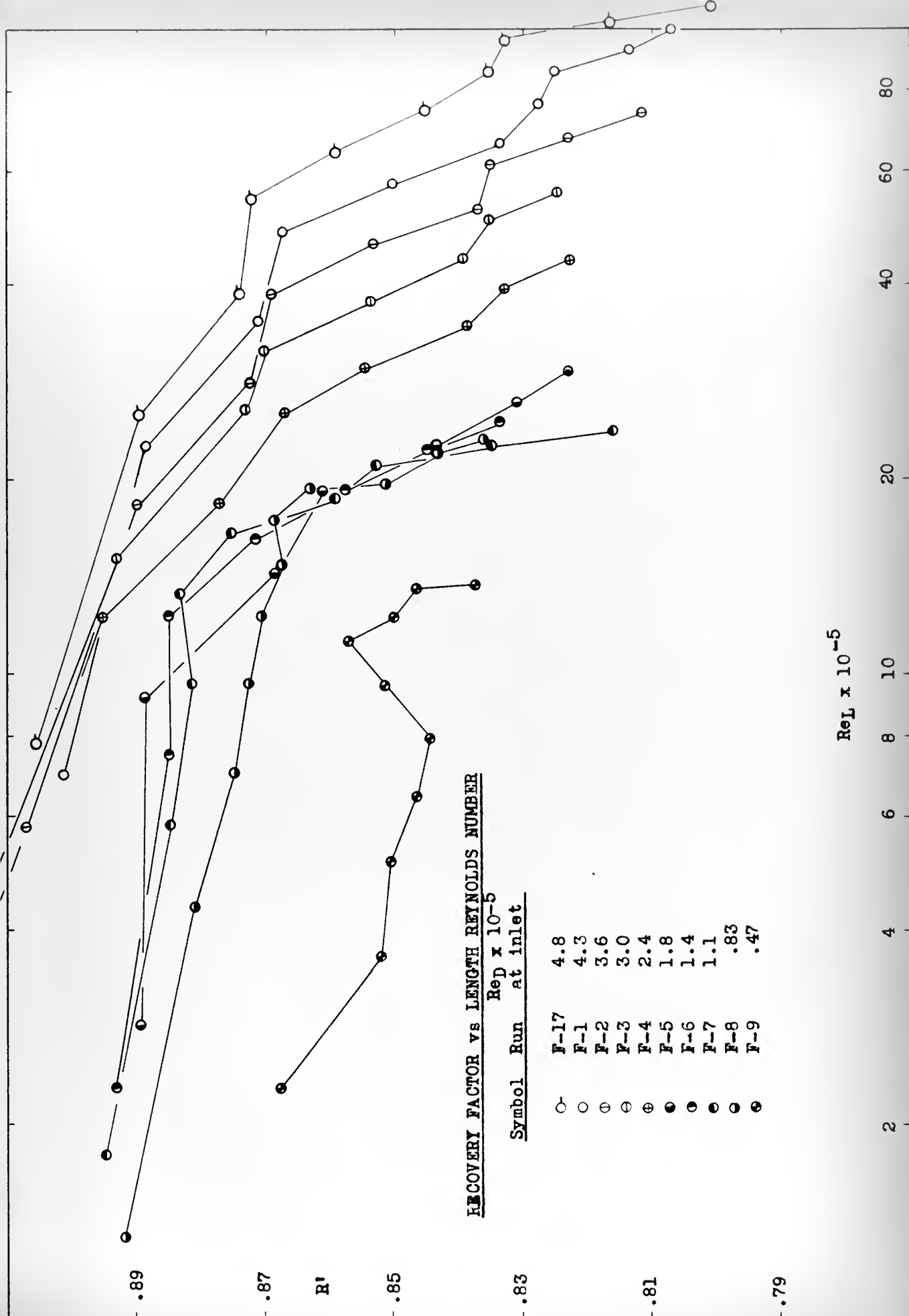


Figure VI-5

FRICTION FACTOR vs LENGTH REYNOLDS NUMBER

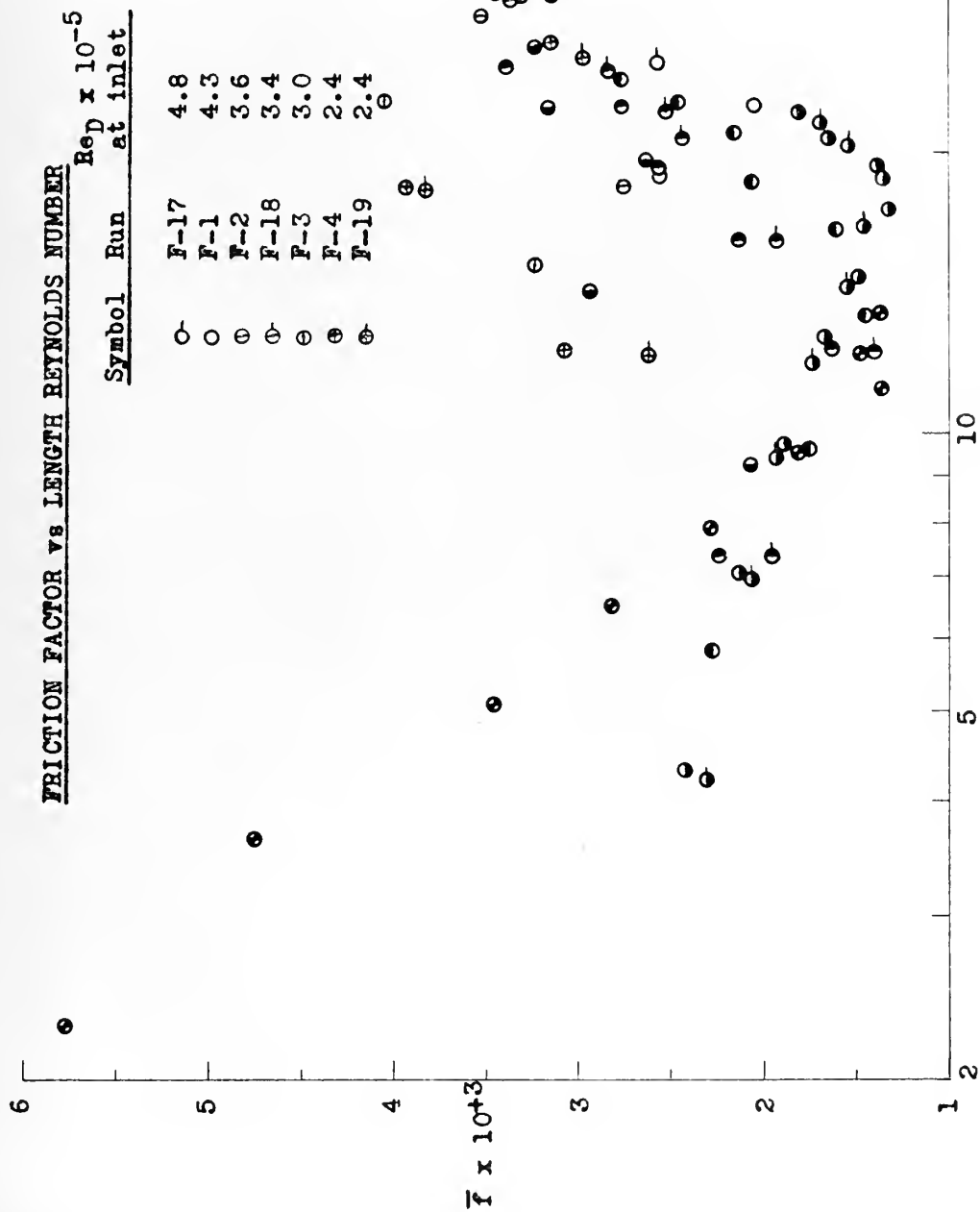


Figure VI-6

MEAN APPARENT FRICTION FACTOR vs L/D

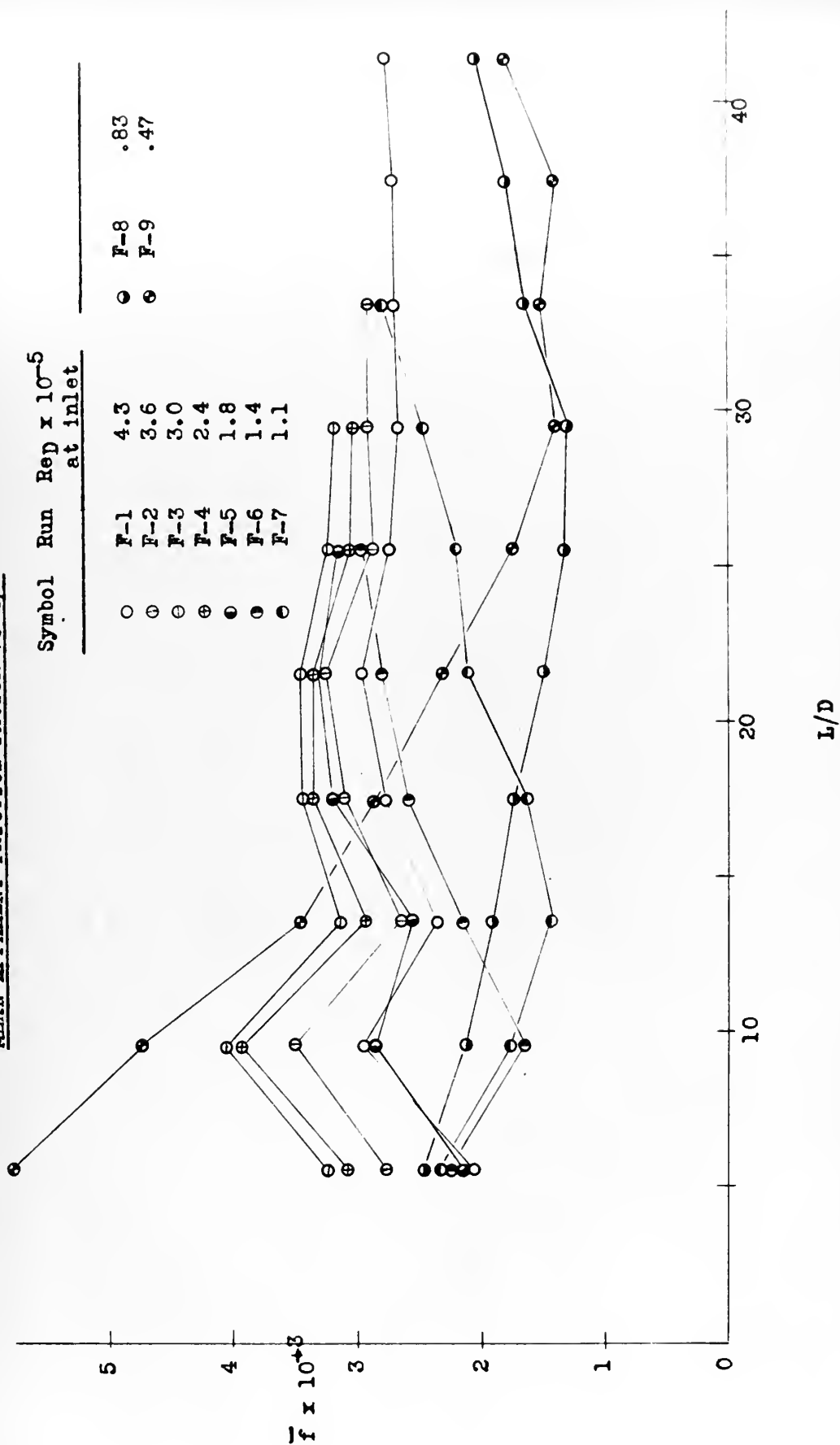
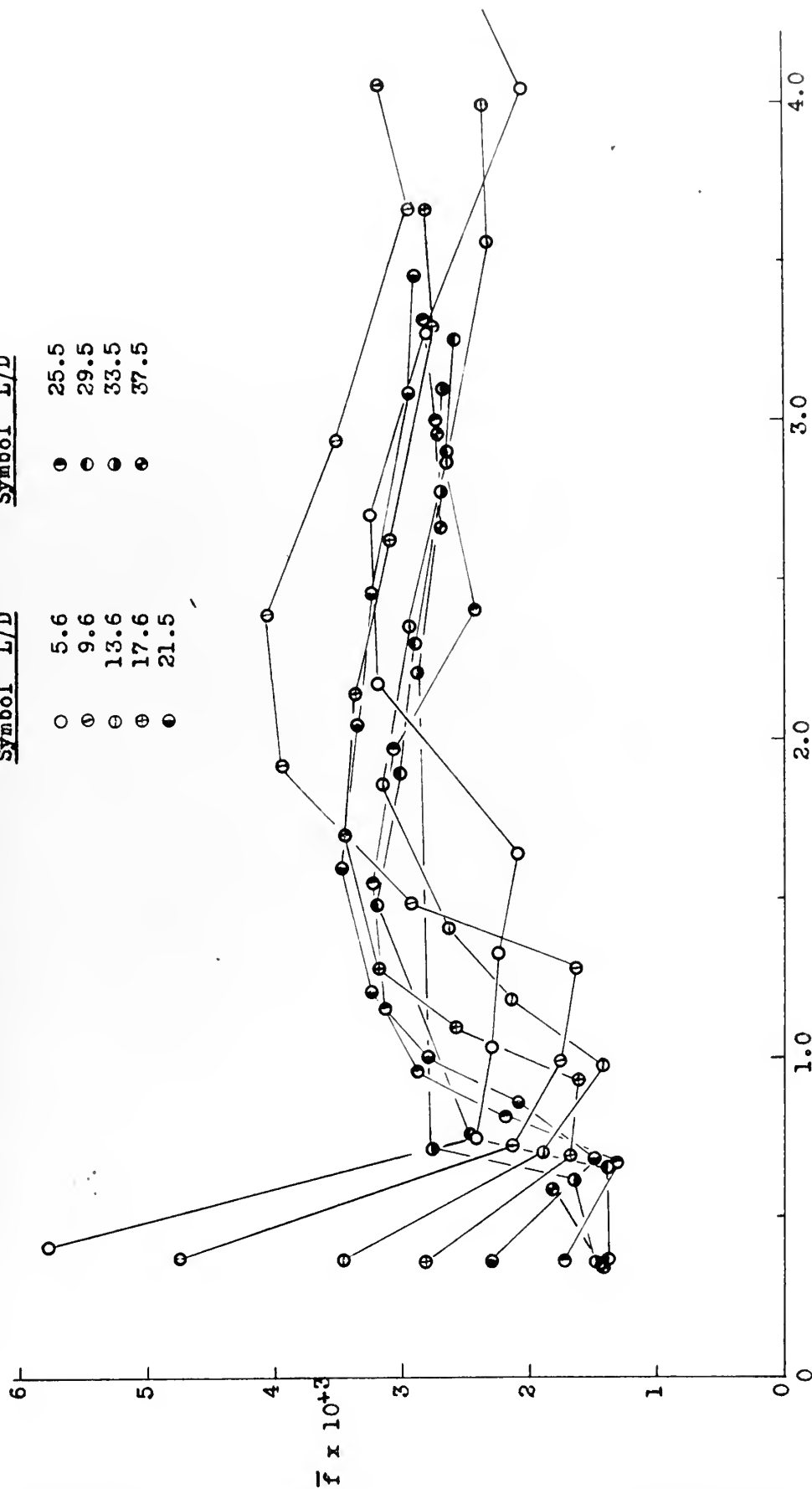


Figure VI-7

MEAN APPARENT FRICTION FACTOR vs DIAMETER REYNOLDS NUMBER

Symbol	L/D	Symbol	L/D
○	5.6	●	25.5
○	9.6	●	29.5
⊖	13.6	●	33.5
⊕	17.6	●	37.5
●	21.5		



$Re_D \times 10^{-5}$

Figure VI-8

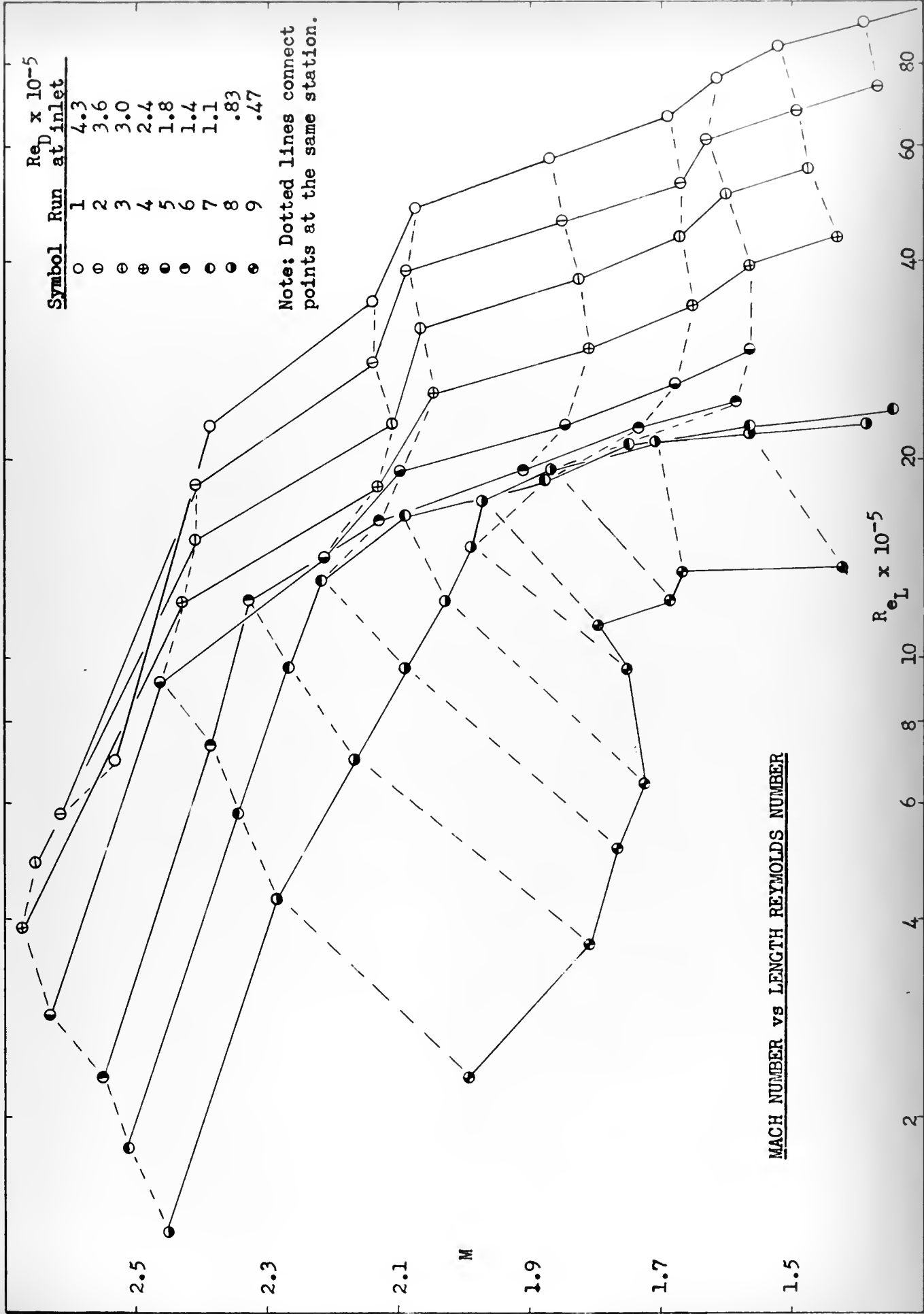


Figure VI-9

RECOVERY FACTOR vs MACH NUMBER

COMPARISON PLOT

Runs F-6 and F-20 were made with original apparatus; F-36 and F-43 with modified apparatus.

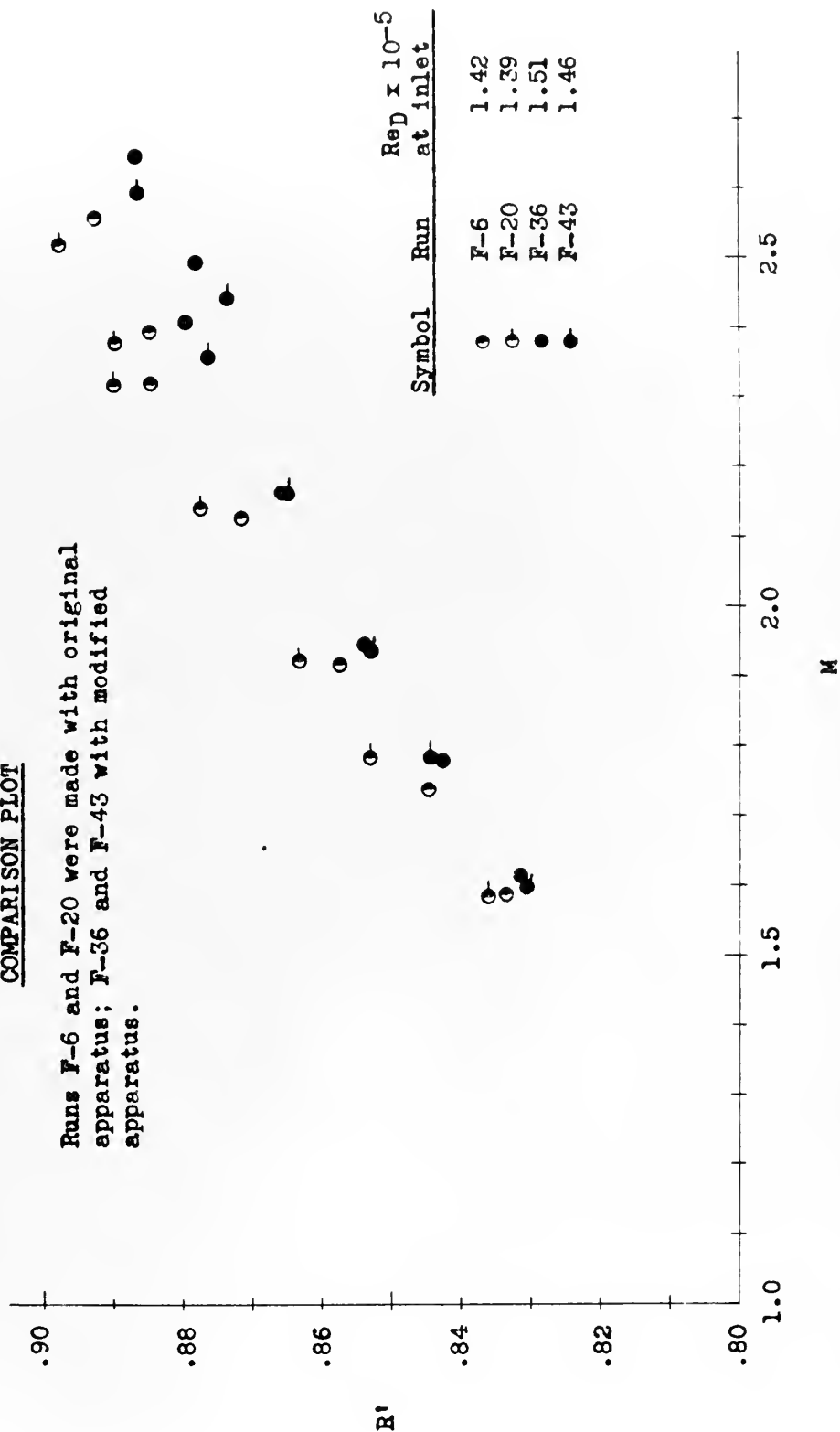


Figure VI-10

PLATE 10

Run F-1

 P_{us} - 72.72 psia T_{us} - 569.47 °Fabs P_{vac} - 0.0067 mm Hg(All Reynolds numbers are $\times 10^{-5}$)
(All friction factors are $\times 10^3$)

STN	P_w/P_{us}	M	T_{aw}/T_{us}	R'	f	f	Re_D	\bar{Re}_D	Re_L	\bar{Re}_L	Re_x
1	.04307	2.533	.9444	.9012	-	-	4.286	-	6.919	-	17.732
2	.04731	2.384	.9405	.8883	2.053	2.053	4.038	4.162	22.615	14.767	32.803
3	.05505	2.140	.9381	.8707	3.847	2.950	3.658	3.848	35.057	28.836	44.294
4	.05816	2.077	.9383	.8669	1.098	2.333	3.568	3.613	48.415	41.736	57.416
5	.06783	1.866	.9383	.8499	4.007	2.751	3.289	3.429	57.740	53.077	66.036
6	.07789	1.689	.9395	.8337	3.734	2.948	3.079	3.184	66.328	62.034	74.096
7	.08279	1.615	.9408	.8274	1.645	2.731	2.997	3.038	70.507	71.418	84.069
8	.08967	1.520	.9447	.8251	2.157	2.649	2.899	2.948	85.549	81.028	92.862
9	.10092	1.388	.9480	.8133	3.005	2.693	2.770	2.835	92.806	89.178	99.795
10	.11363	1.263	.9531	.8064	2.681	2.692	2.663	2.717	99.804	96.305	106.52
11	.14951	1.006	.9717	.8319	3.301	2.753	2.472	2.567	102.52	101.16	108.76

Run F-2

 P_{us} - 58.53 psia T_{us} - 569.61 °Fabs P_{vac} - 0.0035 mm Hg

1	.04075	2.619	.9462	.9069	-	-	3.559	-	5.745	-	14.724
2	.04634	2.411	.9408	.8899	2.757	2.757	3.273	3.416	18.328	12.037	26.786
3	.05555	2.138	.9380	.8722	4.269	3.513	2.931	3.102	28.095	23.212	35.490
4	.05752	2.087	.9389	.8687	.886	2.637	2.872	2.902	38.976	33.536	46.222
5	.06838	1.851	.9401	.8526	4.489	3.100	2.622	2.747	46.034	42.505	52.649
6	.07857	1.674	.9412	.8364	3.760	3.232	2.455	2.539	52.886	49.460	59.080
7	.08153	1.629	.9429	.8353	1.000	2.860	2.414	2.435	61.625	57.256	67.715
8	.09140	1.495	.9452	.8225	3.043	2.886	2.304	2.359	68.000	64.812	73.813
9	.10226	1.370	.9486	.8116	2.835	2.880	2.208	2.256	73.946	70.983	79.517
10	.15488	.973	.9579	.7356	5.526	3.174	1.966	2.087	73.696	73.831	78.656
11	.1784	.957	.9635	.8292	-.093	2.847	1.958	1.962	81.200	77.448	86.140

$P_{us} = 48.55$ psia
 $T_{us} = 570.03$ °F abs
 $P_{vac} = 0.0030$ mm Hg

(All Reynolds numbers are $\times 10^{-5}$)
(All friction factors are $\times 10^3$)

STN	P_w/P_{us}	M	T_{aw}/T_{us}	R'	f	\bar{f}	ReD	\bar{Re}_D	ReL	\bar{Re}_L	Re $_{\infty}$
1	.03973	2.656	.9488	.9125	-	-	2.986	-	4.819	-	12.351
2	.04628	2.409	.9423	.8927	3.236	3.336	2.701	2.844	15.126	9.973	21.941
3	.05679	2.102	.9405	.8731	4.862	4.049	2.387	2.544	22.880	19.003	28.902
4	.05837	2.063	.9402	.8700	.691	2.930	2.350	2.369	31.897	27.389	37.828
5	.06968	1.823	.9414	.8533	4.635	3.356	2.143	2.247	37.623	34.760	43.029
6	.07880	1.667	.9425	.8390	3.341	3.353	2.023	2.083	43.588	40.605	48.693
7	.08336	1.599	.9443	.8354	1.520	3.048	1.974	1.999	50.392	46.990	55.373
8	.09268	1.476	.9466	.8244	2.804	3.013	1.890	1.932	55.790	53.091	60.590
9	.13709	1.077	.9534	.7525	7.599	3.586	1.669	1.780	55.917	55.853	60.128
10	.16882	.900	.9609	.7197	.524	3.129	1.595	1.632	59.972	57.945	63.817
11	.16129	.937	.9757	.8375	.573	2.874	1.609	1.602	66.740	63.350	70.800

Run F-4

$P_{us} = 38.74$ psia
 $T_{us} = 569.88$ °F abs
 $P_{vac} = 0.0060$ mm Hg

1	.03914	2.675	.9495	.9139	-	-	2.392	-	3.861	-	9.890
2	.04533	2.436	.9440	.8946	3.081	3.081	2.172	2.282	12.163	8.012	17.643
3	.05553	2.129	.9418	.8770	4.775	3.928	1.919	2.046	18.395	15.279	23.230
4	.05902	2.043	.9412	.8669	1.522	3.126	1.855	1.887	25.174	21.785	29.855
5	.06970	1.817	.9424	.8542	4.397	3.444	1.701	1.778	29.864	27.519	34.150
6	.07938	1.654	.9432	.8381	3.505	3.456	1.602	1.652	34.510	32.187	38.552
7	.08561	1.564	.9447	.8323	2.025	3.218	1.551	1.577	39.594	37.052	43.507
8	.09580	1.434	.9487	.8224	2.969	3.182	1.482	1.517	43.740	41.667	47.479
9	.16863	.898	.9580	.6944	6.073	3.544	1.268	1.375	42.477	43.109	45.670
10	.18007	.848	.9638	.7084	-1.400	2.990	1.253	1.261	49.909	46.223	50.130
11	.16540	.913	.9775	.8411	1.679	2.863	1.240	1.247	51.424	50.697	54.553

Run F-5

 P_{us} - 28.97 psia T_{us} - 568.58 °Fabs P_{vac} - 0.0026 mm Hg(All Reynolds numbers are $\times 10^{-5}$)
(All friction factors are $\times 10^3$)

STN	P_w/P_{us}	M	T_{aw}/T_{us}	R'	f	\bar{f}	ReD	\bar{Re}_D	ReL	\bar{Re}_L	Re _x
1	.04011	2.627	.9354	.8886	-	-	1.753	-	2.830	-	7.252
2	.04443	2.466	.9376	.8863	2.087	2.087	1.642	1.698	9.195	6.013	13.338
3	.05209	2.216	.9349	.8684	3.737	2.912	1.484	1.563	14.225	11.710	17.969
4	.05672	2.093	.9352	.8612	2.082	2.635	1.414	1.449	19.189	16.707	22.757
5	.06804	1.843	.9368	.8437	4.756	3.165	1.283	1.349	22.526	20.858	25.762
6	.07733	1.680	.9389	.8305	3.465	3.225	1.207	1.245	26.001	24.264	29.046
7	.08530	1.562	.9418	.8227	2.646	3.129	1.157	1.182	29.536	27.769	32.455
8	.15911	.942	.9511	.6754	9.677	4.063	.948	1.053	27.979	28.750	30.371
9	.18303	.832	.9576	.6510	-2.695	3.218	.933	.941	31.255	29.617	33.609
10	.18634	.819	.9620	.6787	-.579	2.796	.931	.932	34.899	33.677	37.247
11	.16674	.904	.9760	.8290	2.722	2.789	.947	.939	39.273	37.086	41.062

Run F-6

 P_{us} - 24.24 psia T_{us} - 568.55 °Fabs P_{vac} - 0.0035 mm Hg

1	.04187	2.552	.9394	.8928	-	-	1.419	-	2.291	-	5.871
2	.04641	2.388	.9385	.8846	2.242	2.242	1.328	1.374	7.437	4.864	10.787
3	.04859	2.317	.9403	.8847	1.053	1.647	1.291	1.310	12.375	9.906	15.632
4	.05527	2.125	.9390	.8715	3.110	2.135	1.194	1.243	16.204	14.290	19.216
5	.06439	1.913	.9398	.8575	3.912	2.579	1.099	1.147	19.295	17.750	22.068
6	.07359	1.739	.9414	.8445	3.584	2.780	1.030	1.065	22.188	20.742	24.787
7	.08345	1.585	.9442	.8332	3.408	2.885	.974	1.002	24.864	23.526	27.322
8	.12750	1.134	.9512	.7616	9.416	3.818	.841	.908	24.871	24.868	26.944
9	.17279	.874	.9583	.6855	-0.474	3.281	.786	.814	26.330	25.600	28.313
10	.18071	.840	.9635	.7049	-1.120	2.792	.780	.783	29.238	27.784	31.266
11	.16520	.909	.9763	.8332	+1.907	2.704	.792	.786	32.845	31.042	34.843

Run F-7

P_{us} - 19.31 psia
 T_{us} - 567.14 °Fabs
 P_{vac} - 0.0051 mm Hg

(All Reynolds numbers are $\times 10^{-5}$)
 (All friction factors are $\times 10^3$)

STN	P_w/P_{us}	M	T_{aw}/T_{us}	R'	f	\bar{f}	ReD	\bar{ReD}	ReL	\bar{ReL}	Re_x
1	.04279	2.511	.9412	.8946	-	-	1.082	-	1.799	-	4.611
2	.04743	2.348	.9393	.8842	2.291	2.291	1.041	1.062	5.831	3.815	8.458
3	.05000	2.268	.9400	.8817	1.222	1.756	1.008	1.025	9.658	7.745	12.200
4	.05168	2.219	.9423	.8836	.782	1.431	.987	.998	13.399	11.529	15.890
5	.05641	2.091	.9419	.8756	2.166	1.615	.939	.963	16.478	14.939	18.846
6	.06578	1.880	.9417	.8591	3.973	2.087	.865	.902	18.625	17.552	20.806
7	.07251	1.753	.9439	.8525	2.629	2.177	.824	.845	21.047	19.830	23.127
8	.08448	1.566	.9455	.8346	4.139	2.457	.770	.797	22.735	21.891	24.678
9	.10312	1.350	.9509	.8161	4.898	2.763	.716	.743	23.969	23.352	25.774
10	.14930	.989	.9581	.7440	5.133	3.026	.644	.680	24.127	24.048	25.751
11	.15030	.984	.9717	.8255	-0.011	2.722	.643	.644	26.653	25.390	28.275

Run F-8

P_{us} - 14.71 psia
 T_{us} - 565.15 °Fabs
 P_{vac} - 0.0018 mm Hg

1	.04430	2.449	.9407	.8914	-	-	.826	-	1.334	-	3.418
2	.04925	2.285	.9390	.8805	2.407	2.407	.773	.800	4.331	2.833	6.282
3	.05315	2.171	.9391	.8745	1.837	2.122	.738	.756	7.078	5.705	8.941
4	.05632	2.088	.9405	.8726	1.428	1.891	.714	.726	9.695	8.387	11.497
5	.05864	2.031	.9405	.8704	1.026	1.674	.698	.706	12.263	10.979	14.024
6	.06038	1.990	.9414	.8678*	.260	1.492	.688	.693	14.812	13.538	16.547
7	.06139	1.968	.9425	.8683	.416	1.312	.682	.685	17.402	16.107	19.122
8	.06598	1.870	.9436	.8630	1.919	1.399	.657	.670	19.378	18.390	21.034
9	.07480	1.709	.9451	.8512	3.378	1.646	.618	.638	10.702	20.040	22.286
10	.08384	1.570	.9483	.8436	3.099	1.808	.588	.603	22.038	21.370	23.521
11	.09819	1.391	.9654	.8759	4.077	2.035	.553	.571	22.922	22.480	24.317

Run F-9

 $P_{us} - 8.83$ psia $T_{us} - 565.27$ °Fabs $P_{vac} - 0.0018$ mm Hg(All Reynolds numbers are $\times 10^{-5}$)
(All friction factors are $\times 10^3$)

STN	P_w	P_{us}	M	T_{aw}/T_{us}	R'	f	\bar{f}	ReD	\bar{ReD}	ReL	\bar{ReL}	ReX
1	.04732	2.333		.9394	.8838	-	-	.470	-	.758	-	1.944
2	.05988	1.990		.9414	.8674	5.784	5.784	.410	.440	2.296	1.527	3.330
3	.06883	1.804		.9415	.8518	3.688	4.736	.381	.396	3.652	2.974	4.613
4	.07109	1.763		.9426	.8505	.863	3.445	.376	.379	5.103	4.378	6.051
5	.07347	1.721		.9428	.8464	.901	2.809	.370	.373	6.496	5.800	7.429
6	.07412	1.710		.9429	.8453	.239	2.295	.369	.370	7.934	7.215	8.863
7	.07143	1.757		.9433	.8517	-1.012	1.744	.375	.312	9.573	8.754	10.519
8	.06928	1.796		.9439	.8572	-.824	1.377	.380	.378	11.215	10.394	12.174
9	.07539	1.689		.9454	.8498	2.295	1.492	.366	.373	12.261	11.738	13.184
10	.07658	1.670		.9451	.8466	.418	1.372	.363	.365	13.607	12.934	14.523
11	.09445	1.425		.9615	.8668	5.554	1.791	.333	.348	13.810	13.709	14.650

Run F-17

 $P_{us} - 79.72$ psia $T_{us} - 565.43$ °Fabs $P_{vac} - 0.0105$ mm Hg

1	.64205	2.575		.9456	.9047	-	-	4.822	-	7.783	-	19.948
2	.64736	2.385		.9412	.8895	2.579	2.579	4.467	4.645	25.016	16.400	35.286
3	.65557	2.145		.9394	.8737	3.776	3.178	4.053	4.260	38.847	31.932	49.072
4	.65726	2.101		.9399	.8719	.760	2.372	3.984	4.019	54.061	46.454	64.112
5	.65716	1.881		.9413	.8585	4.129	2.811	3.657	3.821	64.208	59.135	73.433
6	.67511	1.736		.9419	.8458	3.014	2.852	3.445	3.556	74.434	69.321	83.152
7	.68297	1.614		.9434	.8348	2.689	2.824	3.312	3.384	84.551	79.493	92.908
8	.68671	1.561		.9449	.8322	1.199	2.592	3.251	3.281	95.959	90.255	104.16
9	.69806	1.421		.9470	.8158	3.196	2.668	3.097	3.174	103.76	99.858	111.57
10	.11158	1.283		.9504	.8001	3.018	2.707	2.962	3.030	111.02	107.39	118.49
11	.15552	.973		.9654	.7829	3.654	2.802	2.710	2.836	112.37	111.70	119.21

Run F-18

P_{us} - 59.69 psiaT_{us} - 569.92 °FabsP_{vac} - 0.0091 mm Hg(All Reynolds numbers are $\times 10^{-5}$)
(All friction factors are $\times 10^3$)

STN	P _w	P _{us}	M	T _{aw} /T _{us}	R'	f	f	ReD	ReD	ReL	ReL	Re _x
1	.03980	2.658		.9488	.9125	-	-	3.686	-	5.950	-	15.250
2	.04496	2.459		.9423	.8946	2.558	2.558	3.401	3.544	19.044	12.477	27.623
3	.05382	2.184		.9403	.8777	4.167	3.362	3.042	3.222	29.162	24.103	36.837
4	.05705	2.100		.9402	.8724	1.433	2.719	2.942	2.992	39.930	34.546	47.554
5	.06704	1.878		.9416	.8588	4.172	3.082	2.699	2.821	47.392	43.661	54.201
6	.07655	1.707		.9425	.8437	3.582	3.182	2.532	2.616	54.549	50.971	60.937
7	.08219	1.619		.9442	.8379	1.949	2.977	2.453	2.493	62.628	58.588	68.818
8	.09122	1.497		.9462	.8263	2.773	2.948	2.350	2.402	69.355	65.992	75.284
9	.10057	1.388		.9493	.8180	2.478	2.889	2.264	2.307	75.852	72.604	81.565
10	.15844	.954		.9577	.7526	5.812	3.214	1.994	2.129	74.745	75.299	79.776
11	.16602	.916		.9713	.8000	-.450	2.848	1.976	1.985	81.926	78.336	86.910

Run F-19

P_{us} - 38.69 psiaT_{us} - 571.30 °FabsP_{vac} - 0.0085 mm Hg

1	.03910	2.677		.9467	.9096	-	-	2.383	-	3.846	-	9.858
2	.04432	2.471		.9428	.8961	2.620	2.620	2.192	2.288	12.276	8.061	17.806
3	.05502	2.142		.9406	.8759	5.037	3.829	1.920	2.056	18.400	15.338	23.243
4	.05800	2.067		.9400	.8699	1.310	2.989	1.863	1.892	25.288	21.844	29.990
5	.06895	1.832		.9413	.8540	4.521	3.372	1.702	1.783	29.880	27.584	34.174
6	.07865	1.665		.9426	.8390	3.570	3.412	1.600	1.651	34.476	32.178	38.514
7	.08511	1.570		.9447	.8328	2.133	3.199	1.546	1.573	39.466	36.971	43.367
8	.14979	.996		.9518	.7090	10.13	4.189	1.293	1.469	38.170	38.818	41.433
9	.17964	.850		.9591	.6760	-2.275	3.381	1.248	1.271	41.820	39.995	44.970
10	.18810	.815		.9638	.6915	-1.475	2.841	1.239	1.244	46.436	44.128	49.562
11	.17566	.867		.9709	.7770	2.024	2.760	1.253	1.246	51.971	49.204	55.133

Run F-20

(All Reynolds numbers are $\times 10^{-5}$)
(All friction factors are $\times 10^3$)

P_{us} - 24.23 psia
 T_{us} - 571.00 °Fabs
 P_{vac} - 0.0112 mm Hg

STN	P_w/P_{us}	M	T_{aw}/T_{us}	R'	f	f	ReD	\bar{ReD}	ReL	\bar{ReL}	Rex
1	.04276	2.517	.9429	.8979	-	-	1.389	-	2.243	-	5.748
2	.04678	2.375	.9414	.8895	1.973	1.973	1.313	1.351	7.352	4.798	10.664
3	.04869	2.314	.9430	.8898	.908	1.441	1.280	1.297	12.272	9.812	15.502
4	.05487	2.136	.9416	.8776	2.876	1.919	1.192	1.236	16.170	14.221	19.176
5	.06405	1.920	.9419	.8631	3.963	2.430	1.095	1.144	20.919	18.545	23.925
6	.07118	1.781	.9429	.8529	2.827	2.510	1.039	1.067	22.391	21.655	25.013
7	.08364	1.582	.9453	.8360	4.371	2.820	.967	1.003	24.677	23.534	27.116
8	.13210	1.101	.9524	.7559	9.769	3.813	.828	.898	24.438	24.558	26.527
9	.17659	.857	.9591	.6808	-1.408	3.160	.778	.803	26.066	25.252	28.029
10	.18572	.819	.9640	.6963	-1.514	2.640	.772	.775	28.923	27.495	30.870
11	.17500	.864	.9699	.7686	1.736	2.550	.779	.776	32.322	30.623	34.289

Run F-21

P_{us} - 14.66 psia
 T_{us} - 570.33 °Fabs
 P_{vac} - 0.0087 mm Hg

1	.04497	2.425	.9413	.8915	-	-	.805	-	1.300	-	3.331
2	.04971	2.270	.9396	.8811	2.305	2.305	.756	.781	4.233	2.767	6.140
3	.05366	2.157	.9396	.8747	1.839	2.072	.723	.740	6.926	5.580	8.749
4	.05724	2.064	.9408	.8714	1.620	1.921	.697	.710	9.453	8.190	11.210
5	.06003	1.998	.9415	.8684	1.209	1.743	.679	.688	11.917	10.685	13.629
6	.06214	1.950	.9416	.8650	.910	1.576	.666	.673	14.352	13.135	16.033
7	.06424	1.905	.9425	.8635	.877	1.460	.655	.661	16.720	15.536	18.373
8	.06667	1.856	.9438	.8623	.982	1.392	.643	.649	18.970	17.845	20.591
9	.07288	1.741	.9453	.8553	2.403	1.518	.616	.630	20.631	19.800	22.185
10	.08204	1.596	.9477	.8450	3.201	1.705	.584	.600	21.892	21.262	23.365
11	.09657	1.409	.9587	.8550	4.262	1.961	.547	.566	22.704	22.298	24.085

Run F-20

(All Reynolds numbers are $\times 10^{-5}$)
(All friction factors are $\times 10^3$)

P_{us} - 24.23 psia
 T_{us} - 571.00 °Fabs
 P_{vac} - 0.0112 mm Hg

STN	P_w/P_{us}	M	T_{aw}/T_{us}	R'	f	f	ReD	\bar{ReD}	ReL	\bar{ReL}	Re λ
1	.04276	2.517	.9429	.8979	-	-	1.389	-	2.243	-	5.748
2	.04678	2.375	.9414	.8895	1.973	1.973	1.313	1.351	7.352	4.798	10.604
3	.04869	2.314	.9430	.8898	.908	1.441	1.280	1.297	12.272	9.812	15.502
4	.05487	2.136	.9416	.8776	2.876	1.919	1.192	1.236	16.170	14.221	19.170
5	.06405	1.920	.9419	.8631	3.963	2.430	1.095	1.144	20.919	18.545	23.925
6	.07118	1.781	.9429	.8529	2.827	2.510	1.039	1.067	22.391	21.655	25.013
7	.08364	1.582	.9453	.8360	4.371	2.820	.967	1.003	24.677	23.534	27.116
8	.13210	1.101	.9524	.7559	9.769	3.813	.828	.898	24.438	24.558	26.527
9	.17659	.857	.9591	.6808	-1.408	3.160	.778	.803	26.066	25.252	28.029
10	.18572	.819	.9640	.6963	-1.514	2.640	.772	.775	28.923	27.495	30.870
11	.17500	.864	.9699	.7686	1.736	2.550	.779	.776	32.322	30.623	34.289

Run F-21

P_{us} - 14.66 psia
 T_{us} - 570.33 °Fabs
 P_{vac} - 0.0087 mm Hg

1	.04497	2.425	.9413	.8915	-	-	.805	-	1.300	-	3.331
2	.04971	2.270	.9396	.8811	2.305	2.305	.756	.781	4.233	2.767	6.140
3	.05366	2.157	.9396	.8747	1.839	2.072	.723	.740	6.926	5.580	8.749
4	.05724	2.064	.9408	.8714	1.620	1.921	.697	.710	9.453	8.190	11.210
5	.06003	1.998	.9415	.8684	1.209	1.743	.679	.688	11.917	10.685	13.629
6	.06214	1.950	.9416	.8650	.910	1.576	.666	.673	14.352	13.135	16.033
7	.06424	1.905	.9425	.8635	.877	1.460	.655	.661	16.720	15.536	18.373
8	.06667	1.856	.9438	.8623	.982	1.392	.643	.649	18.970	17.845	20.591
9	.07288	1.741	.9453	.8553	2.403	1.518	.616	.630	20.631	19.800	22.185
10	.08204	1.596	.9477	.8450	3.201	1.705	.584	.600	21.892	21.202	23.365
11	.09657	1.409	.9587	.8550	4.262	1.961	.547	.566	22.704	22.298	24.085

Run F-36

P_{us} - 24.91 psia
 T_{us} - 569.57 °Fabs
 P_{vac} - 0.011 mm Hg
 Re_D at inlet - 1.508×10^5

STN	P_w/P_{us}	M	T_{aw}/T_{us}	R'
1	.03970	2.640	.9342	.8870
2	.04360	2.488	.9327	.8782
3	.04589	2.406	.9353	.8796
4	.05287	2.164	.9350	.8655
5	.06291	1.945	.9370	.8537
6	.07138	1.778	.9391	.8428
7	.08146	1.614	.9424	.8318
8	.12935	1.121	.9501	.7516

Run F-43

P_{us} - 24.28 psia
 T_{us} - 565.02 °Fabs
 P_{vac} - 0.0046 mm Hg
 Re_D at inlet - 1.457×10^5

STN	P_w/P_{us}	M	T_{aw}/T_{us}	R'
1	.04088	2.591	.9349	.8864
2	.04490	2.440	.9314	.8738
3	.04745	2.353	.9349	.8761
4	.05383	2.164	.9348	.8652
5	.06314	1.940	.9368	.8528
6	.07084	1.788	.9392	.8442
7	.08259	1.597	.9427	.8304
8	.13151	1.105	.9511	.7507

CHAPTER VII

Conclusions

For air flowing in a tube at supersonic velocities the recovery factor is very nearly a linear function only of the Mach number in the range of Mach numbers from 1.3 to 2.6 and inlet diameter Reynolds numbers of 0.47 to 4.8×10^5 . The recovery factor varies from 0.81 to 0.905 at Mach numbers of 1.3 and 2.6 respectively.

Preliminary results with the apparatus modified to reduce heat transfer effects to a minimum indicate that the recovery factor is independent of stagnation temperature. In addition the results indicate that the recovery factors measured with the modified apparatus are about 0.5% lower than those reported in this thesis.

Results obtained in this thesis show that it is possible to define three flow regimes in terms of length Reynolds number with a transition regime occurring between the Reynolds numbers of 15×10^5 and 30×10^5 .

In supersonic flow in a tube, the results show that variation of the mean apparent friction factors with length Reynolds number is analogous to the relation between friction factor and diameter Reynolds number in incompressible flow. The mean apparent friction factor reaches a minimum value of 0.0013 as it reaches the transition region and after the transition region it decreases steadily with increasing Reynolds numbers from a maximum value of about 0.0035.

CHAPTER VIII

Recommendations

Based on the results and experience obtained in preparing this thesis, the following recommendations are made:

1. Further runs at stagnation temperatures other than 110°F should be made to determine whether the recovery factor is a function of the stagnation temperature.

2. The range of Mach numbers covered should be extended by using a supersonic nozzle designed for a Mach number of about 4.0.

3. In order to increase the range of flow rates which can be accommodated by the apparatus, the capacities of the ejector and re-generator should be increased.

4. The actual effect on heat transfer of the evacuated chamber surrounding the test section should be investigated to determine whether vacuums of the order obtained in this thesis are sufficient to render heat transfer negligible.

5. In order to eliminate the effect of heat transfer to the air flowing between the stagnation tanks, it is suggested that a study be made of the possibilities of enclosing in an evacuated chamber the apparatus from the inlet of the upstream stagnation tank to the outlet of the downstream stagnation tank. It is further suggested that a means be provided for temperature control of the external surface of the test section.

6. An attempt should be made to correlate the experimental data by using Reynolds numbers based on a viscosity which is evaluated at

some temperature between the mean stream and the wall temperatures.

7. For measuring upstream stagnation pressures greater than 43 psig, a gage which is more accurate than the Bourdon gage now in use should be installed.

8. The supersonic nozzle used in this investigation should be recalibrated while it is not assembled in the recovery factor apparatus in order to better cover the range of expected nozzle throat Reynolds numbers.

9. A filter should be installed in the pipe line through which passes the dry air supplied by the Low Temperature Laboratory.

10. Safety traps should be installed in the low pressure legs of the absolute manometers in order to prevent the loss of silicone oil through flow into the vacuum system manifold.

11. The constant-temperature bath should be provided with a heater of greater power output since the one currently in use is incapable of maintaining a constant temperature of 110°F.

12. A stop valve should be installed in the section of piping immediately upstream of the Cenco-Megavac pump to facilitate the detection of vacuum system leaks through the pump.

13. The use of solid nylon as a material for future test sections should be investigated. Mr. Chase, of the Cummings Machine Works, Boston, has shown that nylon in this form has a greater machinability than lucite.

APPENDIX A

Brief History of Project DIC 6418

The work reported in this thesis was carried out as a part of Project DIC 6418, which is sponsored by the United States Navy through the Office of Naval Research. Since the Project has been in existence over a period of several years and since the results of previous investigators are directly related to those now being reported, a brief history is presented here.

The following is quoted from reference 4, the publication of which immediately preceded this phase of the Project:

"The basic apparatus used to measure both recovery factors and heat transfer coefficients was designed in 1946 by Klingensmith (5). His work included the design of a supersonic ($M = 2.5$) nozzle, the design of a recovery factor test tube made of textolite to which the nozzle would be directly attached, and some calculations for the design of a heat transfer test section. The heat transfer test section was completely designed by Wyant (3) in 1947.

"Junge and Margolskee (6) began construction of the Klingensmith apparatus in February, 1947. The supersonic nozzle and textolite tube were machined at the Boston Navy Yard. The nozzle was calibrated by Ketchum (7) (who was in charge of experimental work between February 1946 and November 1948) in early March, 1947. In early July, 1947, tests were made on the recovery factor apparatus. Prior to the assembly of the apparatus small burrs were visible in the test section at stations 3 and 7. When test runs were made, the pressure distribution was not smooth, so the inside of the test tube was burnished with a glass rod to smooth the edges of the pressure taps. At the same time the test section was shortened by machining off two inches of the tube in order to give a greater length of supersonic flow. Further tests showed that station 5 still gave an unsatisfactory pressure reading, so the hole was sealed with glyptal and a new pressure tap was drilled $1/8$ in. further downstream. At the same time a brass collar was machined to fit between the nozzle and the test section. Additional trial runs were made during which it was observed that the pressure distribution was satisfactory near station 5 when P_{us} was 21 psia, but unsatisfactory when P_{us} was 96 psia.

The nozzle was then rotated 90° relative to the tube, but no appreciable change in pressure distribution was observed. Recovery factor runs JM1-9 were then made (6).

"In October, 1947, Connors and Helfrich (4) took over operation of the apparatus and made runs T1 to T7 to verify the results of Junge and Margolskee (5). A lucite tube was machined and then installed. This tube had eleven stations and an extension which could be installed if desired. A diffuser was also provided, since it was thought that the diffuser would increase the length of supersonic flow in the tube. The diffuser did not perform satisfactorily except at very low upstream stagnation pressures (below 100 cm Hg absolute). At about the same time the manometer system was revised.

"Runs L1 to L20 were then made (4), with a range of stagnation temperatures between 33°F and 140°F . It appeared that the recovery factor might be a function of the upstream stagnation temperature, but careful investigation showed that the apparatus used by Connors and Helfrich was reliable only when t_{us} was about 105°F , so no conclusions could be drawn about a $T_{us} - R'$ relationship.

"In June, 1948, the heat transfer section was installed in place of the lucite recovery factor section by Larkin, Shoulberg, and Ketchum. At the same time the design of an improved recovery factor apparatus was begun."

During the period from June 1948 to May 1949 Shoulberg, Larkin, and England conducted an investigation of heat transfer coefficients for air flowing in a tube at supersonic velocities. Runs K-1 to K-28 were made with the apparatus designed by Wyant. Runs S-1A to S-3B were made after the apparatus had been modified to permit variation of the wall temperature without changing the air flow conditions. The supersonic region investigated lay in the range of Mach numbers from 1.0 to 2.5 and diameter Reynolds numbers from 30,000 to 400,000.

In addition, Shoulberg, Larkin and England completed the design of an improved recovery factor apparatus which was subsequently modified and used for the experiments of this thesis.

Working at the same time as the above, Ketchum, in a thesis for the doctorate degree, compiled the recovery factor and friction factor data obtained by Junge and Margolskee and Connors and Helfrich with the heat transfer coefficients obtained by Shoulberg and made a more thorough analysis of the data obtained. Ketchum also made a very complete review of the literature pertaining to this field.

The work accomplished on the project from the period from June 1949 to May 1950 by Welch, Volonte, Toong, and Young may be summarized chronologically as follows:

1. Design of Foelsch and Sauer supersonic nozzles.
2. Revision of drawings and awarding of contract for the manufacture of the recovery factor apparatus.
3. Making of subsonic heat transfer runs followed by dismantling of heat transfer apparatus.
4. Assembly of new recovery factor apparatus without the test section thermocouples.
5. Installation of pressure gages and valves in the air piping.
6. Overhauling of regenerator and renewal of all filtering material.
7. Design and installation of an orifice plate.
8. Calibration of nozzle and orifice plate with the gasometer.
9. Manufacture, calibration, and installation of test section thermocouples and wiring.
10. Installation of larger copper coil in constant temperature bath.

11. Design and assembly of vacuum system for the recovery factor apparatus and modification of the pressure measuring system.
12. Making of recovery and friction factor runs F-1 to F-35.
13. Modification of the recovery factor apparatus to reduce amount of heat transfer between room and test section.
14. Making of experimental runs F-36 to F-45 to determine the effects of the modification.

APPENDIX B

Calculation of Recovery Factors and Friction Factors

Recovery Factors

In general the method of calculation of recovery factors follows that of Helfrich and Connors.¹ By definition the recovery factor for a perfect gas is given by:

$$R' = \frac{T_{aw} - T_m}{T_{us} - T_m} = 1 - \frac{T_{us} - T_{aw}}{T_{us} - T_m}$$

Since T_{us} is directly measurable and T_{aw} can be closely estimated, it remains only to determine T_m in order to compute the recovery factor.

For a gas flowing isentropically to a supersonic nozzle and adiabatically through the nozzle and duct of constant area, it can be shown that the product $(P_w/P_{us})(A/A^*)$ is the same as for the case of isentropic expansion. The pressure ratio, Mach number, and flow coefficient are related by the expression⁹

$$\left(\frac{1}{C_w}\right)\left(\frac{P_w}{P_{us}}\right)\left(\frac{A}{A^*}\right) = \frac{\sqrt{\left(\frac{2}{\kappa+1}\right)^{\frac{\kappa+1}{\kappa-1}}}}{M\sqrt{1 + \frac{\kappa-1}{2} M^2}}$$

Since (A/A^*) is fixed in this case, the Mach number can be determined when the flow coefficient and pressure ratio are known. Using tabulated values of $(P_w/P_{us})(A/A^*)$ as a function of Mach number from the Gas Tables,⁷ a plot of $(1/C_w)(P_w/P_{us})$ vs. M was constructed and is shown in Figure C-1.

The pressure ratio at a given station can be evaluated from the observed data, and the flow coefficient can be determined from the nozzle calibration

plot of C_w vs Re_D^* (Figure C-2) after Re_D^* has been computed from the following:

$$Re_D^* = \frac{(w/A^*) D^*}{\mu^*} \quad \text{where } D^* \text{ is a constant.}$$

From the isentropic tables for $k = 1.4$

$$T^*/T_{us} = 0.83333.$$

Having computed T^* the viscosity at the nozzle throat can be determined from the temperature-viscosity plot (Figure C-3). From the equation for maximum isentropic mass rate of flow for a perfect gas through a nozzle:

$$(w_s/A^*) = 0.03012 \frac{P_{us}}{\sqrt{T_{us}}}$$

the isentropic flow rate is readily determined. In calculating the throat Reynolds number for the purpose of determining the flow coefficient, it is sufficient to use the isentropic rather than the actual value of flow rate. In an extreme case where a known flow coefficient of 0.9600 is neglected, the error in Re_D^* is 5.8% with a resulting error of 0.09% in estimated flow coefficient, which error is well within the limits of precision with which the nozzle was calibrated.

Once the Mach number has been determined from Figure C-1, the mean stream temperature can be evaluated from the following expression obtained from a one-dimensional analysis of adiabatic flow⁸

$$\frac{T_m}{T_{us}} = \frac{1}{1 + \frac{k-1}{2} M^2}$$

The calculations are simplified by using the tabulation of the temperature ratio as a function of Mach number in the one-dimensional isentropic tables of the Gas Tables.

This method of recovery factor calculation differs from that of Helfrich and Connors in that:

1. The flow coefficient has been included in the expression relating pressure ratio, area ratio, and Mach number; and
2. In accordance with the assumption of a perfect gas the Joule-Thomson effect has been neglected in computing the stagnation temperature at each station.

The recovery factors for Run F-6 have been calculated by the methods of Helfrich and Connors and of Junge and Margolskee;² the results are presented for comparison in Figure B-1.

Friction Factors

From a one-dimensional analysis of compressible adiabatic flow in a tube of constant diameter it can be shown that⁸

$$\frac{4fL_{max}}{D} = \frac{1 - M^2}{\kappa M^2} + \frac{\kappa + 1}{2\kappa} \ln \frac{(\kappa + 1)M^2}{2(1 + \frac{\kappa - 1}{2} M^2)} = \phi(M)$$

Since the ϕ function is tabulated as a function of Mach number for such flow in the Gas Tables, the calculation of friction factors is reduced to a determination of the Mach number, which is evaluated incidental to the calculation of recovery factors.

To compute the local apparent friction factor, i.e., the value which is a mean for two adjacent stations of the test section, it is necessary only to know the Mach numbers at the two stations. Then

$$\frac{4f_1 L_{max1}}{D} - \frac{4f_2 L_{max2}}{D} = \phi_1 - \phi_2$$

Letting f be a value which is the mean of f_1 and f_2

$$\frac{4f}{D} (L_{\max 1} - L_{\max 2}) = \phi_1 - \phi_2$$

But $L_{\max 1} - L_{\max 2}$ is the distance between any two adjacent stations and is constant; therefore

$$\frac{4f}{D} \Delta L = \phi_1 - \phi_2$$

and
$$f = \frac{D}{4 \Delta L} (\phi_1 - \phi_2)$$

To compute the mean apparent friction factor, i.e., the value which is a mean between the first station and any other station, the above expression can be transformed to

$$\bar{f} = \frac{D}{4 \Delta L_x} (\phi_1 - \phi_x)$$

where ΔL_x is the distance between the stations involved.

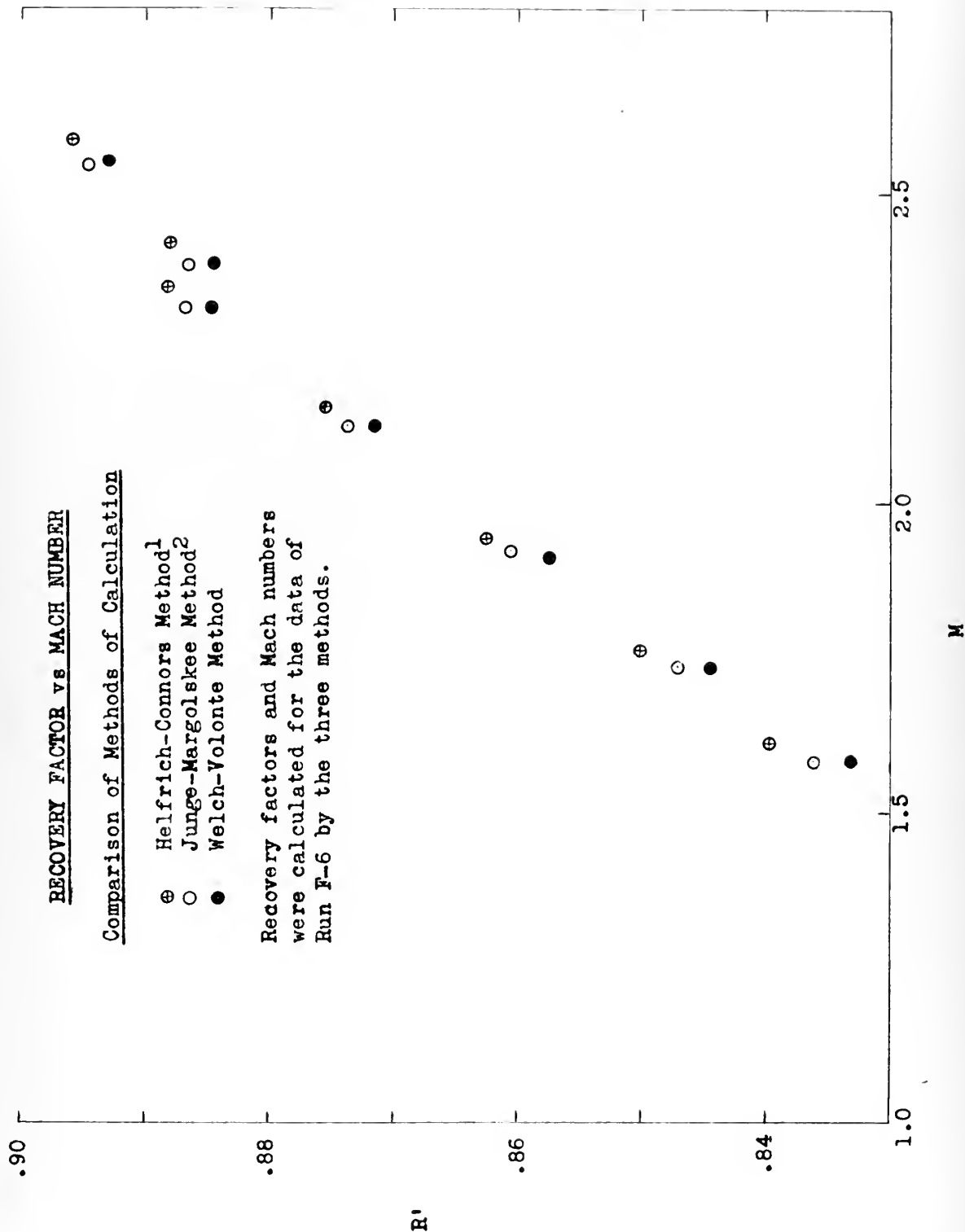


Figure B-1

APPENDIX C

Calculation Data, Constants, and Coefficients

Calculation Data

Although the data used in the calculation of the recovery and friction factors was compiled in tabular form in order to insure consistency among the several persons making the calculations, they are appended here in the form of graphs. The necessary data include the following:

1. M vs $(1/C_w)(P_w/P_{us})$, the source of which is described in Appendix B and which is shown in Figure C-1.
2. C_w vs Re_D^* , the source of which is described in Appendix G and which is shown in Figure C-2.
3. μ vs T , which data is the same as that used in references 1, 2, 4, and 10 and which is shown in Figure C-3.
4. Pressure conversion data plotted in Figure C-4.
5. Thermocouple calibration data, the basis for which is described in Appendix H and which is tabulated in Table C-1.
6. T_m/T_{us} vs M , which was obtained from the tabulation of T/T_0 in Table 30 of the Gas Tables (One-Dimensional Isentropic Compressible-Flow Functions for $k = 1.4$).
7. $4fL_{max}/D$ vs M , which was obtained from Table 42 of the Gas Tables (Fanno Line - One-Dimensional Compressible-Flow Functions for Adiabatic Flow at Constant Area with Friction for $k = 1.4$).

Calculation Constants

The constants used in the calculation of recovery and friction factors

are:

A	- 0.1978 in ²	R	- 53.345 ft-lb/lb-°F
A*	- 0.05662 in ²	r _s	- 0.340 in.
D	- 0.5018 in.	Δr _s	- 0.450 in.
D*	- 0.2685 in.	r _w	- 0.251 in.
g	- 32.174 ft/sec ²	x ₁	- 2.076 in.
k	- 1.400	x ₂	- 4.076 in.
L ₁	- 0.810 in.	x ₃	- 6.076 in.
L ₂	- 2.810 in.	x ₄	- 8.076 in.
L ₃	- 4.810 in.	x ₅	- 10.076 in.
L ₄	- 6.810 in.	x ₆	- 12.076 in.
L ₅	- 8.810 in.	x ₇	- 14.076 in.
L ₆	- 10.810 in.	x ₈	- 16.078 in.
L ₇	- 12.810 in.	x ₉	- 18.076 in.
L ₈	- 14.810 in.	x ₁₀	- 20.076 in.
L ₉	- 16.810 in.	x ₁₁	- 22.076 in.
L ₁₀	- 18.810 in.	°F _{abs}	= °F + 459.69°
L ₁₁	- 20.810 in.		

Calculation Coefficients

Flow Rate

The maximum isentropic mass rate of flow of a perfect gas is given by

$$\frac{w_s}{A^*} = \sqrt{\frac{gK}{R} \left(\frac{2}{\kappa+1} \right)^{\frac{\kappa+1}{\kappa-1}} \frac{P_{us}}{T_{us}}} .$$

Then

$$\frac{w_s}{A^*} = 0.532 \frac{P_{us}}{\sqrt{T_{us}}}$$

and

$$w_s = 0.03012 \frac{P_{us}}{\sqrt{T_{us}}}$$

where w_s is in lb/sec, p_{us} in psia, and T_{us} in °Fabs.

At the nozzle throat the isentropic flow rate per unit area is

$$G_s^* = \frac{w_s}{A^*} = 2543.4 w_s .$$

where G_s^* has the units of lb/sec-ft². At any station along the test section

$$G = \frac{C_w w_s}{A} = 728.13 C_w w_s$$

Diameter Reynolds Number

The Reynolds number based on the diameter is given by

$$Re_D = \frac{GD}{\mu} .$$

At the nozzle throat

$$Re_D^* = \frac{0.02337 G^*}{\mu^*}$$

and at any station along the test section

$$Re_D = \frac{0.04182 G}{\mu_m} .$$

where the G 's have the units of $\text{lb}/\text{sec}\cdot\text{ft}^2$ and the viscosities which are determined at T^* and T_m , respectively, are in $\text{lb}/\text{sec}\cdot\text{ft}$.

Adiabatic Wall Temperature

The coefficient used in calculating the extrapolated adiabatic wall temperature is derived from the following:

$$\frac{t_s - t_{aw}}{\Delta t_s} = \frac{r_s - r_w}{\Delta r_s} .$$

For the constants of this report

$$t_s - t_{aw} = 0.1978 \Delta t_s .$$

Table C-1
Thermocouple Calibration Data**

<u>mv</u>	<u>$t_{us} \& t_{ds}$</u>	<u>$t_s \& \Delta t_s$</u>
-1.0		-16.415°F
-0.9		-11.415
-0.8		- 6.451
-0.7		- 1.523
-0.6	3.58°F	3.369
-0.5	8.40	8.225
-0.4	13.18	13.045
-0.3	17.94	17.828
-0.2	22.65	22.576
-0.1	27.34	27.306
0	32.00	32.000
0.1	36.64	36.648
0.2	41.25	41.260
0.3	45.83	45.854
0.4	50.40	50.431
0.5	54.94	54.971
0.6	59.45	59.493
0.7	63.94	63.997
0.8	68.41	68.465
0.9	72.86	72.915
1.0	77.28	77.347
1.1	81.67	81.744
1.2	86.03	86.104
1.3	90.37	90.446
1.4	94.68	94.770
1.5	98.99	99.076
1.6	103.28	103.364
1.7	107.54	107.635
1.8	111.77	111.869
1.9	115.98	116.085
2.0	120.17	120.283
2.1	124.35	124.463
2.2	128.51	128.625
2.3	132.65	132.769
2.4	136.77	136.895
2.5	140.90	141.003
2.6	144.99	145.112
2.7	149.06	149.184
2.8	153.12	153.238
2.9	157.16	157.274
3.0	161.19	161.292

** See Appendix H.

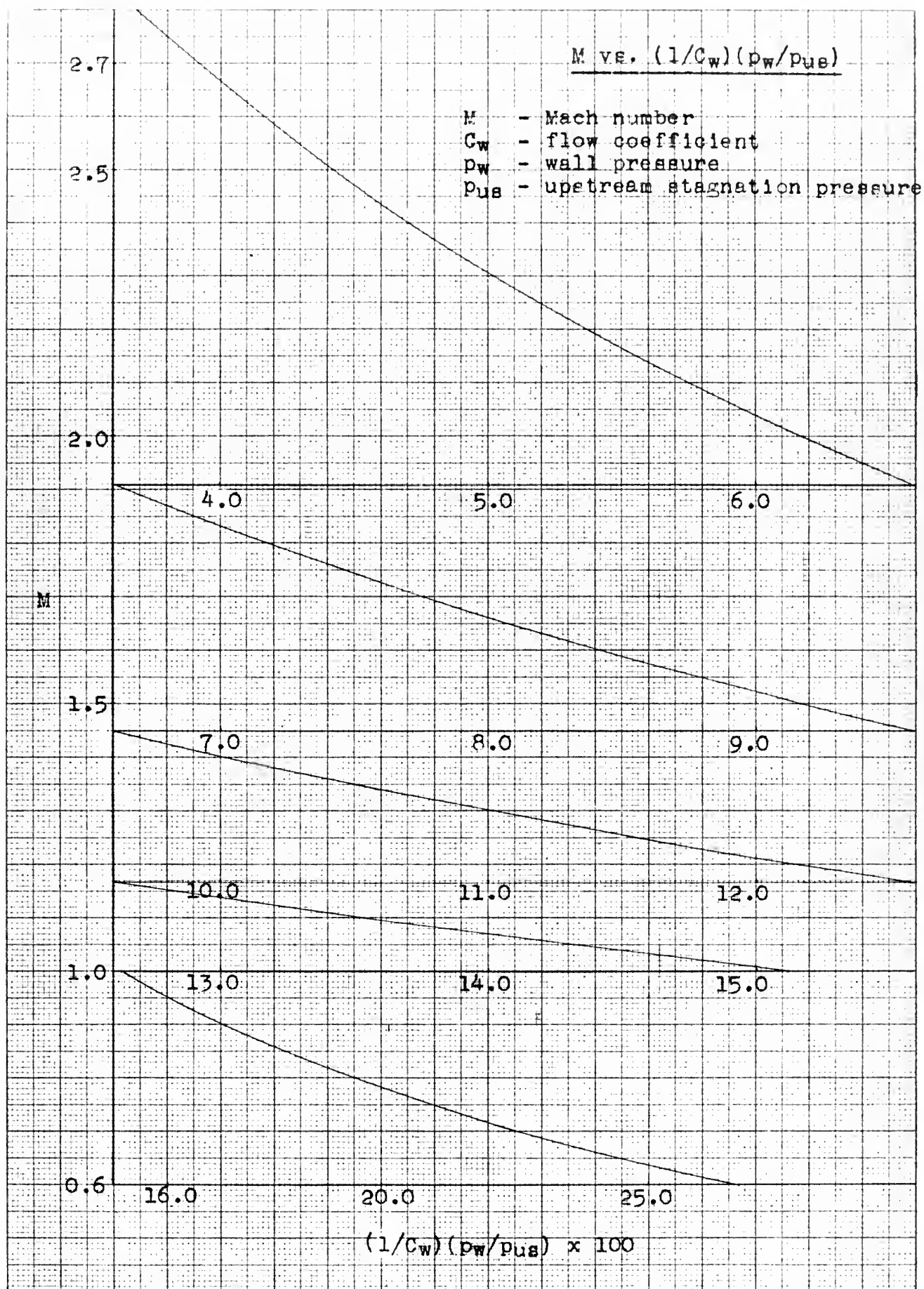


Figure C-1

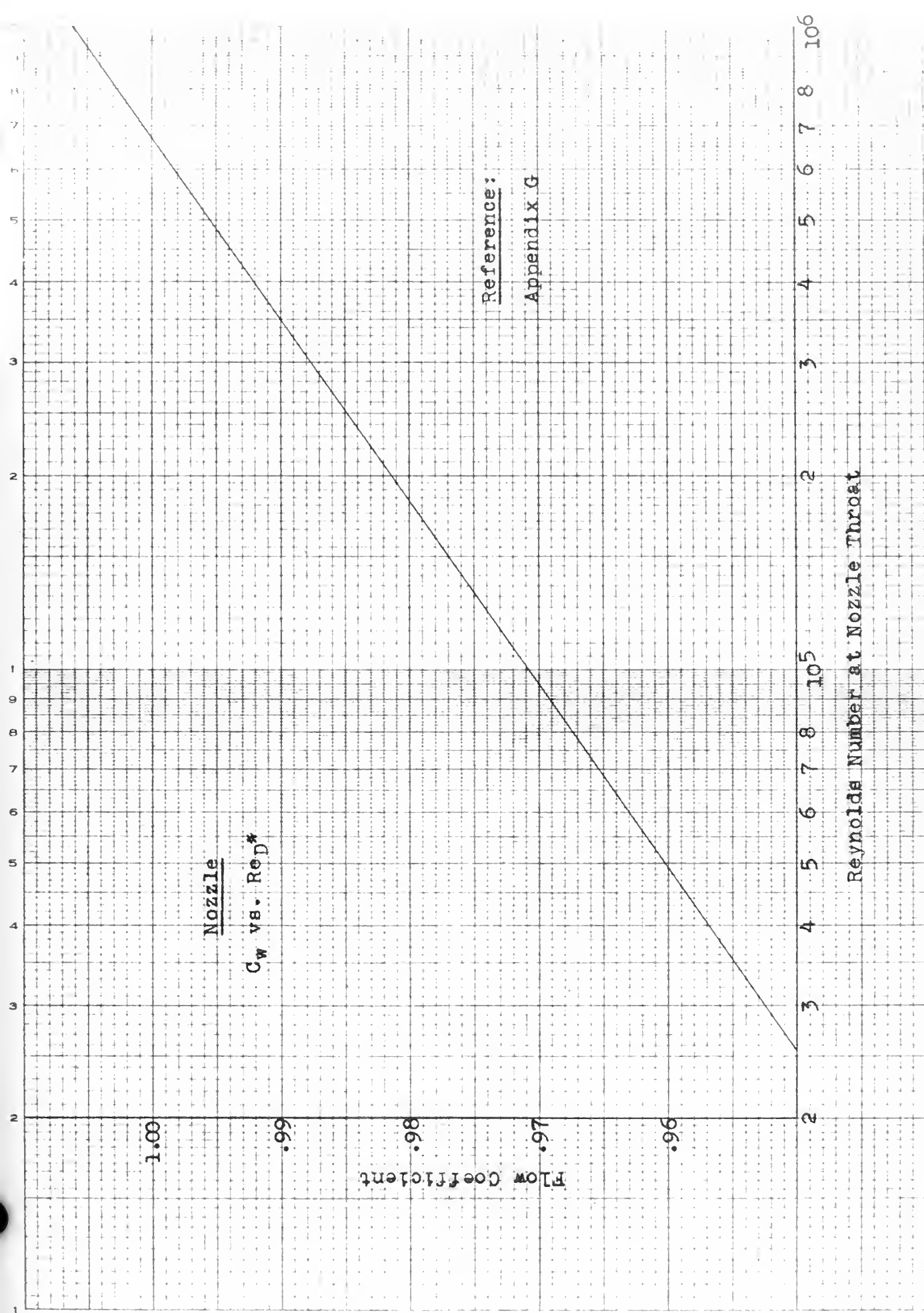


Figure C-2

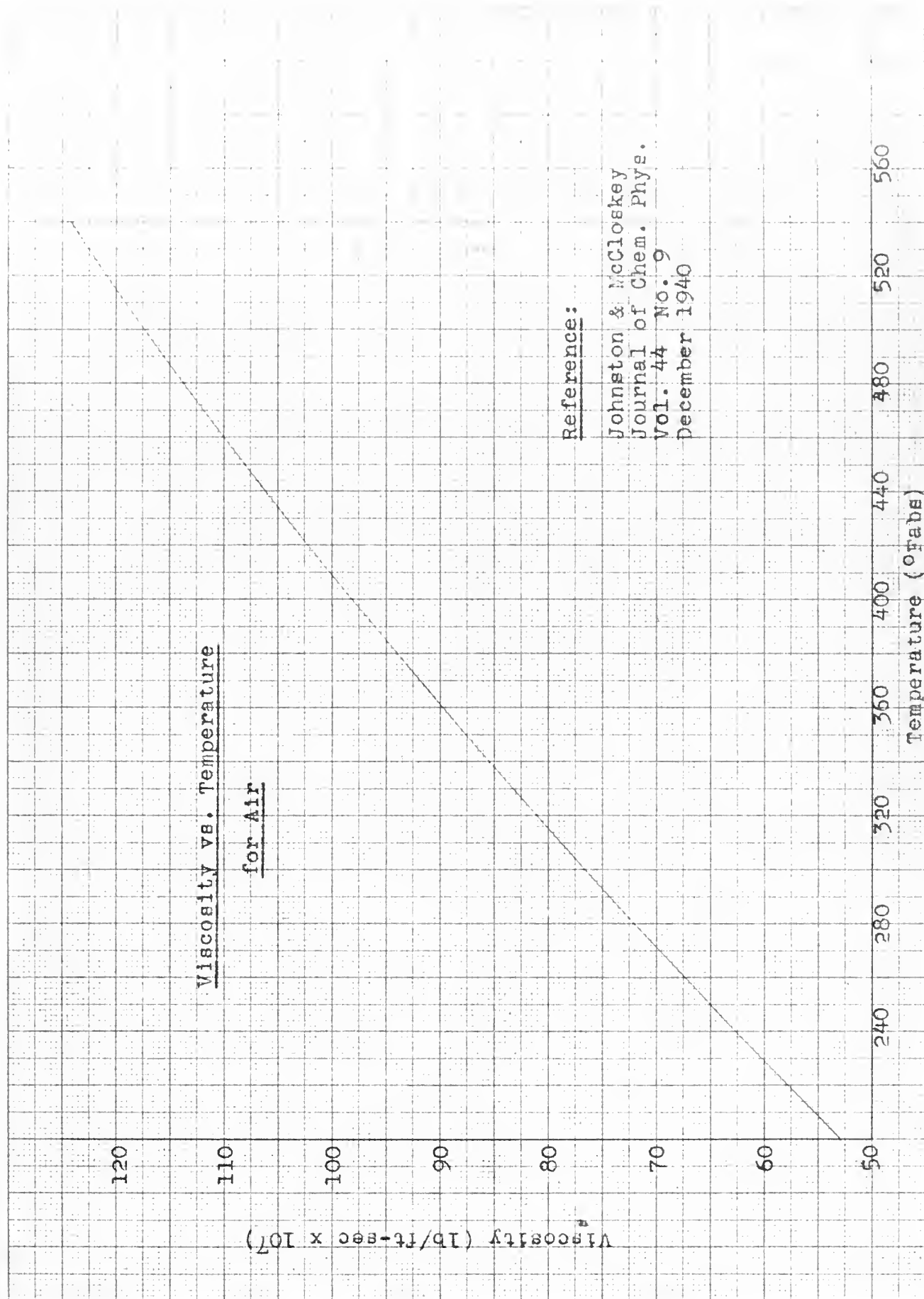


Figure C-3

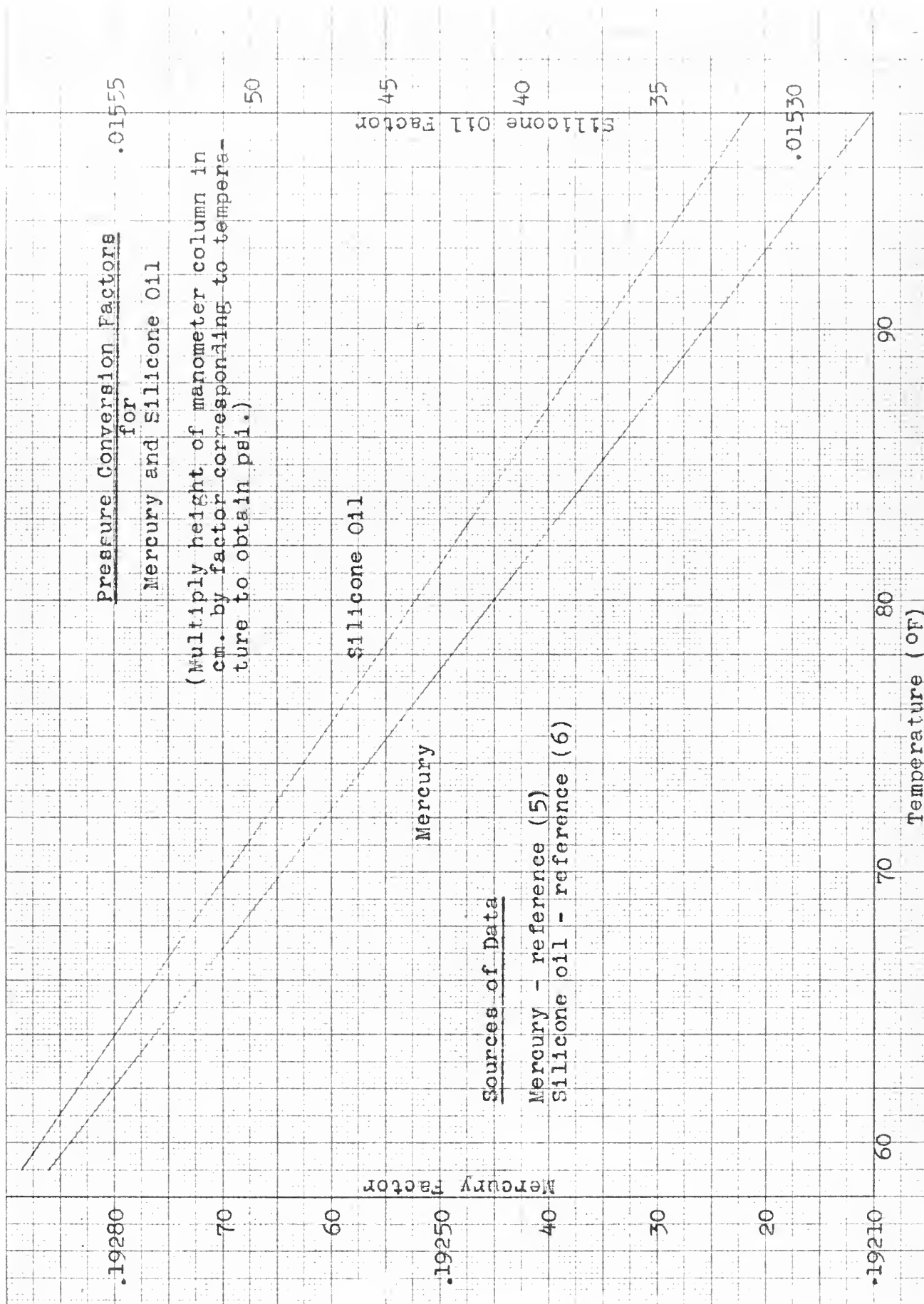


Figure C-4

APPENDIX D

Sample Calculation

Following is a tabulation of the operations involved in the calculation of recovery and friction factors. A sample data and calculation sheet for Run F-6 is included at the end of this appendix. The constants and coefficients used in the calculations are evaluated in Appendix C.

Column	Item	Dimensions	Operation
(1)	L/D	none	L/D values are constant; the values for stations 1-11 are, respectively, 1.614, 5.600, 9.586, 13.571, 17.557, 21.542, 25.528, 29.514, 33.499, 37.485, 41.471.
(2)	x/D	none	x/D values are constant; the values for stations 1-11 are, respectively, 4.137, 8.123, 12.108, 16.094, 20.080, 24.065, 28.051, 32.037, 36.022, 40.008, 43.994.
(3)	T _{room}	°F	Observed data.
(4)	P _{bar}	in. Hg	Observed data (corrected to 32°F).
(5)	P _{bar}	psi	Multiply (4) by 0.49119.
(6)	P _{us}	cm. Hg	Observed data (manometer left column).

Column	Item	Dimensions	Operation
(7)	P _{us}	cm. Hg	Observed data (manometer right column).
(8)	"	"	(7) - (6).
(9)	"	psig	Multiply (8) by conversion factor for mercury evaluated at temperature (3); Figure C-4.
(10)	"	psia	(9) + (5).
(11)	P _w	cm. Hg	Observed data (manometer left column).
(12)	"	"	Observed data (manometer right column).
(13)	"	"	(12) - (11).
(14)	"	psig	Multiply (13) by conversion factor for mercury evaluated at temperature (3); Figure C-4.
(15)	"	psia	(5) - (14).
(16)	"	cm. Silicone	Observed data (manometer left column).
(17)	"	"	Observed data (manometer right column).
(18)	"	"	(17) - (16).

Column	Item	Dimensions	Operation
(19)	P_w	psia	Multiply (18) by conversion factor for silicone oil evaluated at temperature (3); Figure C-4.
(20)	t_{us}	mv	Observed data; three values measured at different times.
(21)	"	$^{\circ}F$	Convert average of three values in (20) using thermocouple calibration data.
(22)	T_{us}	$^{\circ}F_{abs}$	$(21) + 459.69$.
(23)	T^*	$^{\circ}F_{abs}$	$0.83333 \times (22)$.
(24)	μ^*	lb/sec-ft $\times 10^7$	Find value of viscosity at temperature (23); Figure C-3.
(25)	$\sqrt{T_{us}}$	$(^{\circ}F_{abs})^{\frac{1}{2}}$	$\sqrt{(22)}$
(26)	w_s	lb/sec	$0.03012 \times (10)/(25)$.
(27)	G_s^*	lb/sec-ft ²	$2543.4 \times (26)$.
(28)	Re_D^*	none	$0.02337 \times (27)/(24)$.
(29)	C_w	none	Flow coefficient evaluated at (28) from Figure C-2.
(30)	P_w/P_{us}	none	$(15)/(10)$ for mercury manometers. $(19)/(10)$ for silicone oil manometers.
(31)	$(1/C_w)(P_w/P_{us})$	none	$(30)/(29)$.

Column	Item	Dimensions	Operation
(32)	M	none	Evaluated at (31) from Figure C-1.
(33)	T_m/T_{us}	none	Evaluated at (32) from Table 30 of Gas Tables.
(34)	T_m	$^{\circ}\text{Fabs}$	$(33) \times (22)$.
(35)	t_s	mv	Observed data.
(36)	t_s	$^{\circ}\text{F}$	Convert (35) using thermocouple calibration data.
(37)	Δt_s	mv	Observed data.
(38)	$(t + \Delta t)_s$	mv	$(35) + (37)$.
(39)	$(t + \Delta t)_s$	$^{\circ}\text{F}$	Convert (38) using thermocouple calibration data.
(40)	Δt_s	$^{\circ}\text{F}$	$(39) - (36)$.
(41)	$t_s - t_{aw}$	$^{\circ}\text{F}$	$0.1978 \times (40)$.
(42)	t_{aw}	$^{\circ}\text{F}$	$(36) - (41)$.
(43)	$t_{us} - t_{aw}$	$^{\circ}\text{F}$	$(21) - (42)$.
(44)	$T_{us} - T_m$	$^{\circ}\text{Fabs}$	$(22) - (34)$.
(45)	$1 - R'$	none	$(43)/(44)$.
(46)	R'	none	$1 - (45)$.
(47)	T_{aw}/T_{us}	none	$\frac{(42) + 459.69}{(22)}$
(48)	G	lb/sec-ft ²	$728.13 \times (26) \times (29)$.
(49)	μ_m	lb/sec-ft $\times 10^7$	Find value of viscosity at temperature (34); Figure C-3.
(50)	Re_D	$\times 10^{-5}$	$0.04182 \times (48)/(49)$.

Column	Item	Dimensions	Operation
(51)	\bar{Re}_D	$\times 10^{-5}$	Average of values for adjacent stations in (50).
(52)	Re_L	$\times 10^{-5}$	(1) \times (50).
(53)	\bar{Re}_L	$\times 10^{-5}$	Average of values for adjacent stations in (52).
(54)	Re_x	$\times 10^{-5}$	(2) \times (50).
(55)	ϕ	none	Evaluated at (32) from Table 42 of Gas Tables.
(56)	$\Delta\phi$	none	In (55) subtract value for station 2 from value for station 1, station 3 from station 2, etc.
(57)	f	$\times 10^3$	$0.062725 \times$ (56).
(58)	$\phi_1 - \phi_x$	none	In (55) subtract value for each station from value for station 1.
(59)	$D/4 \Delta L_x$	$\times 10^2$	Values are constant; for stations 1-11 they are, respectively, infinity, 6.2725, 3.1363, 2.0908, 1.5681, 1.2545, 1.0454, 0.8961, 0.7841, 0.6969, 0.6273.
(60)	f	$\times 10^3$	(58) \times (59).
(61)	h_1	cm	Observed data.
(62)	h_2	cm	Observed data.

Column	Item	Dimensions	Operation
(63)	$h_1 - h_2 - 1$	cm	$(61) - (62) - 1.$
(64)	$80.25 - h_2$	cm	$80.25 - h_2.$
(65)	P_{vac}	mm Hg.	$(63) \times (64)/975.$

APPENDIX E

Design of Nozzle

In the design of the improved recovery factor apparatus by Shoulberg,⁴ the nozzle contour designed by Klingensmith³ and used in the original recovery factor apparatus was retained with changes only in the dimension reference plane and in the mounting arrangements.

In an effort to obtain a nozzle of shorter length than the Klingensmith nozzle and thus reduce the boundary layer effect upon flow through the nozzle, two nozzles were designed in June-July 1949 by G. J. Van Wylen, research assistant to the Project, and R. V. Welch using methods devised by Kuno Foelsch¹⁴ and R. Sauer¹³ for the design of axially symmetrical supersonic nozzles.

Following the method of Foelsch, the complete nozzle contour from throat to exit was designed for uniform parallel flow at an exit diameter of 0.5015" and an exit Mach number of 2.8 with isentropic flow. It was estimated that the boundary layer effect in this nozzle would reduce the isentropic exit Mach number to an actual value of 2.6. After manufacture and installation of this nozzle in the improved recovery factor apparatus the Mach numbers measured at Station #1, which is 0.81 inches from the nozzle exit plane, range from 2.68 at high to 2.33 at low rates of flow indicating that the average actual exit Mach number is slightly less than the desired value of 2.6.

The Foelsch method linearizes the characteristic equations of axially symmetrical flow by comparing the conditions of flow in a cone with those in a nozzle. Mathematical expressions for the nozzle contour can thus be obtained. The design begins with an assumed source type flow OA (See Fig. E-1) which is altered in region AE to give parallel exit flow. The straight conical section AD assures conical source flow on entering region AE. The throat is designed by using the equation of continuity to determine the throat diameter and constructing TD as a circle tangent to OA at point D and parallel to the axis at throat T. Circular arc TC is a continuation of circular arc TD, and circular arc CI is drawn to produce an inlet nozzle diameter of 1.250 inches.

The Sauer method is a part graphical, part analytical, solution of the characteristic equations of axially symmetrical flow assuming that the flow is isentropic, supersonic and irrotational; it uses successive approximations which converge rapidly. Using the Foelsch contour from points T to A as a starting point, the exit portion of the contour was designed by the Sauer method for an isentropic exit Mach number of 2.8. The contour was then adjusted to obtain uniform parallel flow at an exit diameter of 0.5015". A more complete explanation of the Sauer method follows in Appendix F.

Figure E-2 compares the nozzle contours obtained by the Foelsch and Sauer methods and also shows the Klingensmith nozzle used in the original recovery factor apparatus. The Sauer contour is about 10% shorter than the Foelsch, but the latter has smaller cross-sectional areas

between the throat and exit planes. Since both contours were obtained by assuming isentropic flow in the nozzle, it was felt that the slightly longer, but smaller area, Foelsch contour would have less boundary layer effect than the shorter, but larger area, Sauer contour. For this reason, Professor A. H. Shapiro, Department of Mechanical Engineering, MIT, recommended manufacture of the Foelsch nozzle.

The nozzle was manufactured of stainless steel by the Cummings Machine Works, Boston, Massachusetts, to tolerances of $\pm .0005$ on inside diameters and of $\pm .0001$ on inside concentricity.

It is interesting to note that the design of the nozzle contour by the Foelsch mathematical computation method required about 15 man-hours while that of the Sauer graphical-analytical method required in excess of 160 man-hours.

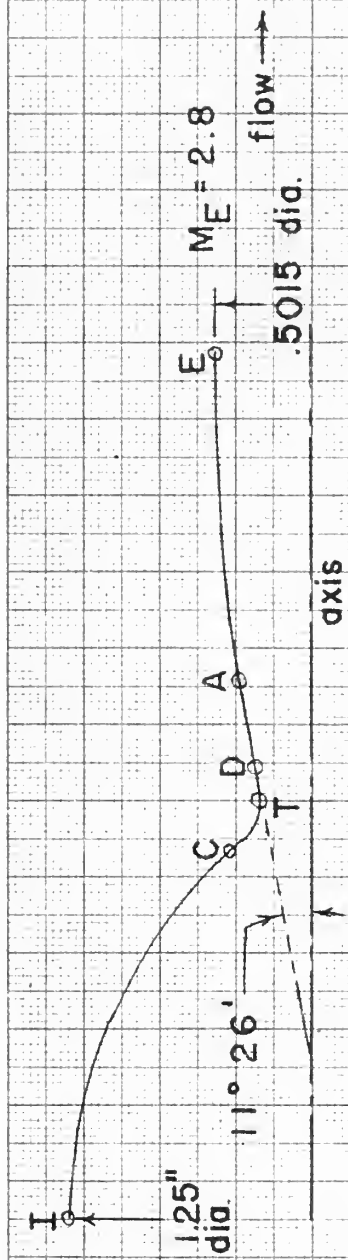


Fig. E-1 Nozzle Contour Regions



Fig. E-2 Comparison of Nozzle Throat to Exit Contours

APPENDIX F

Description of Sauer Method of Nozzle Design

The purpose of this appendix is to outline the Sauer method described in reference 13 which was used in the design of an axially-symmetric, supersonic nozzle with uniform parallel flow at the exit and with an isentropic exit Mach number of 2.8. The reference does not fully explain the application of this method to this type of nozzle to those unfamiliar with the theory of characteristics. Therefore, for the future reference of those who might wish to design a similar nozzle, a brief description of the theory of the Sauer Method and a more detailed description of its application to this type of nozzle is included in this appendix. The nozzle exit contour found by this method appears in Appendix E.

List of symbols:

- ϕ - potential function
- x - longitudinal cylindrical coordinate
- r - radial cylindrical coordinate
- c - velocity of sound
- α - Mach angle
- ξ, η - oblique-angular coordinate system tangent to Mach lines at each point
- $W_{\xi r}$ - component of velocity vector parallel to ξ axis = $\frac{\partial \phi}{\partial \xi}$
- $W_{\eta r}$ - " " " " " " η " = $\frac{\partial \phi}{\partial \eta}$
- V - $\frac{\partial \phi}{\partial r}$
- M_1 - first approximation of Mach net

M_{II} - second approximation of Mach's net

G_I - first approximation of velocity net

G_{II} - second approximation of velocity net

- angle which velocity vector makes with axis in velocity net

Part A - Theory:

Flow is assumed to be steady, isentropic, supersonic, irrotational, and axially-symmetric.

From the definition of the potential function ϕ , equation of continuity, the Euler Equation, and the definition of sound velocity, there results the potential equation:

$$\frac{\partial^2 \phi}{\partial x^2} \left[1 - \frac{(\frac{\partial \phi}{\partial x})^2}{c^2} \right] + \frac{\partial^2 \phi}{\partial r^2} \left[1 - \frac{(\frac{\partial \phi}{\partial r})^2}{c^2} \right] - \frac{2}{c^2} \frac{\partial^2 \phi}{\partial x \partial r} \frac{\partial \phi}{\partial x} \frac{\partial \phi}{\partial r} + \frac{1}{r} \frac{\partial \phi}{\partial r} = 0 \quad \text{Eq. (1)}$$

Assuming at each point in the physical plane a new coordinate system (ξ, η) tangent to the Mach lines at each point, the potential equation is transformed to:

$$\frac{\partial^2 \phi}{\partial \xi \partial \eta} = \frac{\sin^2 \alpha}{r} \frac{\partial \phi}{\partial r} \quad \text{Eq. (2)}$$

If in a given region, we consider that this new coordinate system remains fixed while a given point P undergoes a small displacement, there results:

$$\frac{\partial W_{\xi P}}{\partial \eta} = \frac{\partial W_{\eta P}}{\partial \xi} = \frac{\sin^2 \alpha}{r} v \quad \text{Eq. (3)}$$

For a finite difference, the above may be written:

$$\Delta W_{\xi P} = \frac{\sin^2 \alpha}{r} v \Delta \eta$$

$$\Delta W_{\eta P} = \frac{\sin^2 \alpha}{r} v \Delta \xi \quad \text{Eq. (4)}$$

The significance of these quantities is shown in Figures F-1 and F-2. Consider a Mach net in the physical plane. A constant velocity is assumed in each Mach quadrilateral; hence this area will map in a point in the velocity plane. The center of each area is assumed to be at the intersection of the diagonals. $\Delta\zeta$ and $\Delta\eta$ are the distances between the centers of two adjacent areas measured parallel to the ζ and η axis respectively, and are considered positive in the direction of flow. V is the component perpendicular to the axis of symmetry of the mean velocity vector between the two adjacent areas. r is the distance from the axis to the center of the common side of two adjacent areas.

Part B-Application:

To illustrate the application of this method to the design of a nozzle, the steps in the design of a nozzle will be considered in some detail; values being taken from the design of this nozzle.

I. Source flow in a conical nozzle.

A. First approximation of flow in a conical nozzle:

From the design by Foelsch method, the conical source flow was found to have a half cone angle of $11^{\circ}26'$ and the Mach number at point A was 1.875, which results in a Mach angle

$$\alpha_A = \sin^{-1} \frac{1}{1.875} = 32^{\circ} 14'$$

For the first approximation in the physical plane, M_1 , Figure F-3, the Mach lines are drawn parallel to each other with an inclination of $\pm \alpha_A$ to the x-axis. Having this net, $\Delta\zeta$, $\Delta\eta$ and r can be determined.

Points 1, 2, and 5 can be immediately located in the velocity plane, Figure F-4, since at each of these points the Mach number and the direction of flow is known. An initial approximation for point 3 is located by the intersection of characteristics through 1 and 2, which are inclined at $+\alpha_A$ and $-\alpha_A$ respectively to the x-axis. From point 3 thus located, V for 2/3 and 1/3 is determined, and $\Delta W_{\theta p}$ for 2/3 and ΔW_{np} for 1/3 are calculated from Eq. 4, and point 3 is relocated.

The initial approximations of subsequent points are determined by extending the characteristics of previously determined points and are then corrected in the manner explained for point 3. The points so located determine the velocity plane G_0 . By measuring V and α from G_0 by means of a subsidiary ellipse, the points may be relocated once again to produce velocity plane G_I .

B. Second approximation of flow in a conical nozzle:

From G_I , the direction of the velocity vectors, θ , at each point is measured, and the Mach angle α is determined by using a subsidiary ellipse. The direction of the characteristics at each area in the physical plane is given by $\theta \pm \alpha$. The new Mach net M_{II} is constructed by drawing the new Mach lines with directions as determined by interpolating between the corrected directions. After locating the new centers of the quadrilaterals in the M_{II} plane, they are located in the G_I plane to produce the G_I' net. The points of the G_I' net have the same relative position with respect to the points of the G_I net, as do the centers of areas in

the M_{II} net have with respect to the center^{of} areas in the M_I net. To construct G_{II} , ΔW_{fp} and ΔW_{np} are calculated from M_{II} and G_I' . The corrected Mach directions found from G_{II} are drawn through the centers of areas of M_{II} .

C. Third and higher approximations of flow in conical nozzle:

For the third and higher approximations, the procedure for the second approximation is continued until for a given approximation there is negligible correction necessary to the Mach net in the physical plane.

II. To correct the conical nozzle for parallel outflow:

The corrected nozzle results from joining a new Mach net M^* to the Mach net M_{III} (or higher), so as to obtain parallel flow at exit with an isentropic Mach number $M_E = 2.8$. The point of isentropic Mach number $M_E = 2.8$ is located on the x-axis of the velocity plane of G_{III} and from corresponding characteristic lines is located in the physical plane of M_{III} .

To construct M_I^* , draw characteristic a-a thru M_E . (See Figure F-5.) The centers of areas at junction of M_{III} and M_I nets are to lie on line a-a. In M_I^* the directions of the Mach lines are found by extending the characteristics of M_{III} . Upstream from a-a, the Mach net and velocity nets remain unchanged. Downstream from a-a, the Mach and velocity nets are determined by new boundary conditions; namely, uniform parallel flow of $M_E = 2.8$ along a-b.

A rough estimate of G_O^* is made remembering the new boundary conditions.

G_I^* is constructed with values of $\Delta W_{\varphi p}$ and ΔW_{np} calculated by means of M_I^* and G_O^* . Attention must be paid to the algebraic signs of $\Delta \varphi$ and $\Delta \eta$. Construction must start at point M_E .

With corrected directions of Mach lines in M_I^* , the second approximations and higher are obtained in a manner similar to that outlined for conical flow.

When the correct Mach net is obtained, the contour of the nozzle is drawn. In each area through which the contour passes, the direction is determined by the velocity vector for that area. The ratio of exit area to throat area (as determined by the Foelsch Method) should be that required to give the desired exit Mach number.

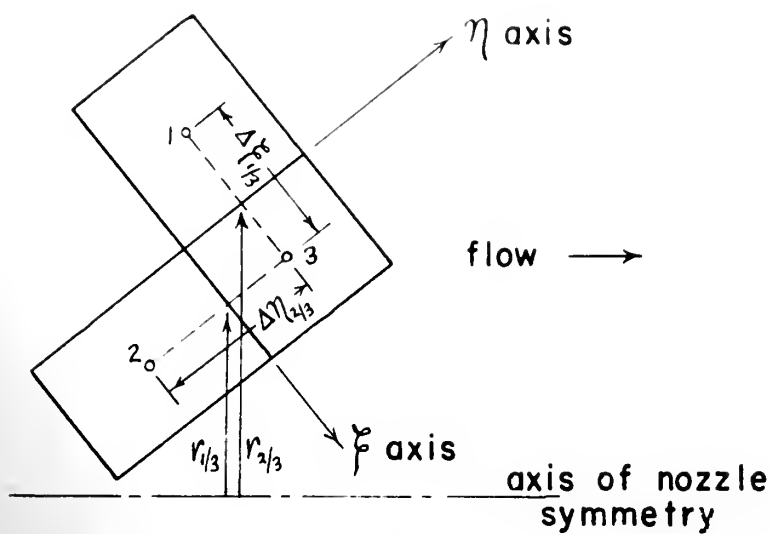


Fig. F-1 Mach Net - Physical Plane

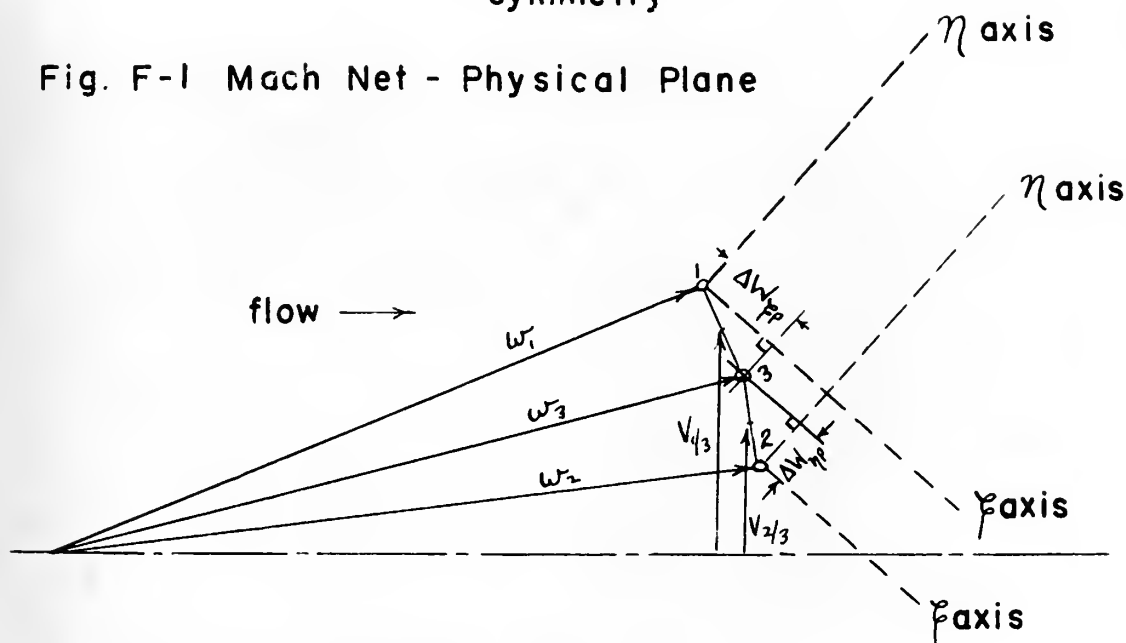


Fig. F-2 Velocity Net

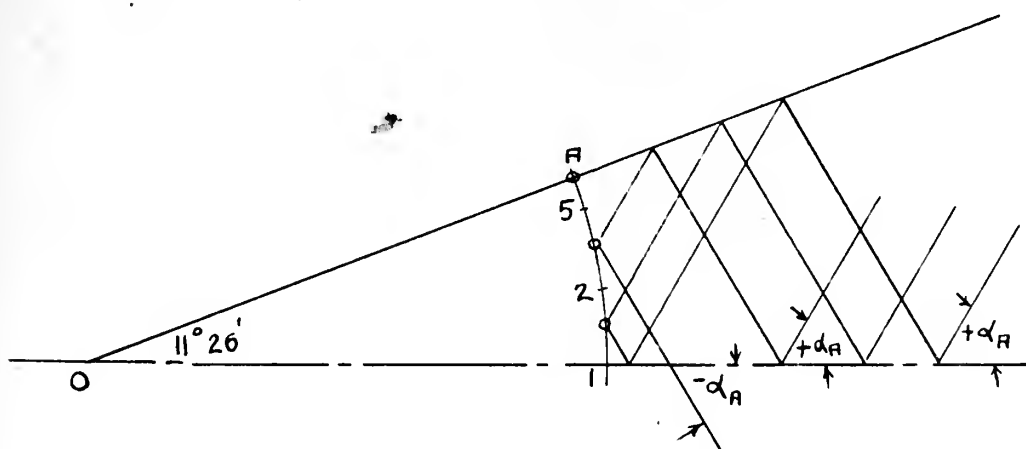


Fig. F-3 Physical Plane M_I

APPENDIX G
Nozzle Calibration

Procedure

Prior to calibrating the nozzle it was installed in the recovery factor apparatus in order that the calibration might yield flow coefficient data which included the influence of all components of the apparatus on the mass flow rate. As a result the process was not strictly a "nozzle calibration."

In order to determine the flow coefficient, i.e., the ratio of actual to isentropic mass rate of flow, twenty-three experimental runs were made using both the gasometer¹¹ in the MIT Mechanical Engineering Laboratory and a sharp-edged orifice to measure the actual flow rate. This appendix will deal only with the data obtained from the gasometer; the results obtained from the orifice, described in Appendix J, were not sufficiently consistent to be of any immediate use.

Ten of the runs, NC-1 through NC-10, were made with apparatus set up as indicated in Figure G-1. In these runs high pressure air was heated in the constant temperature bath and passed through the nozzle, test section, and orifice to the gasometer, the rate of rise of which determined the actual mass flow rate. In the remaining eleven runs, NC-11 through NC-21, the apparatus was set up as indicated in Figure G-2; under these conditions air was passed from the gasometer which had previously been filled from an auxiliary air line, through the constant temperature bath, nozzle, test section, and orifice to a steam-driven ejector. In this case the actual mass flow rate was calculated from the rate of fall of the gasometer.

The latter method more closely simulated the conditions under which the recovery factor runs were made since the ejector maintained low pressures in the section downstream of the nozzle. For this same reason the pressure ratio across the nozzle was always below critical and the conditions for maximum isentropic flow rate always existed. However, since the pressure of the air in the gasometer is limited by the number of weights which can safely be placed on the tank, the range of nozzle throat Reynolds numbers possible was very small and included only values which were generally below 10^5 . The range of Reynolds numbers was extended somewhat by using ice in the constant-temperature bath to reduce the temperature and viscosity of the air.

In the former method the lack of a pressure tap in the nozzle makes it impossible to determine the isentropic mass rate unless the conditions for maximum isentropic rate exist. As a result, it was necessary to experimentally determine the upstream stagnation pressure below which supersonic flow did not exist at the first station in order to determine the range of pressures for which the isentropic flow rate could be computed; it was found that the value was 61 psia. Since it is possible to simultaneously have subsonic flow at the first station (the first point in the test section after the nozzle throat at which there is a pressure tap) and critical flow through the nozzle, there is a small range of upstream stagnation pressures for which the flow, though maximum isentropic in value, could not be computed.

Calculations

The calculation of the actual mass rate of flow is based on the assumption of a perfect gas. From the temperature and pressure of the air in the gasometer the density can be calculated and from the rate of rise or fall the volume rate of flow can be determined since the cross-sectional area of the gasometer is fixed at 19.79 square feet. The product of the volume rate and density yields the mass rate of flow.

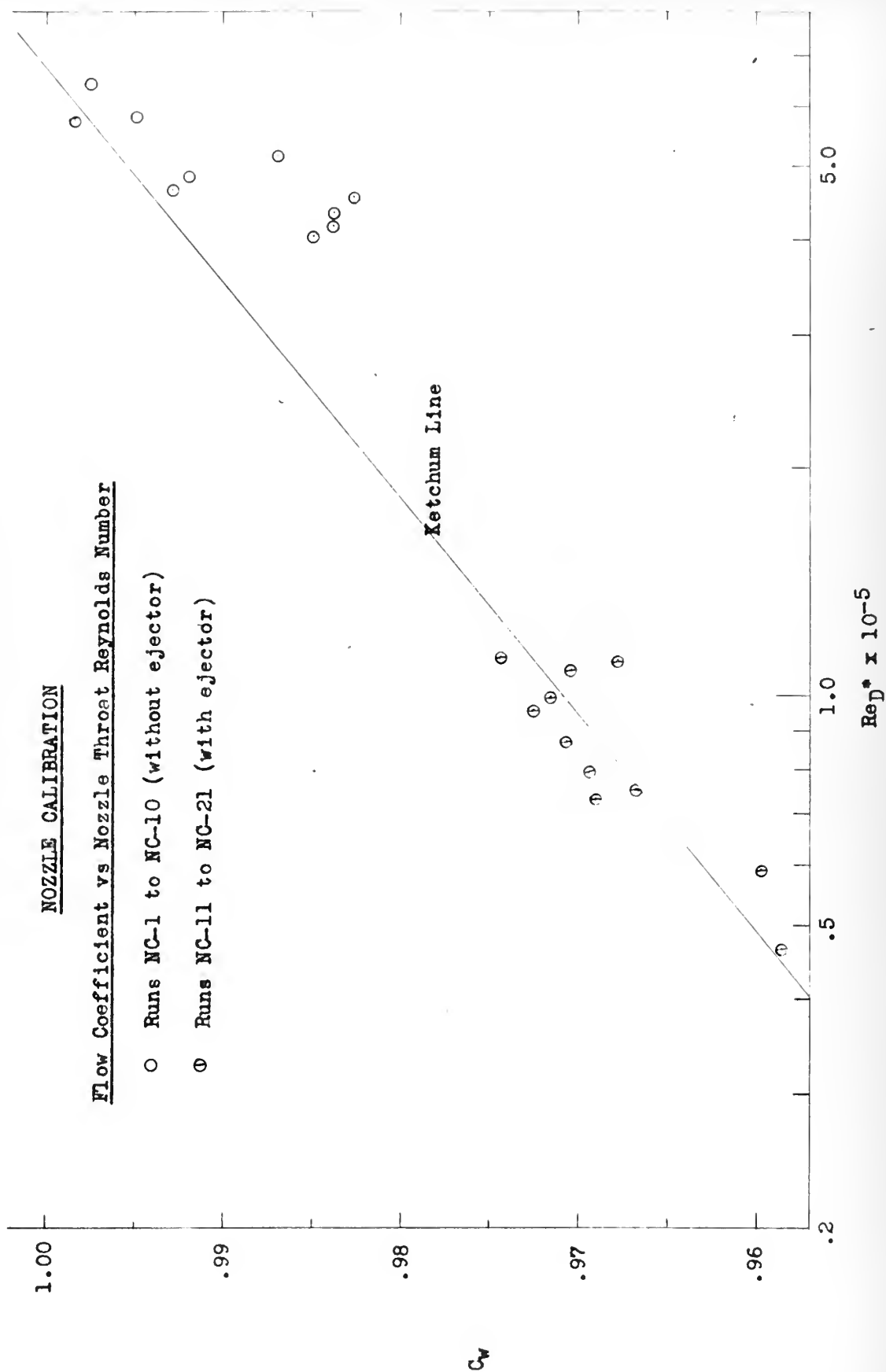
The maximum isentropic mass rate of flow and the nozzle throat Reynolds number are computed by the method outlined in Appendix B.

A summary of the results of the calculations is tabulated in Table G-1 and the plot of flow coefficient as a function of nozzle throat Reynolds number is shown in Figure G-3.

Discussion of Results

From Figure G-3 it can be seen that no calibration data was obtained for the Reynolds number range from 1.1×10^5 to 4.0×10^5 . Although it was possible to obtain flow at Reynolds numbers in this range, the physical limitations of the apparatus made it impossible to calculate the isentropic mass rate of flow. As a result, it was necessary to take advantage of the data obtained by Ketchum¹⁰ in calibrating a similar nozzle.

In carrying out the calculation of recovery factors the relationship between flow coefficient and nozzle throat Reynolds number determined by Ketchum was used. The straight line shown in Figure G-3 represents this function.



The results of the calibration carried out for this report are indicated by the points plotted in Figure G-3. It can be seen that the maximum deviation from the Ketchum line of any point is roughly 1.1% and that the mean deviation is considerably less. For this reason and in view of the fact that no better data was available at the time of the calculations, it is felt that the use of Ketchum's data is justifiable.

Recommendation

In order to determine the flow coefficient as a function of nozzle throat Reynolds number over the range for which no data was obtainable by means of the gasometer, the following procedures are possible:

1. A pressure tap can be located in the nozzle such that the isentropic mass rate of flow may be determined when the flow is not critical; or
2. The nozzle can be removed from the recovery factor apparatus and calibrated independently of the apparatus.

In view of the fact that it is undesirable to disturb the inner surface of the nozzle, it is recommended that the second procedure be carried out to calibrate the nozzle.

Table G-1

Summary of Results of Nozzle Calibration

Run	Rate of Climb	P _{us}	T _{us}	P _{gas}	T _{gas}	ReD*	C _w
	ft/min	psia	°Fabs	psfa	°Fabs	x10 ⁻⁵	-
NC-1	3.683	72.3	560.0	2151	536.3	4.662	.9929
NC-2	3.189	63.2	560.7	2151	535.9	4.036	.9849
NC-3	4.027	77.4	561.6	2096	537.2	5.171	.9869
NC-4	4.520	86.2	561.0	2096	537.2	5.814	.9949
NC-5	3.248	62.7	560.0	2096	536.2	4.189	.9838
NC-6	3.749	71.9	559.5	2096	535.1	4.846	.9920
NC-7	4.930	99.5	559.4	2096	532.7	6.418	.9974
NC-8	4.348	84.4	559.1	2124	532.2	5.744	.9984
NC-9	3.523	69.4	558.7	2124	532.2	4.576	.9826
NC-10	3.274	64.4	558.3	2124	532.2	4.330	.9837
NC-11	-.723	14.81	552.8	2209	535.7	.998	.9715
NC-12	-.633	12.96	551.5	2209	535.7	.874	.9705
NC-13	-.530	10.91	552.6	2209	535.7	.753	.9671
NC-14	-.430	8.90	552.5	2207	535.7	.593	.9597
NC-15	-.338	7.01	551.8	2207	535.7	.466	.9585
NC-16	-.757	15.16	512.6	2246	538.7	1.120	.9678
NC-17	-.761	15.13	511.7	2246	538.7	1.128	.9742
NC-18	-.730	14.62	513.6	2246	537.7	1.080	.9701
NC-19	-.538	10.79	513.6	2246	537.7	.796	.9693
NC-20	-.498	9.96	513.0	2246	538.7	.736	.9690
NC-21	-.644	12.81	510.5	2246	538.7	.956	.9724

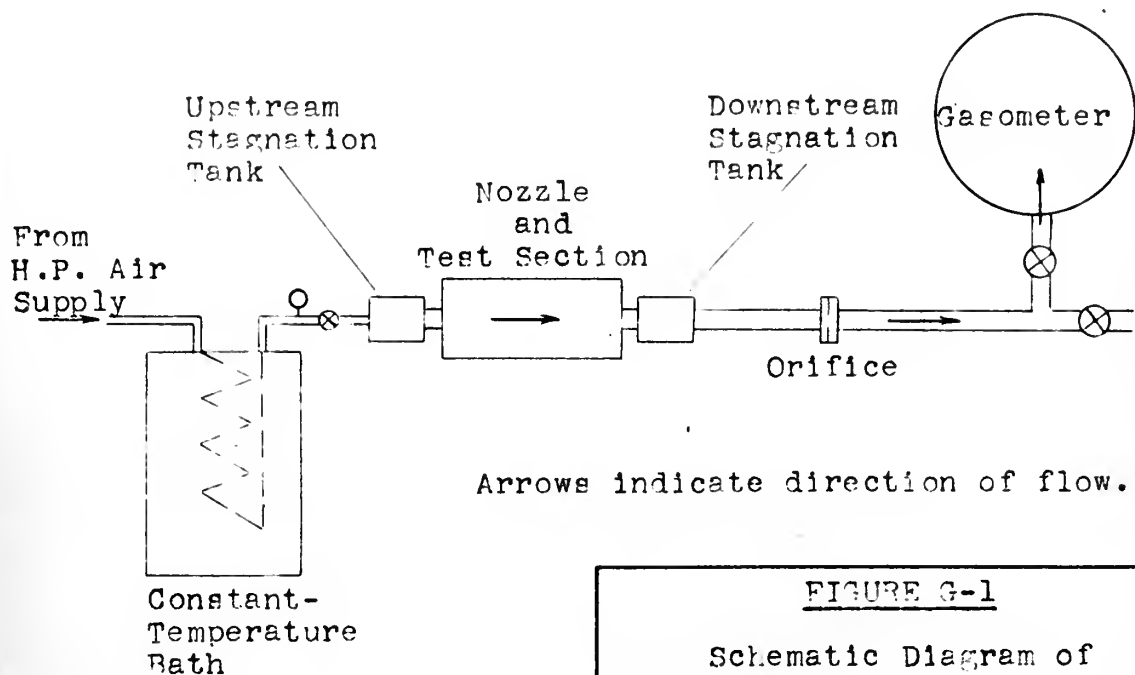


FIGURE G-1

Schematic Diagram of
Nozzle Calibration Apparatus

Runs NC-1 to NC-10

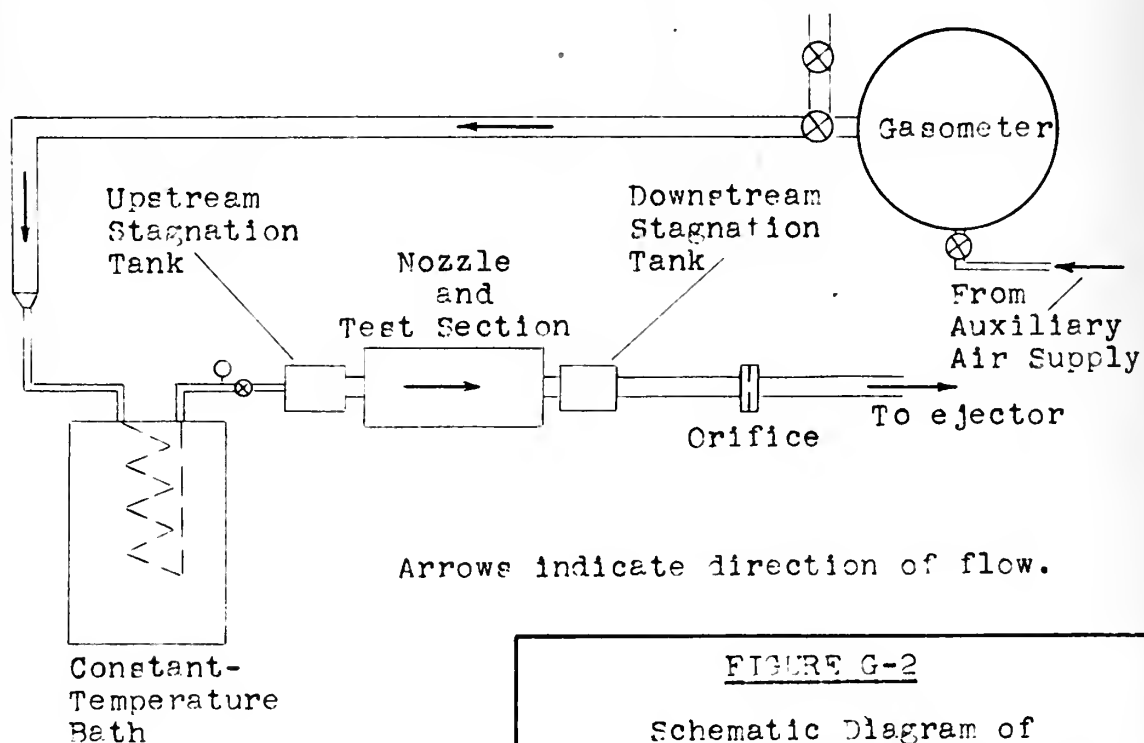


FIGURE G-2

Schematic Diagram of
Nozzle Calibration Apparatus

Runs NC-11 to NC-21

APPENDIX H

Thermocouple Calibration

Thermocouples used for the measurement of the upstream and downstream stagnation temperatures (T_{us} and T_{ds}) were those previously calibrated by Junge and Margolskee². Results of this calibration are also found in Appendix C.

Thermocouples for use in the lucite test section of the improved recovery factor apparatus to measure station temperatures and station radial temperature gradients were made of the same spools of #30 constantan and #30 copper wire as were used for the T_{us} and T_{ds} thermocouples. The manner in which the lucite test section thermocouples were made and installed in the apparatus follows that recommended by Shoulberg⁴. The station temperature thermocouples were calibrated in the MIT Heat Measurement Laboratory with the hot junction in a steam bath and the cold junction in an ice bath. The method of calibration follows:

- Symbols:
- p_b - barometric pressure (corrected)
 - T_p - temperature of boiling point of water °C
 - mv_{rp} - average potentiometer millivolt readings of the eleven stations while at steam temperature
 - T_{rp} - Bureau of Standards Conversion Table (for #30 constantan and #30 copper wire thermocouples) temperature corresponding to mv_{rp} , i.e., average temperature indicated by the eleven stations while at steam temperature
 - mv_r - potentiometer millivolt reading at any temperature between 0 and 100°C.

t_d - difference between T_{rp} and T_p

t_c - temperature correction to be applied to t_r

t_r - Bureau of Standards Conversion Table
temperature corresponding to mv_r

t_t - true temperature at the station = $t_r - t_c$

$$p_b = 758.292 \text{ mm Hg}$$

$$T_p = 100.0 + 0.0369 (p_b - 760) - 0.000020 (p_b - 760)^2 = 99.937 \text{ } ^\circ\text{C}$$

$$mv_{rp} = 4.2884 \text{ mv}$$

$$T_{rp} = 100.27 \text{ } ^\circ\text{C}$$

$$t_d = T_{rp} - T_p = 0.33 \text{ } ^\circ\text{C}$$

Assuming (a) that at $0 \text{ } ^\circ\text{C}$, the potentiometer reading (mv_r) will be zero so that $t_c = 0$ and

(b) that the temperature correction t_c is a linear function of mv_r , then

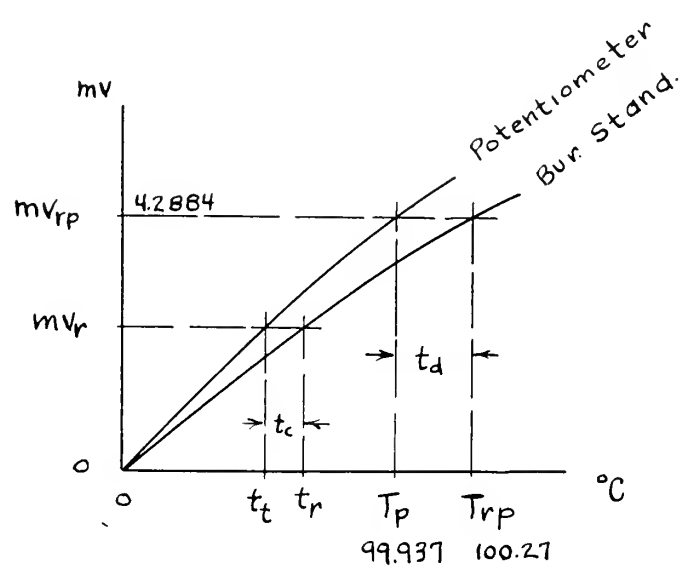
$$\frac{t_c}{mv_r} = \frac{t_d}{mv_{rp}} = \frac{0.33 \text{ } ^\circ\text{C}}{4.2884 \text{ mv}} = .1385 \frac{^\circ\text{F}}{\text{mv}}$$

$$\text{therefore } t_t = t_r - t_c = t_r - mv_r (.1385) \text{ } ^\circ\text{F}$$

A table of values of t_t vs mv_r was then computed by assuming values of mv_r at 0.1 mv intervals, obtaining t_r from the Bureau of Standards Conversion Table and then using the above equation to compute t_t . (See Appendix C.) Linear interpolation between these values results in errors much smaller than the accuracy of the thermocouple measurements.

At steam temperature the average deviation between the station millivolt reading and the averaged millivolt readings of the eleven

stations (mv_{rp}) is ± 0.0025 mv or ± 0.09 °F. At temperatures between 0 and 100°C, the average deviation will be proportionately less.



APPENDIX I

Vacuum System Precautions

The vacuum system itself is adequately described in Chapter V. The purpose of this appendix is to give the more important precautions to be observed in the operation of the vacuum system in order to maintain a low vacuum of 0.003 to 0.005 mm Hg pressure.

One of the major sources of potential trouble is the diffusion pump primarily because the pump is made of metal and its operating fluid cannot be observed nor can mal-operation of the pump quickly be detected by means of the vacuum measuring system. The condition and amount of octoil in the pump is not readily determinable since inspection requires breaking the seal on the not too accessible pump drain plug, removing the octoil and replacing the oil after measuring and inspecting. Inspection of the trap placed between the diffusion pump and the megavac pump to prevent carry over of octoil into the megavac pump is also difficult since its drain plug is quite inaccessible. Because of the danger of disturbing the joint seals in nearby piping and also because about 5 hours of running time is required to remove all dissolved gases from any fresh octoil placed in the system, removal of the octoil from the diffusion pump for inspection is not recommended at intervals of less than two months unless some of the following precautions have been violated or the pump is definitely not operating satisfactorily. Because of the fractionating principle, however, one filling of octoil should last indefinitely if not subjected to abuse or action of chemical vapors. Therefore, the diffusion pump should be quite

dependable if the following precautions for the prevention of decomposition and contamination of the octoil are observed:

1. Do not turn on the diffusion pump heater until the megavac pump has reduced the vacuum system pressure to less than 0.1 mm Hg because the hot oil vapors will decompose on exposure to air at pressures above 0.1 mm Hg.
2. In order to condense the hot oil vapors before coming into contact with the air, continue circulating cooling water after turning off the pump heater for at least 15 minutes before opening the vacuum system to the atmosphere.
3. Open vacuum system to the atmosphere very slowly.
4. When system is open to the atmosphere, the circulating water must not be turned on since water vapor will condense inside the pump and contaminate the oil.
5. It is preferable to leave the vacuum system at pressures below atmospheric when system is not in use than to leave system open to the atmosphere.
6. Regulate the circulating water such that the cooling coil and entire surface of the diffusion pump beneath the coil are quite cold during operation. Water leaving the cooling coil should be slightly warm to the touch.
7. When octoil is to be removed for storage during long periods of pump idleness, it should be stored in glass stoppered, amber colored bottles.

8. Cleaning of the pump should be undertaken whenever the vacuum system is dismantled. Acetone should be used for this purpose, followed by air circulation, and then evacuation of the pump. Carbon tetrachloride must not be used since this solvent clings to the metal parts and is difficult to remove.

The megavac pump requires no special care other than proper lubrication of the motor, maintaining correct level of clean high vacuum oil in the pump, prevention of overheating, etc. The pump should give trouble-free and efficient operation for about 100,000 hours.

The remaining causes of poor vacuum come under the heading of leaks through the numerous joints and seals in the vacuum system. Constant vigilance and application of glyptal and air-drying varnish to suspected joints is mandatory. It is preferable to apply the glyptal and varnish when the vacuum system is open to the atmosphere and time should be allowed for thorough drying before placing the system in operation, if possible. The covering of glyptal and varnish should be removed by means of glyptal thinner or benzene before dismantling a joint. When assembling any part of the vacuum system piping or test section, it is essential to use every means possible, such as, cleaning of parts before assembly, use of high-vacuum grease on all rubber gaskets and screw threads, proper tightening of bolts and compression fittings, etc., to prevent future leakage.

Some precautions to be observed in the vacuum measuring system are:

1. Even though a safety trap is provided, care should be taken when comparing the pressure in the absolute pressure manometer manifold

with that in the vacuum system to prevent silicone oil being forced into the recovery factor test section as a result of the pressure in the manometer manifold being much greater than that in the vacuum system.

2. After measuring the pressure in the vacuum system by means of the McLeod gage, lower the mercury reservoir to its lower position to facilitate evacuation of that part of the apparatus.

3. The mercury reservoir mentioned above should be lowered slowly to prevent an air bubble entering the mercury column from the mercury column air cushion and thus raise the pressure in the vacuum system appreciably.

APPENDIX J

Orifice

Design and installation

A standard orifice plate for measuring the downstream flow rate was designed and installed in the downstream section of the recovery factor apparatus in order to provide a comparison with the calculated nozzle flow rate and to detect leaks in the apparatus.

The orifice was designed in accordance with reference 12 for maximum possible flow rate occurring at the highest expected upstream stagnation pressure and the lowest expected upstream stagnation temperature. Thus:

$$W_o = .5319 A^* \frac{P_{us}}{\sqrt{T_{us}}} = .5319 (.05662) \frac{100}{\sqrt{492}} = .1355 \text{ lb/sec}$$

The area of the orifice to be installed in the 2 1/2"-pipe with radius pressure taps was determined for the above flow rate from the following equation taken from Section VII of reference 12:

$$W_o = \frac{K E Y A_2}{12} \sqrt{\frac{2g}{RT_1} P_{10} \Delta P_o} \quad (1)$$

in which the orifice upstream pressure (P_{10}) and the pressure differential (ΔP_o) across the orifice are selected from a consideration of the manometers to be used for their measurement. From the area (A_2) thus determined, the diameter (D_2) was found to be about 1.5".

The orifice plate was then machined from 1/8" stainless steel plate with an orifice diameter of 1.498 inches and with a 45°-bevel on the downstream face. The plate was installed between two 2 1/2-inch pipe flanges

with a rubber gasket on each side of the plate. The length of straight piping provided upstream of the orifice was 22 pipe diameters while that downstream was 10 pipe diameters, both of which are greater than the minimum required by Section IV of reference 12. The upstream pressure tap was installed at a distance of 1 pipe diameter from the orifice plate and the downstream tap at a distance of 1/2 pipe diameter.

Calibration

The orifice was calibrated after installation, using air flow measured by the gasometer at the same time the nozzle was calibrated. The orifice flow coefficient was calculated from the following equation:

$$K_o = \frac{W_{\text{gasometer}}}{0.668 A_2 E Y \sqrt{\frac{P_{10} \Delta P_o}{R T_{0s}}}} \quad (2)$$

Results of the calibration are shown in Figure J-1, but it should be noted that this calibration is valid only for $\frac{\Delta P_o}{P_{10}} \leq 0.2$ which corresponds roughly to upstream stagnation pressures (P_{us}) greater than 25 psia when T_{us} is near 110 °F.

Calculation of Flow

The method of calculating the orifice flow rate is adequately described on page 56, reference 12. There remains only the necessity of indicating how the values were measured. Referring to equation (1): P_{10} was obtained from the orifice upstream pressure tap reading converted to psia; ΔP_o was obtained directly from the pressure differential manometer across the orifice; T_1 was assumed to be equal to T_{ds} ; E, the area multiplier for

thermal expansion of the primary element due to the pipe temperature, is equal to 1 at room temperature; and Y , the expansion factor, was calculated, knowing the ratio of orifice to pipe diameter and the ratio of ΔP_o to P_1 .

Results:

As can be seen from Figure J-1, the orifice flow coefficients determined from the gasometer flow vary as much as $\pm 5\%$ from the mean value of the orifice coefficient. Assuming the gasometer flow to be correct, because it yielded nozzle flow coefficients that were quite close to values previously determined, the orifice flow determination is not accurate enough to permit the orifice to be used for the purpose for which it was designed.

The orifice is limited to flow rates in which $\frac{\Delta P_o}{P_1} \leq 0.2$ and thus for P_{us} greater than 25 psia when T_{us} 110 °F. This limitation can be improved by redesigning the orifice for the smaller flow rates. However, it was felt that re-design with a smaller orifice area would not improve the large variation of the orifice flow coefficient to within the $\pm 0.5\%$ necessary to make the orifice usable as a means of determining leaks or errors in the determination of nozzle flow rates. Therefore, re-design was not attempted.

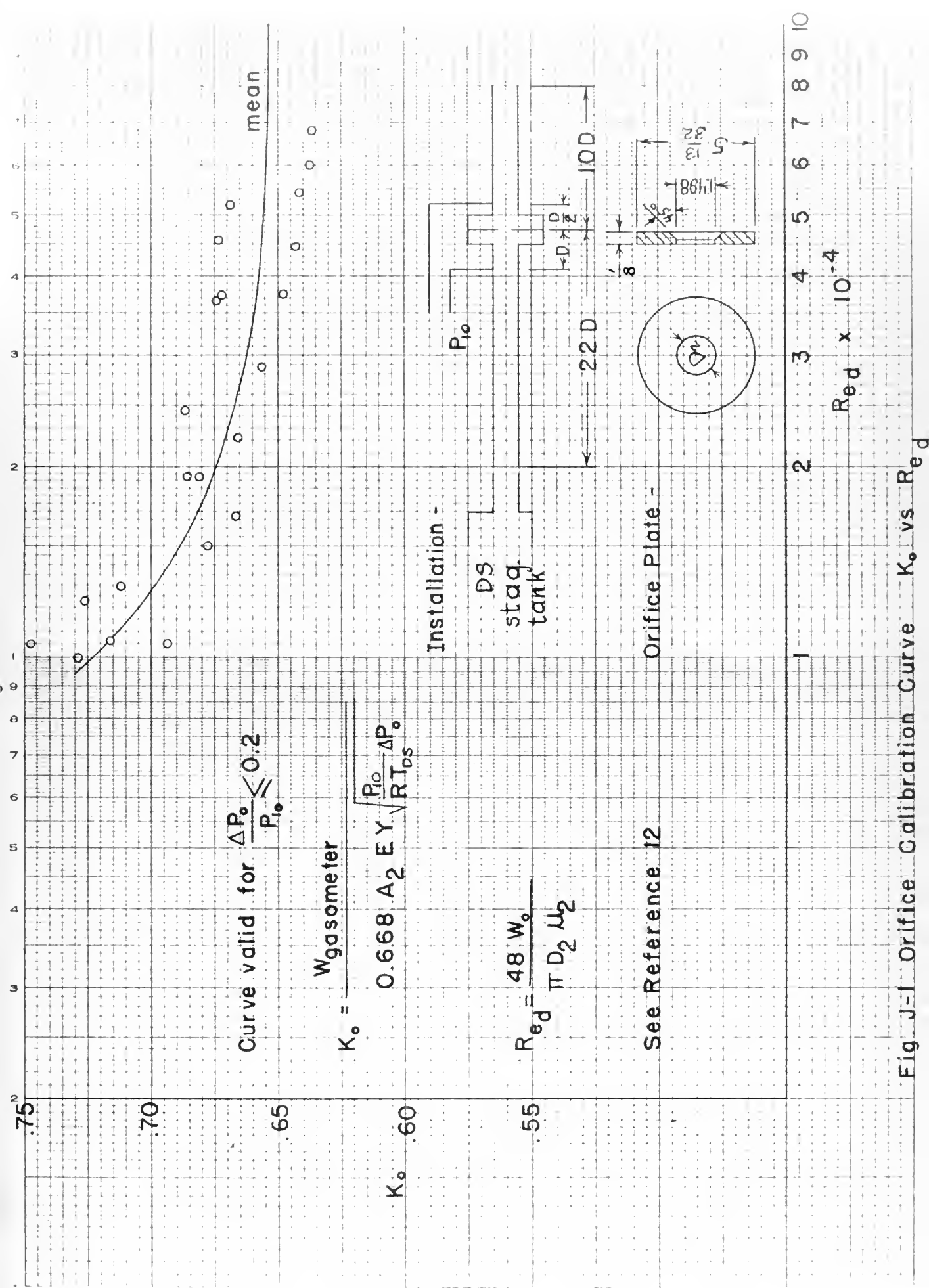


Fig. J-1 Orifice Calibration Curve K_o vs R_{ed}

APPENDIX K

Modification to the Recovery Factor Apparatus

After completion of runs F-1 to 35, the recovery factor test section was modified to reduce the heat conduction and radiation between the 1/8-inch O.D. copper tubing used for measuring the station wall pressures, and the lucite test section. One end of the copper tubing is exposed to room temperature, while the other is fastened to the lucite test section. As discussed in Chapter VI, experiments with dry ice placed on the exposed ends of the copper tubing showed that an appreciable amount of heat was being transferred from the room to the test section via the copper tubing; or vice versa, depending upon the relation between the station wall temperature and room temperature.

The modification consisted primarily of removing all copper tubing inside the recovery factor apparatus, leaving only a length of 1 1/4 inches at the upstream end plate and at the station boss compression fitting. The removed copper tubing was replaced with low conductivity, 1/8-inch plastic tubing. The ends of the plastic tubing were slipped over the short lengths of the remaining copper tubing and a tight joint was effected by means of small tube clamps and a coating of glyptal. This change effectively prevents all but small amounts of heat transfer by conduction and radiation between the room and the test section by the pressure tubing.

To reduce the other possible radiation effects in the apparatus, such as that between the lucite test section and the textolite outer tube, aluminum foil was wrapped loosely around the test section, around each pressure tube, and then around the assembly of the pressure tubing and test section. Both

end plates were covered with several layers of aluminum foil and a layer was loosely secured to the inside of the textolite outer tube. The recovery factor apparatus was wrapped with aluminum foil externally, as well.

In order to determine the temperature surrounding the lucite test section, and also to determine the temperature gradient existing between the test section and the textolite outer tube, two thermocouples were installed inside the apparatus. The thermocouple wires were led out of the apparatus through four 45° holes drilled in the downstream end plate in a manner similar to the thermocouple holes drilled in the upstream end plate, and thence through the joint between the downstream end plate and the textolite outer tube. A tight seal was effected by means of high vacuum grease applied to the wires, the end plate gasket and the joint between the end plate and outer tube. Externally, this joint was coated with glyptal and air-drying varnish.

One of the above thermocouples, called T_L , was located about $1/2$ inch from the lucite test section between the bosses of stations #5 and 6. Two layers of aluminum foil separate the thermocouple from the lucite itself. The other thermocouple, T_T , was placed on the same horizontal plane and in the same longitudinal position as T_L but was fastened by adhesive tape directly to the inside of the textolite outer tube.

After the modification was completed, run F-36 was made at $T_{us} = 109.89^\circ\text{F}$ and the recovery factors obtained were found to agree quite well with those previously obtained at similar upstream stagnation temperatures. This indicates that the modification does not appreciably change the data on

recovery factors already obtained at T_{us} near 110 °F. This was the expected result since at this T_{us} the wall temperature in the lucite test section is approximately equal to room temperature and thus only small heat transfer was possible via the copper tubing. At other stagnation temperatures, however, the heat transfer before the copper tubing was removed was proportionately greater and this modification will result in much more accurate recovery factors.

APPENDIX L

Effects of Measurement Errors

The equipment used to measure observed quantities in the recovery factor and friction factor runs is the same as that used by previous investigators working on other phases of this project. Since the limitations on the precision of measurements have been discussed in references 2 and 4, it is the purpose of this appendix to present an analysis of the effects of the measurement errors on the calculated quantities.

The recovery factor is dependent on the Mach number, which is a computed quantity, and the adiabatic wall temperature and upstream stagnation temperature, both of which are measured quantities. The Mach number in turn is a function of the local wall pressure, upstream stagnation pressure, and flow coefficient.

Consider the equation (See Appendix B):

$$\left(\frac{P_w}{P_{us}}\right)\left(\frac{A}{A^*}\right) = \frac{C_w \sqrt{\left(\frac{2}{\kappa+1}\right)^{\frac{\kappa+1}{\kappa-1}}}}{M \sqrt{1 + \frac{\kappa-1}{2} M^2}}$$

Using the technique of taking the logarithm of both sides of the equation and differentiating leads to:

$$\frac{d(P_w/P_{us})}{P_w/P_{us}} = \frac{dC_w}{C_w} - \frac{dM}{M} - \frac{1}{2} \frac{(\kappa-1)M^2}{\left(1 + \frac{\kappa-1}{2} M^2\right)} \frac{dM}{M}$$

for A/A^* and κ both constant.

For small changes in variables the differentials in the above expression may be replaced by delta-quantities to indicate small finite differences. To

study the effects of errors in flow coefficient only assume that there are no errors in the pressure measurements. Then

$$\frac{\Delta C_w}{C_w} = \left(1 + \frac{k-1}{2} \frac{M^2}{1 + \frac{k-1}{2} M^2} \right) \frac{\Delta M}{M}$$

Assuming $k = 1.400$ and rearranging:

$$\frac{\Delta M}{M} = \frac{(1 + .2 M^2)}{(1 + .4 M^2)} \frac{\Delta C_w}{C_w}$$

The above equation expresses the interdependence of the percent error in calculated Mach number, percent error in flow coefficient, and Mach number; the function is plotted in Figure L-1.

From the same original equation and in a similar manner the effects of errors in measurements of wall pressure and upstream stagnation pressure can be determined. The resulting error equations are:

$$\frac{\Delta M}{M} = \frac{(1 + .2 M^2)}{(1 + .4 M^2)} \frac{\Delta P_{us}}{P_{us}}$$

and

$$\frac{\Delta M}{M} = - \frac{(1 + .2 M^2)}{(1 + .4 M^2)} \frac{\Delta P_w}{P_w}$$

These functions are also plotted in Figure L-1.

To determine the effect of errors in Mach number on calculated recovery factors, the same technique is applied to the definition of recovery factor

$$R' = 1 - \frac{1 - (T_{aw}/T_{us})}{1 - (T_m/T_{us})}$$

Since T_m/T_{us} is a function of Mach number and since T_{aw}/T_{us} is appreciably constant, the following can be derived:

$$\frac{\Delta R'}{R'} = \frac{10 (1 - T_{aw}/T_{us})}{M^2 \left[1 - (1 - T_{aw}/T_{us}) (5/M^2 + 1) \right]} \frac{\Delta M}{M}$$

For $T_{aw}/T_{us} = 0.94$

$$\frac{\Delta R'}{R'} = \left(\frac{0.639}{M^2 - 0.319} \right) \frac{\Delta M}{M}$$

Figure L-2 shows the percent error in recovery factor as a function of percent error in Mach number for the above value of T_{aw}/T_{us} .

From the definition of recovery factor it can be shown that

$$\frac{\Delta R'}{R'} = \frac{1}{1 - \frac{(T_m/T_{us})}{(T_{aw}/T_{us})}} \frac{\Delta T_{aw}}{T_{aw}}$$

This function is plotted in Figure L-3 for various values of Mach number and for T_{aw}/T_{us} constant at 0.94.

As a result of this analysis the probable errors in calculated recovery factors due to the limitations on the precision of measurements are tabulated below:

<u>Measured Quantity</u>	<u>Probable Measurement Error</u>	<u>Maximum Probable Error (%)</u>	<u>Maximum Probable R' Error</u>	
			<u>M = 1</u>	<u>M = 2.5</u>
P_{us} (Bourdon gage)	0.5 psi	1.3%	1%	0.1%
P_{us} (Hg manometers)	0.10 cm	0.2%	0.2%	0.05%
P_w (Hg manometers)	0.10 cm	2%	1.6%	0.3%
P_w (absolute manometers)	0.10 cm	0.5%	0.4%	0.05%
C_w	0.01	1%	0.8%	0.1%
T_{aw} ($T_{aw}/T_{us} = .94$)	0.4°F	0.1%	0.8%	0.2%

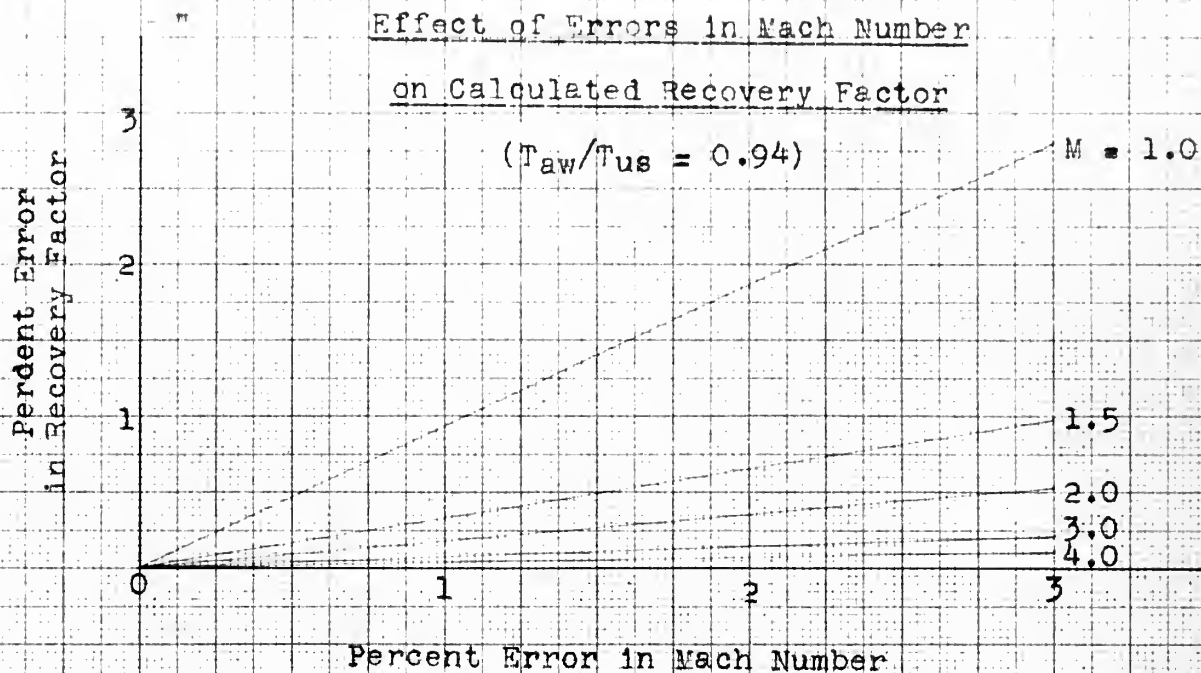


Figure L-2

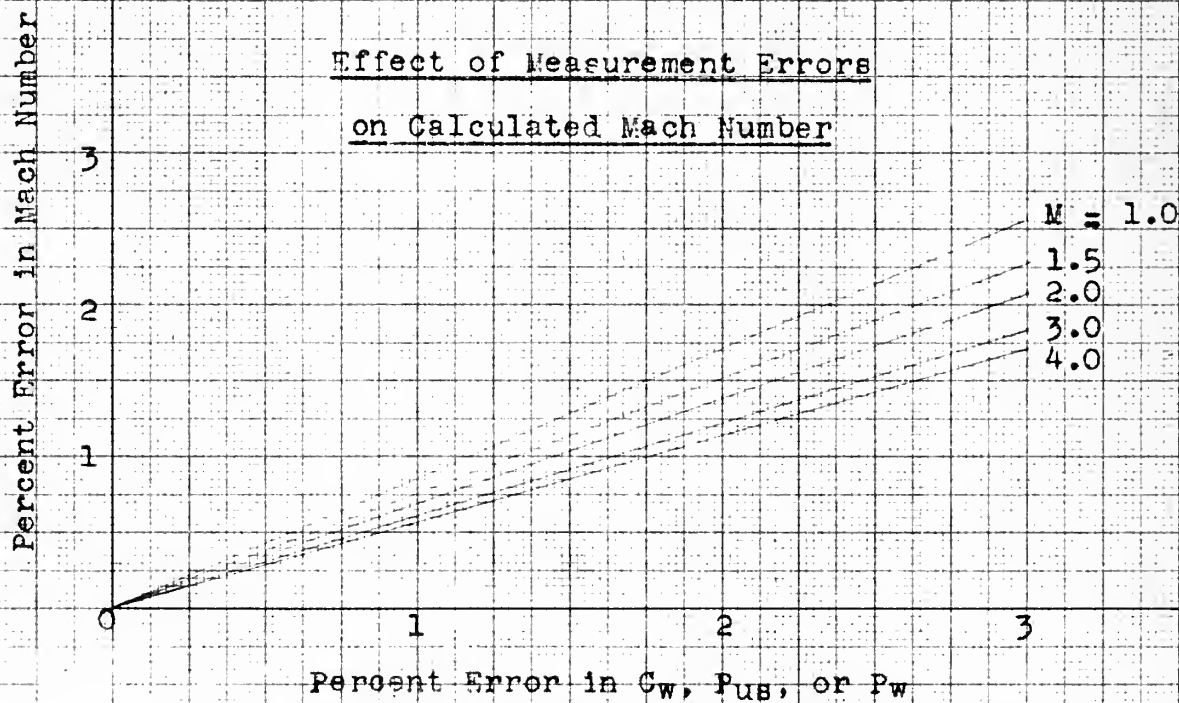


Figure L-1

Figure L-3

Effect of Errors

in T_{aw}

on Calculated Recovery Factor

$(T_{aw}/T_{us} = 0.94)$

Percent Error in Recovery Factor

15

10

5

0

1

2

Percent Error in T_{aw}

1.0

$n = 1.5$

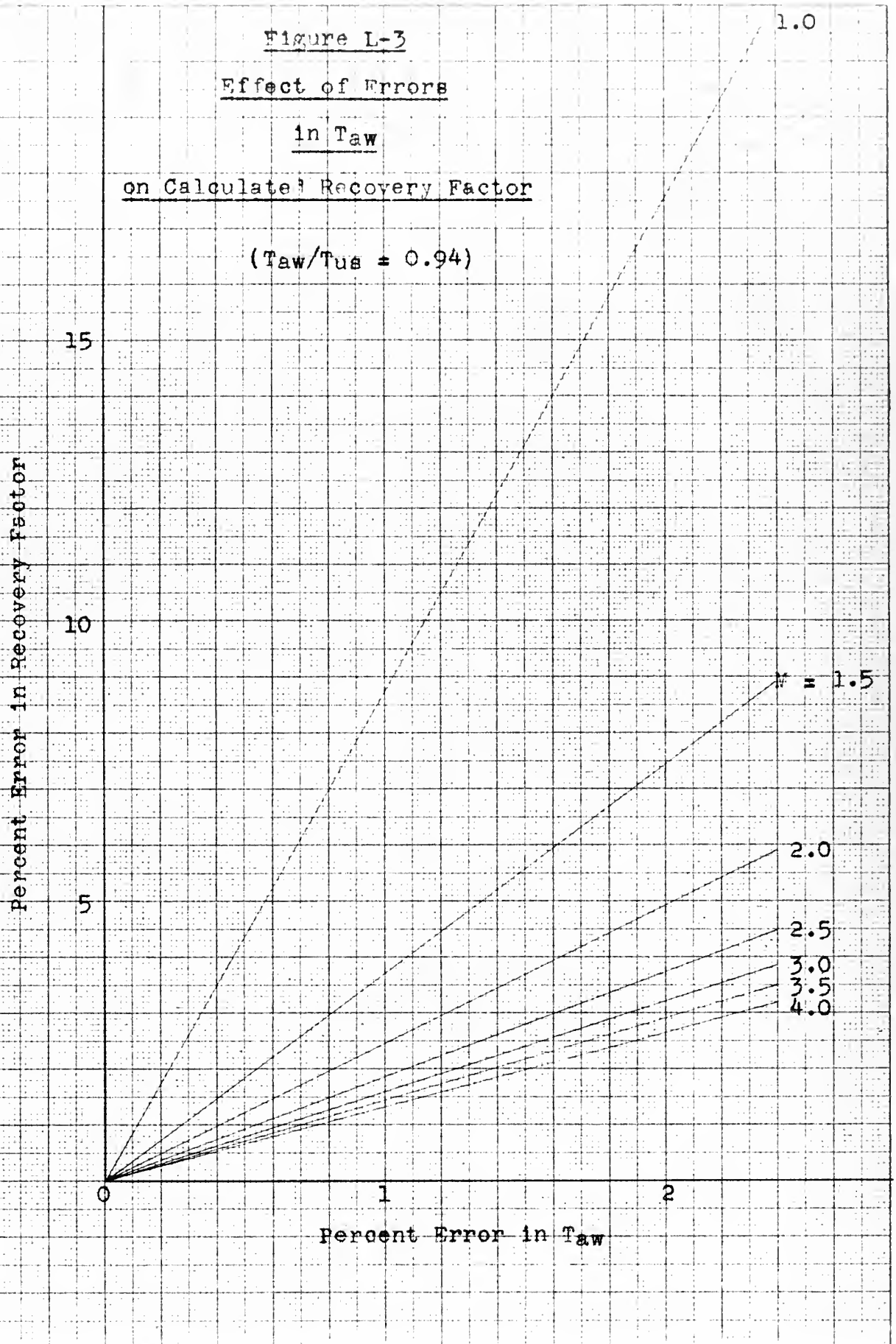
2.0

2.5

3.0

3.5

4.0



APPENDIX MBibliography

1. Helfrich, W.E. and J.W. Connors; Experimental Investigation of Recovery Factors for Air Flowing in a Tube at Supersonic Velocities; S.M. Thesis, Dept. of Mech. Eng., M.I.T.; 1948.
2. Junge, R.M. and J.M. Margolskee; Experimental Investigation of Recovery Factors for Air Flowing in a Tube at Supersonic Velocities; S.M. Thesis, Dept. of Mech. Eng., M.I.T.; 1947.
3. Klingensmith, K.K.; Design of Apparatus for Measuring Recovery Factors and Heat Transfer Coefficients for Air Flowing in Tubes at Supersonic Velocities; S.M. Thesis, Dept. of Mech. Eng., M.I.T.; 1947.
4. Shoulberg, R.H., W. J. Larkin and W.L. England; Experimental Investigation of Heat Transfer Coefficients for Air Flowing in a Tube at Supersonic Velocities; S.M. Thesis, Dept. of Mech. Eng., M.I.T.; 1949.
5. Beattie, Blaisdell, Kaye, Gerry and Johnson; Thermal Expansion and Compressibility of Vitreous Silica and the Thermal Dilatation of Mercury; Proceedings of the American Academy of Arts and Sciences, Vol. 74, No. 11, Dec. 1941, page 386.
6. Dow Corning Silicone Notebook Fluid Series No. 2 issued July 1946; Silicone Fluids for Use in High Vacuum Diffusion Pumps.
7. Keenan, J.H., and J. Kaye; Gas Tables; John Wiley and Sons, New York, 1948.
8. Shapiro, A.H., W.R. Hawthorne, and G.M. Edelman; The Mechanics and Thermodynamics of Steady One-Dimensional Gas Flow with Tables for Numerical Solutions; Meteor Report No. 14; M.I.T., 1947.
9. Shapiro, A.H.; Flow of Compressible Fluids; Course 2.492 Notes; Dept. of Mech. Eng., M.I.T., 1947.
10. Ketchum, G.M.; Recovery Factors, Friction Factors, and Heat Transfer Coefficients for the Flow of Air at Supersonic Velocities in a Tube; Sc. D. Thesis; Dept. of Mech. Eng., M.I.T., 1949.
11. McElrath, T. Jr.; Investigation and Application of a Laboratory Gasometer; S.M. Thesis; Dept. of Mech. Eng., M.I.T., 1941.

12. Instruments and Apparatus Special Subcommittee on the Measurement of Fluid Flow; Flow Measurement 1940. Information on Instruments and Apparatus, Part 5. Measurement of Quantity of Materials, Chapt. 4. Flow Measurement by Means of Standardized Nozzles and Orifice Plates. A.S.M.E. Power Test Codes, The American Society of Mechanical Engineers, New York City, N.Y., 1940.
13. Sauer, R.; Method of Characteristics for Three Dimensional Axially Symmetrical Supersonic Flows; N.A.C.A. Tech. Memo. 1133, Jan. 1947.
14. Foelsch, Kuno; Analytical Design of Axially Symmetric Laval Nozzle for a Parallel and Uniform Jet; Journal Aeronautical Science, Vol. 16, No. 3, March 1949.
15. Wyant, J.D.; Design of a Heat Exchanger for the Measurement of Local Heat Transfer Coefficients for Air in Supersonic Flow Through a Tube; S.M. Thesis, Dept. of Mech. Eng., M.I.T., 1947.
16. Kaye, J., J.H. Keenan, and W.H. McAdams; Report of Progress on Measurements of Friction Coefficients, Recovery Factors, and Heat Transfer Coefficients for Supersonic Flow of Air in a Pipe; M.I.T., 1949.
17. Keenan, J.H. and E.P. Neumann; Friction in Pipes at Supersonic and Subsonic Velocities; N.A.C.A. TN 963; January, 1945.
18. Emmons, H.W. and J.G. Brainerd; Temperature Effects in a Laminar Compressible Fluid Boundary Layer Along a Flat Plate; Journal of Applied Mechanics; September 1941.
19. Eckert, E. and W. Weise; The Temperature of Unheated Bodies in a High Speed Gas Stream; N.A.C.A. TM 1000, 1941.
20. Ackermann, G.; Forschung Ing. Wes.; Vol. 13, 1942.
21. Nicolai, L.A.; Measurements of Friction Factors, Recovery Factors, and Coefficients of Heat Transfer in a Tube for Subsonic Flow of Air; Sc. D. Thesis, Dept. of Chem. Eng., M.I.T., 1944.
22. Eber, G.; Experimentelle Untersuchung der Bremstemperatur. und des Wärmeüberganges an einfachen Körpern bei Überschallgeschwindigkeit; Archiv 66/57, Nov., 1941.
23. Frossel, W.; Flow in Smooth Straight Pipes at Velocities above and below Sound Velocity; N.A.C.A. TM No. 844, 1938.

24. Pohlhausen, E.; Der Wärmeaustausch zwischen festen Körpern und Flüssigkeiten mit kleiner Reibung und kleiner Wärmeleitung;
Zeitschrift für angewandte Mathematik und Mechanik; 1921.

H. S. N. A. P.

89

8

DATE DUE

[illegible]

Thesis

W3935 Welch

13244

Experimental investigation of recovery factors and friction factors for air flowing in a tube at supersonic velocities.

Thesis

W3935 Welch

13244

Experimental investigation of recovery factors and friction factors for air flowing in a tube at supersonic velocities.

thesW3935

Experimental investigation of recovery f



3 2768 001 95207 0

DUDLEY KNOX LIBRARY